IEC 61000-4-23

Edition 2.0 2016-10

INTERNATIONAL STANDARD

colour inside

BASIC EMC PUBLICATION

Electromagnetic compatibility (EMC) – Part 4-23: Testing and measurement techniques – Test methods for protective devices for HEMP and other radiated disturbances

IEC 61000-4-23:2016-10(en)

IEC Central Office
3, rue de Varembé
CH-1211 Geneva 20
Switzerland

Tel.: +41 22 919 02 11
Fax: +41 22 919 03 00
info@iec.ch
www.iec.ch

About the IEC
The International Electrotechnical Commission (IEC) is the leading global organization that prepares and publishes International Standards for all electrical, electronic and related technologies.

About IEC publications
The technical content of IEC publications is kept under constant review by the IEC. Please make sure that you have the latest edition, a corrigenda or an amendment might have been published.

IEC Catalogue - webstore.iec.ch/catalogue
The stand-alone application for consulting the entire bibliographical information on IEC International Standards, Technical Specifications, Technical Reports and other documents. Available for PC, Mac OS, Android Tablets and iPad.

IEC publications search - www.iec.ch/searchpub
The advanced search enables to find IEC publications by a variety of criteria (reference number, text, technical committee,…). It also gives information on projects, replaced and withdrawn publications.

IEC Just Published - webstore.iec.ch/justpublished
Stay up to date on all new IEC publications. Just Published details all new publications released. Available online and also once a month by email.

Electropedia - www.electropedia.org
The world's leading online dictionary of electronic and electrical terms containing 20 000 terms and definitions in English and French, with equivalent terms in 15 additional languages. Also known as the International Electrotechnical Vocabulary (IEV) online.

IEC Glossary - std.iec.ch/glossary
65 000 electrotechnical terminology entries in English and French extracted from the Terms and Definitions clause of IEC publications issued since 2002. Some entries have been collected from earlier publications of IEC TC 37, 77, 86 and CISPR.

IEC Customer Service Centre - webstore.iec.ch/csc
If you wish to give us your feedback on this publication or need further assistance, please contact the Customer Service Centre: csc@iec.ch.

IEC 61000-4-23

Edition 2.0 2016-10

INTERNATIONAL STANDARD

colour inside

BASIC EMC PUBLICATION

Electromagnetic compatibility (EMC) –
Part 4-23: Testing and measurement techniques – Test methods for protective devices for HEMP and other radiated disturbances

INTERNATIONAL ELECTROTECHNICAL COMMISSION

ICS 33.100.99

ISBN 978-2-8322-3687-1

Warning! Make sure that you obtained this publication from an authorized distributor.

CONTENTS

INTERNATIONAL ELECTROTECHNICAL COMMISSION

____

ELECTROMAGNETIC COMPATIBILITY (EMC) –

Part 4-23: Testing and measurement techniques – Test methods for protective devices for HEMP and other radiated disturbances

FOREWORD

1) The International Electrotechnical Commission (IEC) is a worldwide organization for standardization comprising all national electrotechnical committees (IEC National Committees). The object of IEC is to promote international co-operation on all questions concerning standardization in the electrical and electronic fields. To this end and in addition to other activities, IEC publishes International Standards, Technical Specifications, Technical Reports, Publicly Available Specifications (PAS) and Guides (hereafter referred to as "IEC Publication(s)"). Their preparation is entrusted to technical committees; any IEC National Committee interested in the subject dealt with may participate in this preparatory work. International, governmental and non-governmental organizations liaising with the IEC also participate in this preparation. IEC collaborates closely with the International Organization for Standardization (ISO) in accordance with conditions determined by agreement between the two organizations.
2) The formal decisions or agreements of IEC on technical matters express, as nearly as possible, an international consensus of opinion on the relevant subjects since each technical committee has representation from all interested IEC National Committees.
3) IEC Publications have the form of recommendations for international use and are accepted by IEC National Committees in that sense. While all reasonable efforts are made to ensure that the technical content of IEC Publications is accurate, IEC cannot be held responsible for the way in which they are used or for any misinterpretation by any end user.
4) In order to promote international uniformity, IEC National Committees undertake to apply IEC Publications transparently to the maximum extent possible in their national and regional publications. Any divergence between any IEC Publication and the corresponding national or regional publication shall be clearly indicated in the latter.
5) IEC itself does not provide any attestation of conformity. Independent certification bodies provide conformity assessment services and, in some areas, access to IEC marks of conformity. IEC is not responsible for any services carried out by independent certification bodies.
6) All users should ensure that they have the latest edition of this publication.
7) No liability shall attach to IEC or its directors, employees, servants or agents including individual experts and members of its technical committees and IEC National Committees for any personal injury, property damage or other damage of any nature whatsoever, whether direct or indirect, or for costs (including legal fees) and expenses arising out of the publication, use of, or reliance upon, this IEC Publication or any other IEC Publications.
8) Attention is drawn to the Normative references cited in this publication. Use of the referenced publications is indispensable for the correct application of this publication.
9) Attention is drawn to the possibility that some of the elements of this IEC Publication may be the subject of patent rights. IEC shall not be held responsible for identifying any or all such patent rights.

International Standard IEC 61000-4-23 has been prepared by subcommittee 77C: High power transient phenomena, of IEC technical committee 77: Electromagnetic compatibility.

It forms Part 4-23 of IEC 61000. It has the status of a basic EMC publication in accordance with IEC Guide 107.

This second edition cancels and replaces the first edition published in 2000. This edition constitutes a technical revision.

This edition includes the following significant technical changes with respect to the previous edition:

a) updates to the shielding effectiveness (SE) test method in Clause 5;
b) a new Annex F describing methods for testing 'inside-to-out' has been added.

The text of this standard is based on the following documents:

CDV	Report on voting
77C/253/CDV	77C/257/RVC

Full information on the voting for the approval of this standard can be found in the report on voting indicated in the above table.

This publication has been drafted in accordance with the ISO/IEC Directives, Part 2.

A list of all parts in the IEC 61000 series, published under the general title *Electromagnetic compatibility (EMC)*, can be found on the IEC website.

The committee has decided that the contents of this publication will remain unchanged until the stability date indicated on the IEC website under "http://webstore.iec.ch" in the data related to the specific publication. At this date, the publication will be

- reconfirmed,
- withdrawn,
- replaced by a revised edition, or
- amended.

A bilingual version of this publication may be issued at a later date.

IMPORTANT – The 'colour inside' logo on the cover page of this publication indicates that it contains colours which are considered to be useful for the correct understanding of its contents. Users should therefore print this document using a colour printer.

INTRODUCTION

IEC 61000 is published in separate parts, according to the following structure:

Part 1: General

General considerations (introduction, fundamental principles)

Definitions, terminology

Part 2: Environment

Description of the environment

Classification of the environment

Compatibility levels

Part 3: Limits

Emission limits

Immunity limits (in so far as they do not fall under the responsibility of the product committees)

Part 4: Testing and measurement techniques

Measurement techniques

Testing techniques

Part 5: Installation and mitigation guidelines

Installation guidelines

Mitigation methods and devices

Part 6: Generic Standards

Part 9: Miscellaneous

Each part is further subdivided into several parts, published either as international standards, as technical specifications or technical reports, some of which have already been published as sections. Others will be published with the part number followed by a dash and a second number identifying the subdivision (example: IEC 61000-6-1).

The IEC has initiated the preparation of standardized methods to protect civilian society from the effects of high power electromagnetic (HPEM) environments. Such effects could disrupt systems for communications, electric power, information technology, etc.

This part of IEC 61000 is an international standard that establishes the test concepts, set-ups, required equipment, and test procedures for protective devices against HEMP radiated disturbances.

Annex F provides examples of the SE test method placing the TX antenna inside the barrier.

ELECTROMAGNETIC COMPATIBILITY (EMC) –

Part 4-23: Testing and measurement techniques – Test methods for protective devices for HEMP and other radiated disturbances

1 Scope

This part of IEC 61000 provides a protective devices test method for HEMP and other radiated disturbances. It is primarily intended for HEMP testing but can be applied to other externally generated radiated disturbances where appropriate. It provides a brief description of the most important concepts for testing of shielding elements. For each test, the following basic information is provided:

– theoretical foundation of the test (the test concepts);
– test set-up including outside-to-in and inside-to-out measurements;
– required equipment;
– test procedures;
– data processing.

This international standard does not provide information on requirements for specific levels for testing.

This part of IEC 61000 has been updated to include a new test method.

Due to the available space, a transmitting antenna position outside the barrier has mainly been suggested. However, nowadays, many EMP protection facilities in practical use do not actually have enough space available outside the electromagnetic barrier due to physical constraints such as concrete walls or soil to allow the method described in IEC 61000-4-23:2000 (edition 1) to be applied correctly. From experience many facilities have available space for a 1 m separation or less only.

Therefore, in many practical cases it is not possible to measure shielding effectiveness according to the test method of previous documents. The constructors for EMP protection facilities are also unwilling to build facilities with extra space for measurements with the transmitting antenna outside the barrier due to the great expense and inefficiency of the operational working area for new or existing buildings.

This document provides additionally a method that allows the transmitting antenna to be placed inside the enclosure and the receiving antenna outside the barrier (‘inside-to-out’ method). Annex F includes test set-up and procedure examples.

2 Normative references

The following documents are referred to in the text in such a way that some or all of their content constitutes requirements of this document. For dated references, only the edition cited applies. For undated references, the latest edition of the referenced document (including any amendments) applies.

IEC 60050-161, *International Electrotechnical Vocabulary (IEV) – Part 161: Electromagnetic compatibility* (available at www.electropedia.org)

IEC 61000-2-9, *Electromagnetic compatibility (EMC) – Part 2: Environment – Section 9: Description of HEMP environment – Radiated disturbance*

IEC 61000-5-3, *Electromagnetic compatibility (EMC) – Part 5-3: Installation and mitigation guidelines – HEMP protection concepts*

3 Terms and definitions

For the purposes of this document, the terms and definitions given in IEC 60050-161, as well as the following apply.

3.1
aperture
opening in an electromagnetic barrier (shield) through which EM fields may penetrate

3.2
aperture point-of-entry
intentional or inadvertent holes, cracks, openings or other discontinuities in a shield surface

Note 1 to entry: Intentional aperture points-of-entry are provided for personnel and/or equipment entry and egress and for ventilation through an electromagnetic barrier.

3.3
attenuation
reduction in magnitude (as a result of absorption and scattering) of an electric or magnetic field, a current or a voltage, usually expressed in decibels

3.4
bandwidth (of a device)
width of a frequency band over which a given characteristic of an equipment or transmission channel does not differ from its reference value by more than a specified amount or ratio

[SOURCE: IEC 60050-161:1990, 161-06-09, modified – the note has been deleted.]

3.5
bandwidth (of an emission or signal)
width of the frequency band outside which the level of any spectral component does not exceed a specified percentage of a reference level

[SOURCE: IEC 60050-161:1990, 161-06-10]

3.6
bounded wave simulator
type of simulator for producing electromagnetic fields in a localized region of space referred to as a "test volume"

3.7
box
enclosure that contains electrical equipment

Note 1 to entry: Such boxes usually contain modules of subsystems.

3.8
broadband

3.8.1
broadband
<emission> emission which has a bandwidth greater than that of a particular measuring apparatus or receiver

3.8.2
broadband device
device whose bandwidth is such that it is able to accept and process all the spectral components of a particular emission

[SOURCE: IEC 60050-161:1990, 161-06-12]

3.9
circuit
collection of interconnected electronics forming one or more closed paths

3.10
conductive point-of-entry
electrical wire or cable or other conductive object, such as a metal rod, which passes through the electromagnetic barrier

3.11
coupling
interaction of electromagnetic fields with electrical systems, whereby part of the energy of the field is transferred to the system

3.12
current injection test
test technique by which, through some external means, a current is forced to flow in a circuit at a desired location

Note 1 to entry: For EMP testing purposes, it is a process by which simulated EMP transient current pulses are introduced into a component, circuit or system to measure damage or upset thresholds.

3.13
cut-off frequency
<waveguide> lowest frequency for which there is no attenuation of the electromagnetic fields propagating in a lossless waveguide

Note 1 to entry: Below this frequency, the fields attenuate exponentially with distance along the waveguide.

3.14
dipole
straight antenna, usually fed in the center, that produces maximum radiation in a plane normal to its principal axis

3.15
direct drive
excitation of an electrical system by directly applying a voltage or current source (either transient or continuous wave) to system cables or surfaces as a means of simulating the effects of transient EM pulses

Note 1 to entry: See current injection test (3.12).

3.16
direct field penetration
penetration of the system shielding by the EM field

3.17
direction of propagation
direction of the electromagnetic plane-wave propagation vector k, which is perpendicular to the plane containing the vectors of the electric and the magnetic fields

3.18
electric field strength
E
magnitude of the electric field vector of an electromagnetic wave or of a field created by an electric charge distribution, measured in volt per meter

3.19
electromagnetic barrier
shield
topologically closed surface made to prevent or limit EM fields and conducted transients from entering the enclosed space

Note 1 to entry: The barrier consists of the shield surface and PoE treatments and it encloses the protected volume.

3.20
electromagnetic disturbance
any electromagnetic phenomenon which may degrade the performance of a device, equipment or system, or adversely affect living or inert matter

[SOURCE: IEC 60050-161:1990, 161-01-05]

3.21
electromagnetic environment
totality of electromagnetic phenomena existing at a given location

[SOURCE: IEC 60050-161:1990, 161-01-01, modified – the note has been deleted.]

3.22
electromagnetic pulse
EMP
all types of electromagnetic fields produced by a nuclear explosion

Note 1 to entry: Electromagnetic pulse is also referred to as nuclear electromagnetic pulse (NEMP).

3.23
(electromagnetic) radiation

a) phenomenon by which energy in the form of electromagnetic waves emanates from a source into space
b) energy transferred through space in the form of electromagnetic waves

[SOURCE: IEC 60050-161:1990, 161-01-10, modified – the note has been deleted.]

3.24
electromagnetic topology
description of the interconnection of shields or electromagnetic barriers in a system that limit the EMP environment within the system

3.25
external coupling
process by which an incident electromagnetic field strikes the exterior portions of a conducting system enclosure and induces currents and charges

3.26
gasket
element, normally electrically conductive and flexible, used to seal an aperture in an enclosure

3.27
inside-to-out
test method where the transmitting antenna is placed inside and the receiving antenna is placed outside the shielded enclosure

3.28
hardening
process of decreasing the vulnerability of a system or component by design techniques, for example by protecting against, or decoupling from, an undesirable external environment such as EMP

3.29
high-altitude electromagnetic pulse
HEMP
electromagnetic pulse produced when a nuclear explosion occurs outside the earth's atmosphere, typically above an altitude of 30 km

3.30
hyperband
spectrum of EM field with a band ratio greater than 10

3.31
impulse radiating antenna
IRA
half IRA
full IRA
full IRA with a full parabolic dish or half IRA with a divided parabolic dish on a conducting ground plane and an impedance transformer from 50 Ω to 100 Ω

3.32
inside-to-out
alternative test method where the receiving antenna is placed outside and the transmitting antenna is placed inside of the shielded enclosure

3.33
magnetic field strength
H
magnitude of the magnetic field vector of an electromagnetic wave, or the field produced by a current flowing in a wire, loop antenna, etc., measured in amperes per meter

3.34
outside-to-in
conventional test method where the receiving antenna is placed inside and the transmitting antenna is placed outside of the shielded enclosure

3.35
overall shielding
global shielding
protection of an entire entity by use of a single shielding enclosure or some practical equivalent, such as the protection of the contents of an entire building by shielding the entire building

3.36
penetration
transfer of electromagnetic energy through an electromagnetic barrier from one volume to another

Note 1 to entry: This can occur by field diffusion through the barrier, by field leakage through apertures, and by electrical current passing through conductors connecting the two volumes (wires, cables, conduits, pipes, ducts, etc.).

3.37
point-of-entry
PoE
physical location (point/port) on the electromagnetic barrier, where EM energy may enter or exit a topological volume, unless an adequate PoE protective device is provided

Note 1 to entry: A PoE is not limited to a geometrical point. PoEs are classified as aperture PoEs or conductor PoEs according to the type of penetration. They are also classified as architectural, mechanical, structural or electrical PoEs according to the architectural engineering discipline in which they are usually encountered.

3.38
PoE protective device
PoE treatment
protective measure used to prevent or limit EM energy from entering a protected volume at a PoE

Note 1 to entry: Common PoE protective devices include waveguides below cut-off, closure plates for aperture PoEs, and filters and surge arresters on penetrating conductors.

3.39
protected volume
three-dimensional space enclosed by an electromagnetic barrier

3.40
pulse
abrupt variation of short duration of a physical quantity followed by a rapid return to the initial value

[SOURCE: IEC 60050-161:1990, 161-02-02]

3.41
radio frequency
RF
frequency of the electromagnetic spectrum that is between the audio frequency portion and the infrared portion

Note 1 to entry: Sometimes, audio frequencies are considered to be included as part of the RF spectrum.

3.42
penetrating field
field inside the shielded volume that may penetrate via shield imperfections

3.43
shielded enclosure
screened room
mesh or sheet metallic housing designed expressly for the purpose of separating electromagnetically the internal and external environment

[SOURCE: IEC 60050-161:1990, 161-04-37]

3.44
shielding degradation
general or localized reduction of electromagnetic shielding effectiveness as a result of openings, penetrations, wear, improper utilization, etc.

3.45
shielding effectiveness
SE
measure of the reduction or attenuation in the electromagnetic field strength at a point in space caused by the insertion of a shield between the source and that point, usually expressed in decibels (dB)

3.46
skin effect
tendency of alternating current to concentrate in the surface layer of a conductor, resulting in the effective resistance of the conductor increasing with frequency

3.47
system
collection of equipment, subsystems, skilled personnel, and techniques capable of performing or supporting a defined operational role

Note 1 to entry: A complete system includes related facilities, equipment, subsystems, materials, services and personnel required for its operation to the degree that it can be considered self-sufficient within its operational or support environment

3.48
transient, adjective and noun
pertaining to or designating a phenomenon or a quantity which varies between two consecutive steady states during a time interval short compared with the time-scale of interest

[SOURCE: IEC 60050-161:1990, 161-02-01]

3.49
protection device
device providing protection to a conductive PoE

Note 1 to entry: It may, for example, consist of one or more of the following: a spark gap, a metal oxide varistor (MOV) or a filter. These devices are used to reduce the electrical disturbance which penetrates an electromagnetic barrier.

3.50
waveguide below cut-off
waveguide whose primary purpose is to attenuate electromagnetic waves at frequencies below its lowest cut-off frequency, while at the same time providing a physical opening into a shielded enclosure

3.51
wire mesh
connected wire fabric normally used for protection of apertures in an electromagnetic barrier

4 HEMP test concepts

4.1 General

A key aspect in HEMP protection is describing and using the electromagnetic shielding topology of the system. This amounts to locating and characterizing the various surfaces (or electromagnetic barriers) within the system enclosing regions (volumes) protected against HEMP. In real systems, openings shall be present in the shields for the normal operation and functioning of the equipment inside. These openings degrade the shielding, and if the degradation is too large, various types of HEMP protection devices shall be provided at these penetration points in the shield. The location of the various penetration points and the types of protective devices determine the location and type of test to be conducted to verify the system shielding.

As an example, a hypothetical case of a building containing a highly shielded screen room is considered. Inside the screen room, it is assumed that there are several equipment enclosures, linked together by shielded cables and connectors. The first shielding surface in this system is the building enclosure. Depending on the type of building, this may or may not provide significant shielding for the interior volume. After energy penetration along inappropriately protected signal and power lines field penetration through apertures in the wall (including cracks and inappropriate joints) and diffusion through the wall are the main pathways for external energy to leak into the shielded room. Large apertures in the form of doors and windows, as well as conducting penetrations for electrical power and communications lines, may be present. Tests of these individual penetration mechanisms shall be required to evaluate the shielding provided by this enclosure.

Inside the building, the HEMP field is attenuated somewhat by the building walls or enclosure. Thus, the electrical disturbance experienced by the internal screen room is lower than that of the ambient external HEMP field. Because the internal shielded room is specifically designed to reduce the EM fields inside, it is expected that it will function properly – if the various protection devices applied to the shield penetrations are operational. Field penetration through cracks and joints in the walls, diffusion through the shield material and conductive penetrations along signal wires are the main pathways for energy to leak into the shielded room.

Inside the screen room, the conducting exteriors of the equipment housing and the shielded cables form the third barrier in this hypothetical system. As before, the EM energy is able to penetrate into these internal boxes by conductive penetrations, aperture penetrations and by diffusion. Moreover, energy penetration through braided cables and cable connectors may occur on the lines linking the various internal equipment enclosures.

Annex A describes test concepts for both conductive and radiated disturbances. In Clause 4, various methods are described for testing protective measures against the radiated HEMP environment only. These tests involve the direct generation of EM fields acting on equipment enclosures or shields, or the injection of current and charge onto shields to simulate the radiated field interaction to the structures. In the remainder of Clause 4, a brief introduction into the various HEMP test concepts and techniques for radiated field disturbances is given. The specific test procedures are presented in Clause 5.

4.2 Testing of shielding enclosures

4.2.1 General

There are several different ways of characterizing the behaviour of protective enclosures. Below, various test concepts are examined that serve to describe the shielding behaviour of the individual shielding elements in question. Annex A should be consulted for more information regarding these types of HEMP tests. Instead, test methods for verifying the protection levels provided by individual shielding components within the system will be examined and indication given as to what should be measured in the tests.

Field transfer functions

A common measure of shielding is obtained by examining the strength of the internal EM field relative to the intensity of the external excitation EM field (i.e. the field with the building removed). Because the external and internal EM environments can be defined in terms of either the E-field or the H-field, and because these fields are vector quantities, a large number of field combinations is possible. Moreover, these fields are time-varying in nature, due to the transient nature of the HEMP threat.

Considering the internal and external fields to be decomposed into their frequency-domain spectra, a measure of the attenuation provided by the building is provided by the field transfer function $T(\omega)$ which is the ratio of suitably chosen field quantities as

$$T(\omega) = \frac{A_{\text{in}}(\omega)}{A_{\text{out}}(\omega)} \tag{1}$$

where

$A_{\text{out}}(\omega)$ represents the spectral magnitude and phase components of a particular vector component of either the E or H excitation field outside the facility; and

$A_{\text{in}}(\omega)$ represents a magnitude and phase component of either E or H inside the building.

Depending on the choice of the internal and external fields, this ratio can be dimensionless or have dimensions of an impedance (in ohms) or an admittance (in siemens).

The field transfer function in Equation (1) is a complex valued function, having both a magnitude and phase. An illustration of a measured transfer function between the external excitation and the internal H-fields for a sample shielding enclosure is illustrated in Figure 1. If an accurate representation of the internal transient fields is to be determined from measurements of $T(\omega)$, both quantities shall be measured. If only a relative indication of the attenuation as a function of the frequency is desired for the building, then it is sufficient to measure only the magnitude $|A_{\text{in}}|$ and $|A_{\text{out}}|$.

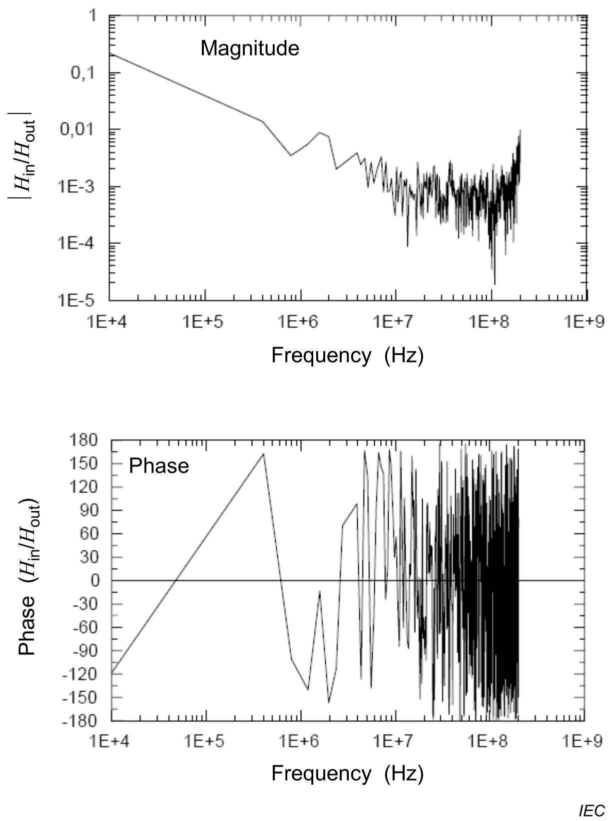

Figure 1 – Example of measured magnitude and phase of the transfer function $T(\omega) = H_{\text{in}}/H_{\text{out}}$ for a shielded enclosure

Shielding effectiveness

The shielding effectiveness of a facility is closely related to the shield transfer function discussed above in that it compares the relative magnitudes of two similar field components in the frequency domain. However, this quantity contains less information because the phase information is lacking. Shielding effectiveness of the enclosure is defined as follows:

$$SE_{\mathrm{A}} = 20\log_{10}\left(\frac{|A_{\mathrm{out}}|}{|A_{\mathrm{in}}|}\right) = 20\log_{10}\left(\frac{1}{|T_{\mathrm{A}}(\omega)|}\right)\ \mathrm{dB} \tag{2}$$

where

A_{out} and A_{in} represent suitable external and internal E- or H-field quantities.

Thus, it is closely related to the magnitude plot of the transfer function for the fields.

Because of the fundamental differences in electric and magnetic shielding mechanisms at low frequencies, the shielding effectiveness for electric fields, denoted by SE_{E}, and for magnetic fields, SE_{H}, are significantly different at low frequencies. Figure 2 illustrates the theoretical shielding provided by a closed aluminum shell of a thickness of 0,5 mm. Generally, SE_{H} is less than SE_{E} at low frequencies (below 100 kHz), due to the fact that the low-frequency magnetic field is able to diffuse through the protective enclosure walls more easily than does the electric field. It is for this reason that magnetic field SE is typically used at lower frequencies (below 10 MHz), and at higher frequencies (above 10 MHz) the SE for electric or magnetic field can be used to characterize an enclosure.

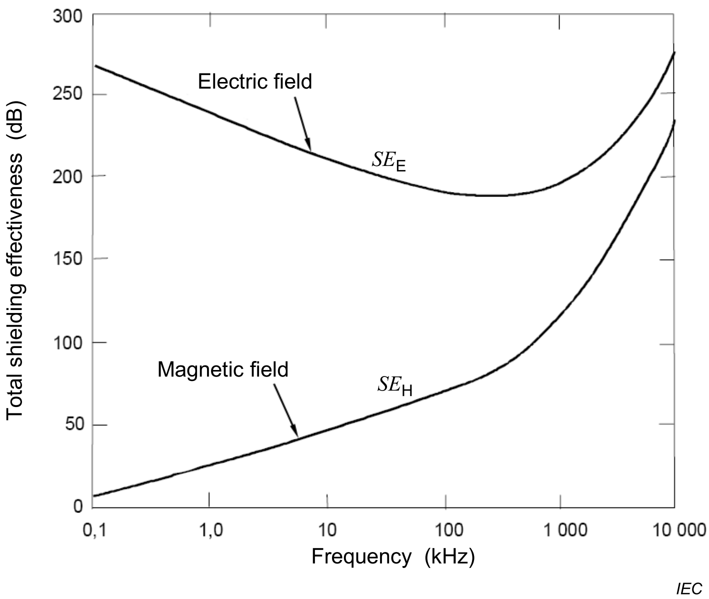

Figure 2 – Electric field and magnetic field shielding effectiveness of a 0,5 mm thick aluminum enclosure [29][1]

As a further example of the measured magnetic field shielding effectiveness of a real enclosure, Figure 3 illustrates the behaviour of SE_{H} as measured for the same building discussed in Figure 1. It should be noted that the shielding has several peaks and nulls, corresponding to internal and external resonances of the enclosure, as well as frequency-dependent penetrations that occur in addition to the simple diffusive penetration of fields through the shield material.

1 Numbers in square brackets refer to the Bibliography.

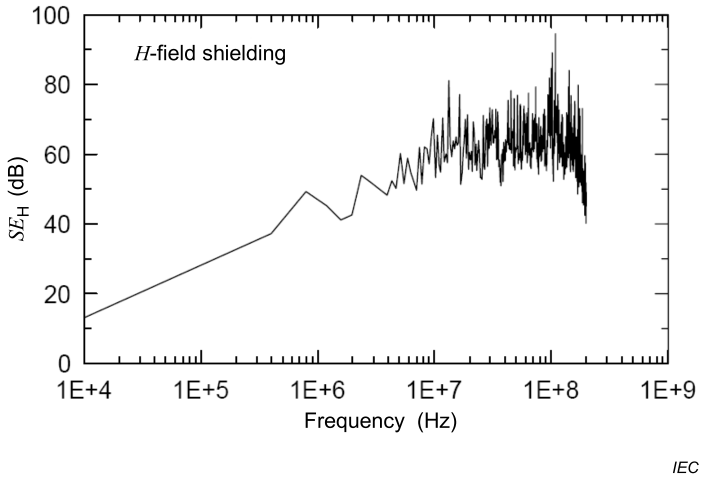

Figure 3 – Measured magnetic field shielding effectiveness SE_H for a building

4.2.2 Buildings

For a building such as that illustrated in Figure 4, the internal HEMP-induced response arises mainly from conductive and aperture-type penetrations. Thus, any test of the global enclosure shielding should strive to adequately excite these penetrations. The field penetration by diffusion through the building shield (i.e. the walls of the enclosure) is generally smaller than that of the conducting shield inside the walls.

The HEMP test concept for physically large buildings requires either the excitation by HPEM ultra-wideband (UWB), continuous wave (CW) signals simulating fields on the exterior of the test object (see the discussion of the various test interface locations in Figure A.1). For this excitation, the measurement of a suitable internal response induced by this external field is needed.

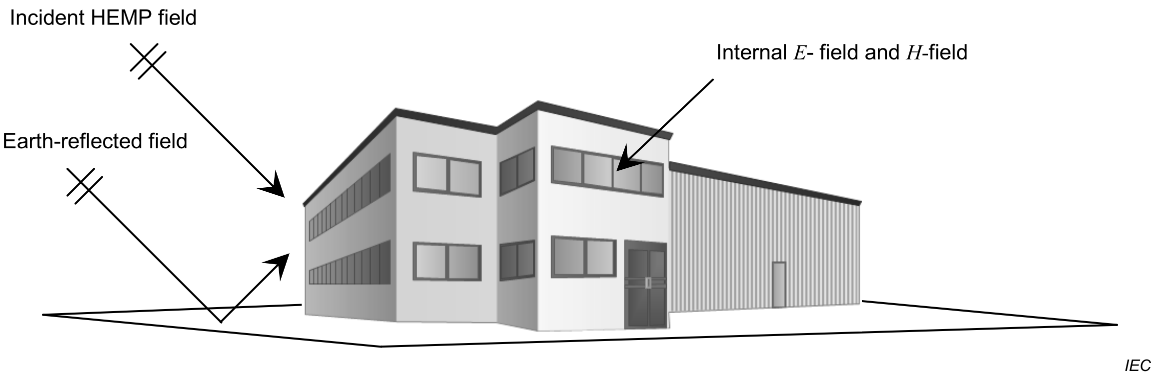

Figure 4 – Conceptual illustration of the HEMP test of a building

On the exterior of the building, the radiated or simulated HEMP excitation field is expressed by the following parameters (see IEC 61000-2-9):

– the incident field (plus ground-reflected field, if any) waveform characteristics (such as its amplitude, rise time, and fall time);
– the excitation field polarization;
– the amount of the system exterior illuminated by the radiated or simulated field.

Details of how this external field may be produced or approximated are presented in 5.2.

Different types of internal responses can be chosen to describe the shielding of the facility enclosure. These include the internal *E*- or *H*-fields or the induced voltage and current on internal conductors. Consequently, different measures for the shielding can be generated for any particular system. Moreover, the location of the internal observation point can vary, again giving rise to wide variations of shielding figures of merit.

4.2.3 Shelters and shielded rooms

For a shelter or a shielded room, it is assumed that the radiated HEMP environment is still being applied to the exterior of the enclosure where the incident HEMP fields are assumed to provide the main excitation to the structure. Consequently, the test concepts for these enclosures are similar to those for large buildings. These smaller enclosures can again be characterized by either

– a complex-valued field transfer function, or

– a shielding effectiveness.

It should be kept in mind, however, that there will also be transient signals conducted into this facility on conducting PoEs such as power lines and data lines, and these shall be addressed separately, as discussed in IEC 61000-5-3.

The main difference between large buildings without conducting shielded enclosures and shelters or shielded rooms is that the HEMP protection levels provided by these smaller enclosures will be significantly higher, since they are specifically designed to provide a high degree of shielding. Consequently, the internal signal levels are usually smaller than in the case of just buildings. This makes the measurements more susceptible to noise. In addition, due to the smaller size, the effects of internal cavity resonances will occur at higher frequencies. As a result, quasi-static shielding concepts are applicable over a wider range of frequencies for these enclosures (see IEC 61000-5-3).

Figure 5 illustrates a generic shielded room with several PoEs of the shielding barrier identified.

NOTE Power and signal conducting penetrations are not illustrated, as they are considered separately in IEC 61000-4-25.

Characterizing the overall barrier shielding by a field transfer function $T(\omega)$, or by shielding effectiveness SE, provides a global measure of the penetration effects from all of the penetration mechanisms indicated in Figure 5. That is to say, the internal fields arise from the penetrations from all of the PoEs taken together, along with the diffusion through the material in the walls of the shield. Other measurement techniques are available for characterizing the protection provided by the individual penetrations (such as the gasket, air vent, shielded conduit, etc.) and these are discussed in 4.4.

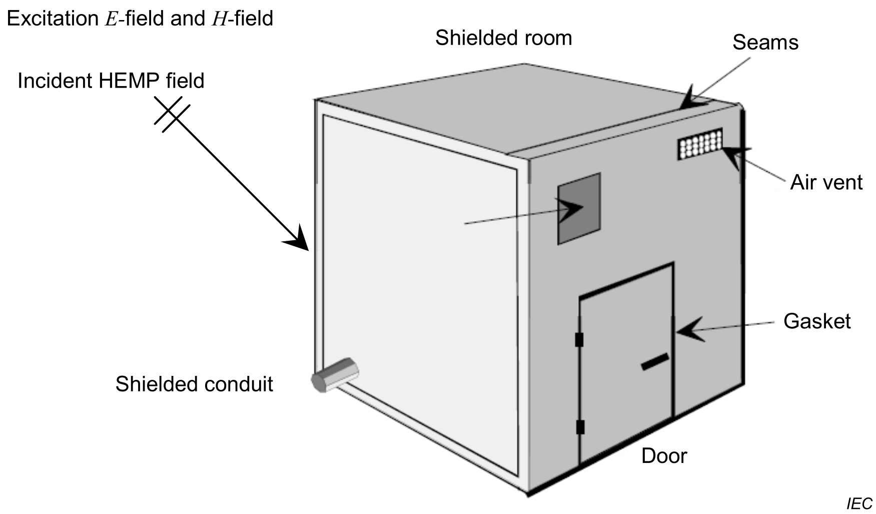

Figure 5 – Illustration of a shielded room or enclosure excited by HEMP fields

4.2.4 Cabinets, racks and boxes

These enclosures are typically located within an existing EM barrier, which significantly modifies the electromagnetic field environment exciting the system. An internal box or an equipment cabinet is excited by a combination of the internal EM field plus injected currents on cable shields coming from other equipment that have also been excited by the local fields. This is illustrated in Figure 6.

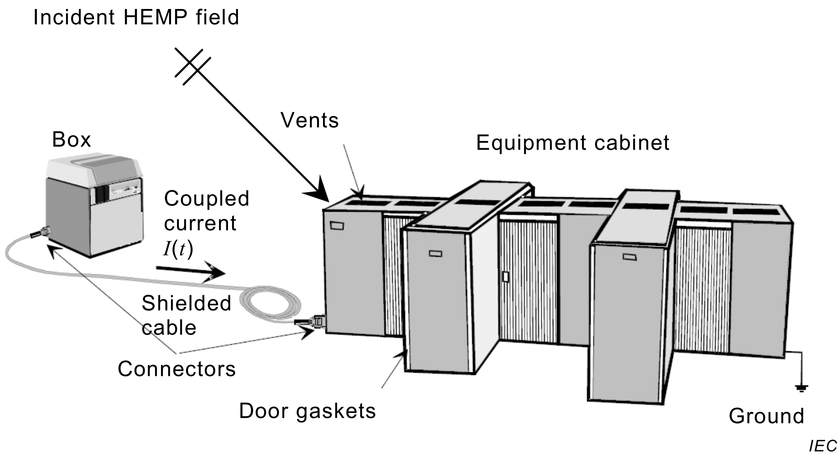

Figure 6 – Illustration of equipment racks, cabinets and box excited by internal HEMP disturbance

Field illumination test

For tests of these enclosures involving the EM fields inside a larger enclosure, the previous concept of field illumination can be adopted to measure the global shielding provided by the equipment. As before, this shielding may be characterized by

– a complex-valued field transfer function, or

– a shielding effectiveness of the enclosure.

Due to the smaller size of these enclosures, however, difficulties in this measurement can arise from the dense internal packing of internal electronic components. Often this makes it difficult to locate suitable EM field sensors inside the box. Furthermore, because the testing is conducted on the box or enclosure surface, there are large uncertainties in the characterization of the HEMP field environment. Finally, the interconnection between the various equipment items can be rather complex, and if a single box or equipment rack is tested, its measured response may be considerably different from that found when it is connected to the rest of the system.

Shield transfer impedance

An alternative to the field testing of boxes and small enclosures is to use the concept of a transfer impedance of the enclosure (see Annex E). This is similar to the treatment of a shielded cable discussed in 5.3, and involves testing at a box level interface in the system. In this case, a current $I(t)$ is injected onto the surface of the box or rack, and an open-circuit voltage $V_{\text{oc}}(t)$ on a suitable internal sense wire is measured. In this form of testing, it is important to ensure that the injected current flows over the exterior of the box in the same way as when the box is connected to the rest of the system. This implies that the current exit point (the ground connection) has to be maintained so that the injected current can be removed properly.

Figure 7 illustrates a general shielded enclosure excited by an external current injection. Just inside the shell at points a and b, a sense wire is connected to the shield, and the open-circuit voltage V_{oc} is measured. The transfer impedance of this enclosure is a complex valued quantity, defined in terms of the frequency domain spectral components as

$$Z_{\text{t}}(\omega) = \frac{V_{\text{oc}}(\omega)}{I(\omega)} \qquad (3)$$

where

$I(\omega)$ is the injected current, and

$V_{\text{oc}}(\omega)$ is the measured open-circuit voltage on the sense wire.

This shield transfer impedance value varies, depending on the location of terminals inside the enclosure for determining the open-circuit voltage. For adequate sensing of the shielding provided by the entire enclosure, the voltage sense points should be located within the enclosure, near the current injection locations.

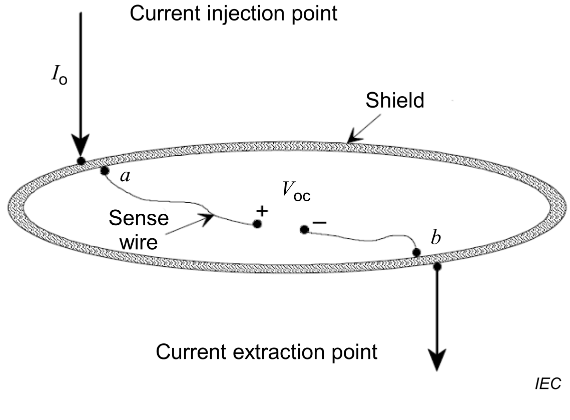

Figure 7 – A general shield excited by current injection

The shield transfer impedance is a function of the electrical properties of the shielding material, as well as the shield dimensions and the nature of any imperfections in the enclosure such as seams, apertures, etc. In the special case of a thin spherical shield in which there are no aperture penetrations, it is possible to calculate the H-field shielding effectiveness SE_{H}, given the shield transfer impedance and the d.c. resistance of the shield through the relationship:

$$SE_{\mathrm{H}} = 20\log_{10}\left|\frac{\left(\frac{a}{\Delta}(\gamma\Delta)^2\right)}{3\frac{Z_{\mathrm{t}}}{R'}}\right| \qquad (4)$$

where

a is the radius of a thin spherical shield (in m);

Δ is the thickness of the shield (in m);

γ is the propagation constant in the shielding material, given by $\gamma \approx \sqrt{j\omega\mu\sigma}$;

σ is the electrical conductivity of the shield material (in S/m);

Z_{t} is the shield transfer impedance (in Ω/m);

R' is the per unit length d.c. resistance of the shield (in Ω/m).

4.3 Testing of shielded cables and connectors

4.3.1 General

Shielded cables are frequently used to transmit information between equipment contained within two protective enclosures. As such, one can define two distinct transmission lines: an external line having currents and charges flowing on the exterior of the cable, together with a possible ground-plane return, and an internal line consisting of the conductors inside the shield. HEMP fields can excite the external transmission line, and if the cable shield is imperfect, some of the external currents and charges can penetrate through the shield and excite the internal line. This leads to an unwanted response in the "protected" equipment. In 4.3, test concepts for this coupling mechanism are examined.

Annex B summarizes important aspects of the characterization of a cable shield. This involves two parameters: the shield transfer impedance and the transfer admittance. For most practical cable shields, the transfer impedance is a complex valued, frequency-dependent function, described by real and imaginary parts, or equivalently, by a magnitude and phase function. The transfer admittance, however, is primarily reactive, and is effectively modelled by a frequency independent capacitance.

While the transfer impedance is a function of the shield properties only, the transfer admittance depends on both the shield and the configuration of the external transmission line. It is possible, however, to present the measured transfer admittance parameter in another form: that of the shielding leakage parameter, which is independent of the external circuit. Subclause 4.3.2 considers test methods for the transfer impedance and admittance quantities, keeping in mind that the latter quantity depends on the details of the external circuit, such as the external line height, wire radius, and nature of the local ground plane near the cable.

4.3.2 Testing of cable shields

4.3.2.1 Determination of the transfer impedance

Although there are several different test configurations for measuring the transfer impedance of a cable shield, they are all related to the basic configuration shown in Figure 8. An external voltage source V_{s} feeds the x = 0 end of a cable shield of length L which is connected to the ground (i.e. the reference conductor) through a short-circuit at the opposite end of the cable. The resistance Z_{s} at the source limits the current flowing in the cable exterior.

The inner (coaxial) conductor of the shielded cable is shorted to the shield at the $x = L$ end of the line, and the open-circuit voltage, V_{i}, is measured at the x = 0 end. Under the assumptions that

– the internal and external transmission lines are electrically short ($L << \lambda$), and

– that there is negligible field excitation of the inner cable due to fields entering through the ends of the line,

the frequency-dependent transfer impedance of this cable shield can be approximated from Equation (B.8) as

$$Z_t'(\omega) = R_t'(\omega) + jX_t'(\omega) \approx \frac{V_i}{I_e L} \approx \frac{Z_s}{L} \frac{V_i}{V_s} \ \Omega/\text{m} \quad (5)$$

where

Z'_t is the cable transfer impedance (in Ω/m);

ω is the angular frequency (in 2π × Hz);

V_i is the open-circuit voltage on the internal conductor;

I_e is the open-circuit current on the shield;

V_s is the excitation voltage of the external circuit of the cable shield (in V);

L is the length of the shield conductor (in m);

Z_s is the effective source impedance of the external voltage source (in Ω).

When using these expressions, it is very important to ensure that the line is electrically short. As the frequency increases, the current distribution on the exterior cable begins to have periodic nulls and peaks due to reflections from the shorted end of the line. Moreover, there are internal reflections from the short on the interior cable. These oscillations are the cause of significant errors in the measurement of transfer impedance at high frequencies.

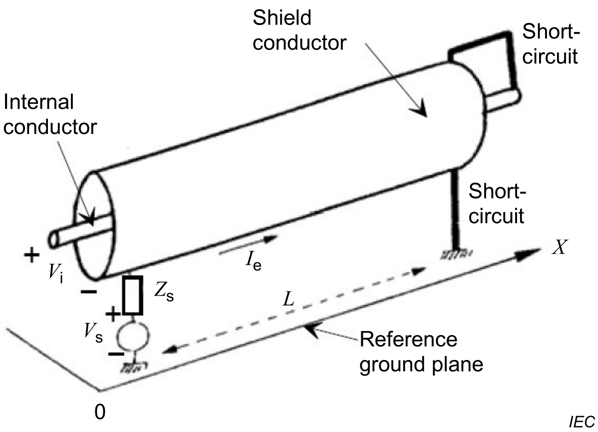

Figure 8 – Basic configuration for transfer impedance measurement

Figure 8 illustrates the typical frequency domain behaviour of the measured transfer impedance for four different braided cables having reasonably good shielding. At low frequencies, Z'_t is primarily resistive, with a value equal to the per-unit-length d.c. resistance of the shield. At higher frequencies, the field penetration through the apertures in the braid of the shield begins to affect the internal response and the shielding behaviour is slightly degraded. Accompanying this increase in transfer impedance at high frequencies is an electrical phase variation – a quantity that it is essential to know if any detailed calculations are to be performed using the measured Z'_t.

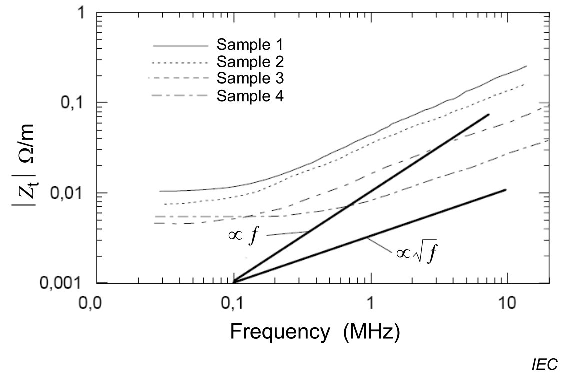

a) – Magnitude

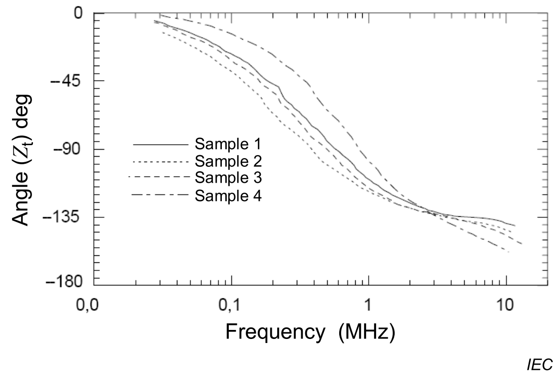

b) – Phase

NOTE At high frequencies the curves are proportional to $\sqrt{f}$ rather than f, which indicates that responses are not well represented by a simple inductance.

Figure 9 – Measured transfer impedance magnitude and phase of transfer impedance per unit length for four braided shield cables with good shielding properties

4.3.2.2 Determination of the transfer admittance

The evaluation of the transfer admittance of the cable shield utilizes the general test configuration shown in Figure 10. This is similar to the configuration for the transfer impedance measurements, but with different terminations at the cable ends. Using Equation (B.9), together with the same assumptions as for the transfer impedance, the transfer admittance of the shield can be expressed as

$$Y_t' \approx -\frac{1}{L}\frac{I_i}{V_s} \approx -j\omega C_i' C_e' S \text{ S/m} \tag{6}$$

where

Y'_t is the cable transfer admittance (in S/m);

I_i is the internal conductor current (in A);

V_s is the excitation voltage of the external circuit of the cable shield (in V);

L is the length of the cable (in m);

ω is the angular frequency (in $2\pi \times$ Hz);

S is the shield leakage parameter (in m/F);

C'_i is the internal per-unit-length capacitance of the coaxial cable (in F/m);

C'_e is the external per-unit-length capacitance of the coaxial cable (in F/m).

Thus, a measurement of the internal conductor current arising from the external source voltage provides the transfer admittance. Under the approximation that Y'_t is purely reactive, the shield leakage parameter can be determined, if the internal and external per-unit-length capacitances of the coaxial cable are known. The parameter S is a single, real-valued number, and depends only on the characteristics of the braided cable. Hence, it is a useful descriptor for cable shields.

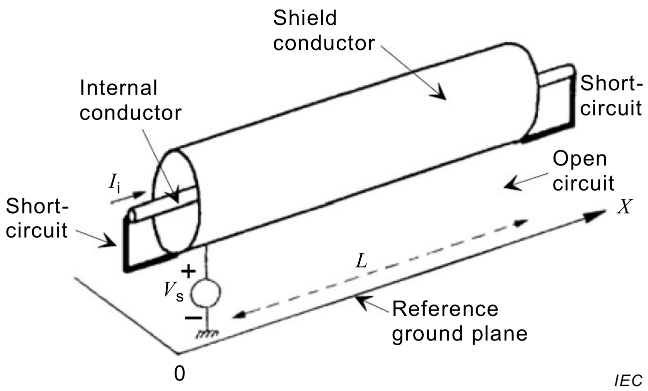

Figure 10 – Basic configuration for transfer admittance measurement

4.3.3 Testing of cable connectors

Connectors on shielded cables are often more important in determining the overall shielding of the cable system than is the cable shield. This is because the connector introduces an interruption to the shield, and, as such, presents an imperfection in the shielding topology. One way to represent the effects of the connector (as seen by the internal, or shielded, transmission line circuit) is by using discrete voltage and current sources at the location of the connector. The strengths of these sources are related to the external current and voltage on the connector multiplied by discrete transfer impedance and admittance parameters representing the connector, much as in the case of the distributed cable shield penetrations.

As in the case of a braided shield, the lumped transfer impedance of a connector contains both a resistive and reactive part, and the transfer admittance of a connector is primarily capacitive. However, cable connectors are always designed so that there is very small E-field penetration through the device. Consequently, the transfer admittance effects of the connector are almost always much lower than the effects from the transfer impedance. Usually, the lumped transfer impedance parameter is the only one required.

The test configuration for cable connectors is similar to that for the cable shield transfer impedance discussed previously. Figure 11 illustrates the general test configuration for such measurements. The same requirements for the test equipment for the cable shield test are required here, and the construction of the outer shield shall be such that it is a much better shield than the connector. This implies that a solid shield is preferable to a braided shield for this measurement.

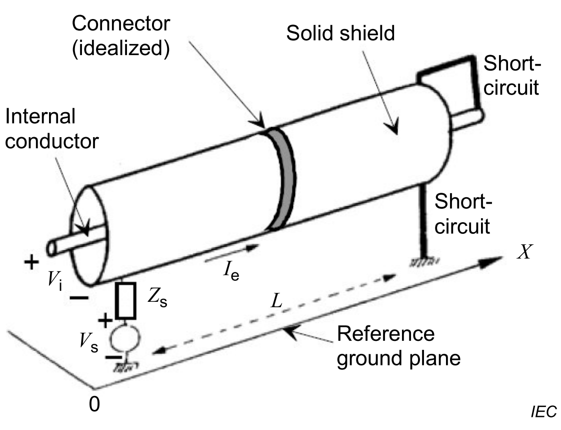

Figure 11 – Test configuration for transfer impedance measurement of a cable connector

Given a measurement of the internal open-circuit voltage, the transfer impedance of the connector is determined by the expression

$$Z_{\mathrm{t}}(\omega) = R_{\mathrm{t}}(\omega) + jx_{\mathrm{t}}(\omega) \approx \frac{V_{\mathrm{i}}}{I_{\mathrm{e}}} \approx Z_{\mathrm{s}} \frac{V_{\mathrm{i}}}{V_{\mathrm{s}}}\ \Omega \tag{7}$$

where

V_{i} and V_{s} have been defined in 4.3.2.1,

Z_{t} is the transfer impedance of the connector (in Ω), and

Z_{s} is the impedance of the external circuit (in Ω).

It should be noted that while the length of the cable, L, does not appear explicitly in this expression, it is necessary that $L << \lambda$. Thus L should be as short as possible to maximize the frequency range of validity for the measurements.

4.4 Testing of shielding materials

4.4.1 General

Imperfections in the shielding topology of a system can often be protected by using localized methods such as gaskets (on seam or between doors and their jambs), conducting sheets or screens (covering apertures), and other specialized measures like honeycombs and waveguides beyond cut-off. Characterizing these protection measures is less obvious because their behaviour depends not only on their individual electrical composition, but also on how the devices are connected to the shielding topology. For example, a very long crack might be protected by filling it with a conducting material. This could be effective in protecting against currents flowing across the crack: the conducting material lets the current pass over the crack without much distortion and the H-field on the shielded side is minimized. However, for currents parallel to the crack, the presence or absence of the protective filling is unimportant. The current is not significantly affected by the slit, and any protection against this current component is unnecessary.

In describing tests suitable for these components, therefore, an attempt is made to characterize the intrinsic shielding property of the protection device, independently of how it is used in a particular installation. This means that a particular component might be classified as a "good" protective device in one installation, but due to the particularities of how it is used in another facility, considered to be a "poor" component in another installation. Evaluating the global behaviour of a system, together with all of its protection devices, is the role of system level testing, a subject which is beyond the scope of this standard.

4.4.2 Conducting gaskets

Figure 12 shows several configurations of a conducting gasket serving as a HEMP protection device. The basic mechanism for protection is that the gasket forms a conducting path between the two parts of the enclosure; this keeps current and charge from "leaking" into the inside (i.e. into the protected region). Each of the three configurations in the figure has a different shielding behaviour, due to the differences in the geometry of the enclosure walls that surround the gasket.

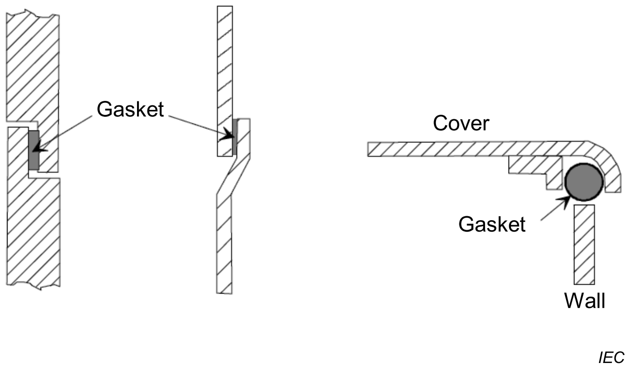

Figure 12 – Examples of conducting gaskets used as HEMP protection devices

A simple yet general circuit model for a gasket seal can be made by noting the important parts of the geometry in Figure 12. Current flowing from one conductor to another has to pass through the gasket and this will present an electrical resistance to the current. Similarly, the flat plates on either side of the gasket appear locally as a capacitance through which a displacement current can flow. Finally, the metal conductors of the two walls form an inductance in this circuit.

Figure 13 shows the equivalent circuit representation of such a gasketed opening. The resistance of the gasket and the capacitance of the gasket opening appear in parallel, and this combination is in series with the inductances representing the current paths through the walls of the enclosure. Specific values for L and C depend on the local geometry of the seal, whereas the value of R depends on both the geometry and on the intrinsic electrical properties of the gasket material.

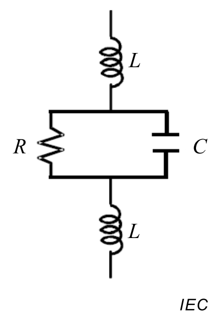

Figure 13 – Circuit model representing the behaviour of a conducting gasket for HEMP protection

These circuit values can be measured or calculated using simple models for the specific shape and geometry under consideration for a given problem. For characterizing the electrical properties of the gasket material, however, measurements of electrical resistivity of the gasket material can be used. This quantity is independent of the surroundings of the gasket and can be used to rank the effectiveness of one type of gasket with another. It should be noted, however, that such gaskets are usually made of flexible material, and, therefore, their characteristics are dependent on contact pressure as in all examples of Figure 12. The age of gasket materials is also a factor.

Figure 14 illustrates the measurement configuration for the resistivity. This is the four-electrode method, and it is specially designed so that measurements of materials with very low resistivities can be made. For this measurement, a block of the gasket material is sandwiched between two electrodes made from copper or another highly conducting material. An external d.c. voltage source is connected across the two outer electrodes and a current is allowed to pass through the electrode. The resulting voltage drop across the sample is measured using a high input impedance voltmeter, so as not to disturb the current flow in the sample. With these parameters measured, the d.c. resistivity of the sample material is given by the expression:

$$\rho_{DC} = \frac{V_s}{I_o} \frac{A}{L} \quad \Omega{\cdot}m \tag{8}$$

where

ρ_{DC} is the d.c. resistivity of the sample material in ($\Omega{\cdot}$m);

A is the cross-sectional area of the gasket material (in m^2);

L is the thickness of the gasket sample (in m);

I_o is the current passing through the sample (in A);

V_s is the voltage drop across the sample (in V).

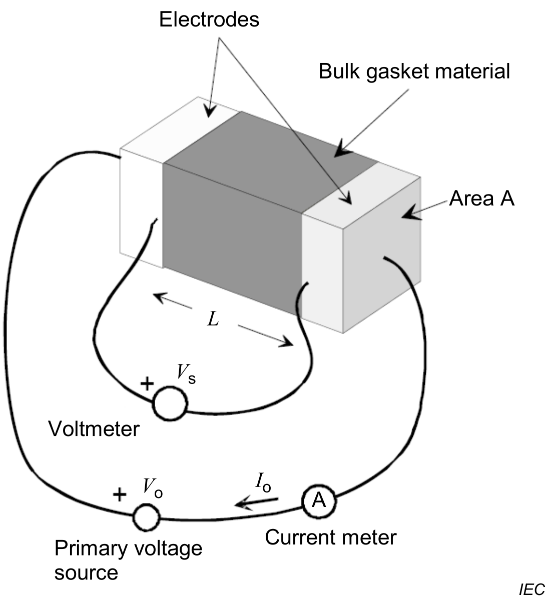

Figure 14 – Measurement configuration for the resistivity of a sample

Similar measurements can be made at higher frequencies and a frequency-dependent gasket impedance can be measured. However, this quantity is of limited use, because its frequency variations are easily confused with those of the gasket-mounting hardware and surroundings. Consequently, the d.c. resistivity is the most commonly used parameter for characterizing the gasket material.

4.4.3 Conducting sheets and screens

4.4.3.1 General

Conducting screens or sheets of conducting material are often used to limit the HEMP penetration through apertures in the shield. Such protection devices include

– wire mesh screens;
– conductive paint coatings;
– vacuum metallized coatings;
– flame/arc sprays;
– metallic foils lining equipment bays;
– metallic fillings added to plastic enclosures.

As in the case of gasketing material, it is possible to characterize these protection devices either by measurements of their shielding behaviour as installed in a specific topological configuration, or by an alternate measurement of some intrinsic electrical property of the shielding material. While this latter measurement may not accurately indicate how the protection device will function in an arbitrary installation, it does provide a useful technique for distinguishing between one protection material and another in a self-consistent manner. Two test concepts for conducting aperture protective devices are discussed in 4.4.3.2 and 4.4.3.3: one which measures the resistivity of the conducting material, and another which measures the shielding effectiveness of the material used for shielding under controlled conditions.

4.4.3.2 Measurement of material resistivity

The resistivity of the material comprising the protective cover of an aperture is one parameter that may be used to characterize its shielding. As in the case of the conducting gasket described in 4.4.2, the resistivity of a conducting sheet can be determined using the test configuration shown in Figure 14. An alternative approach is to use a measurement technique in which the d.c. resistivity is measured with probes located on the surface of the sample as indicated in Figure 15.

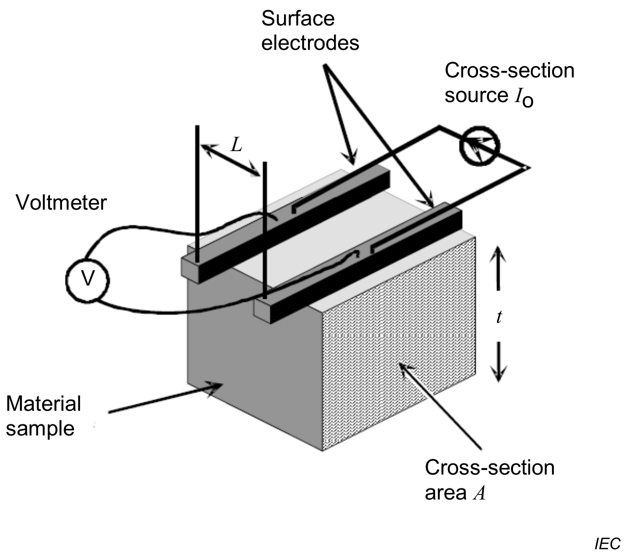

Figure 15 – Test concept for measuring the resistivity with surface probes

In this test, a constant d.c. current source I_o is connected to two electrodes separated by a distance L and in good electrical contact with a block of conducting material. In response to this current, a voltage V_s is induced across the two electrodes. This voltage may be measured by a high impedance voltmeter and the resistivity is again given by the expression in Equation (8). The same expression is used in the present case, because it is assumed that the block is a good conductor and the current tends to flow uniformly across the cross-sectional area A of the material from one electrode to the other.

It is important to note that this measurement procedure is applicable only at low frequencies where the skin depth of the material in question is very large compared to the thickness of the sample. If the frequency of the current source were allowed to increase, the skin depth (given by $\delta = \sqrt{\rho/(\pi f \mu)}$) decreases and, at some point, begins to be comparable with the thickness of the material under test. At this point, the details of the current distribution in the conductor cross-section shall be taken into account, as discussed in Annex E.

As noted in Annex E, both the surface impedance (relating the tangential E-field outside the protective barrier to the excitation surface current) and the transfer impedance (relating the tangential E-field inside the protective barrier to the excitation surface current) may be calculated (see Equations (E.14) and (E.18)), once the material resistivity is known. Thus, the d.c. measurement of the resistivity can be used to infer the shielding properties of the material for higher frequencies.

4.4.3.3 Shielding effectiveness measurements

A more direct approach for characterizing the shielding behaviour of a wire mesh or conducting screen is to measure its shielding effectiveness under standard conditions. It is well known that in the near field (or equivalently, for low frequencies), the electric and magnetic fields penetrate into a conductor differently. Consequently, a shield shall be characterized in general by two different shielding effectiveness parameters. For far-field shielding, where the incident field on the shield is a plane wave, the two shielding effectiveness values become equal, and this single value may be used to characterize the protection.

Figure 15 illustrates a measurement concept for the plane-wave shielding effectiveness of screens and sheets. Figure 15 a) shows the ideal situation, in which a plane wave is incident upon an infinite screen. The shielding of this screen can be characterized by the following equation (see Equation (2)):

$$SE_{\mathrm{A}} = 20\log_{10}\left(\frac{|A_{\mathrm{out}}|}{|A_{\mathrm{in}}|}\right)\,\mathrm{dB} \tag{9}$$

where

A_{out} represents the principal component of the incident field E^{inc} (or H^{inc}) at an observation point with the conducting screen removed;

A_{in} is the same component of the field that is transmitted through the screen: E^{tr} (or H^{tr}).

The resulting shielding effectiveness depends on the angle ψ that the incident field makes with the normal to the sheet. Normally, the angle ψ = 0° is chosen for defining the shielding properties of the infinite plane.

For actual measurements, the idealized configuration of Figure 16a) cannot be realized, due to the fact that the source producing the incident field is not of infinite size, nor is it infinitely far from the screen. Moreover, the screen is not infinitely large. This implies that the measurements made using the test configuration in Figure 16b) can be different from those expected from a theoretical treatment of the infinite plane geometry, due to the following effects:

– the non-plane-wave nature of the incident fields from the source;
– the radiation pattern from the source;
– diffraction from the edges of the screen.

To minimize this difficulty, it is common to require the following conditions to be maintained in the measurement configuration:

– the size of the screen $a >> \lambda$;
– the observation and source positions d_{o} and $d_{\mathrm{s}} < a$;
– = 0° (normal incidence).

With these assumptions, an approximation to the plane-wave shielding effectiveness of the screen is obtained by making two measurements of the selected primary field components at the observation location. The first measurement is with the plate removed and is denoted as $E^{\mathrm{m}}_{\mathrm{removed}}$ (or $H^{\mathrm{m}}_{\mathrm{removed}}$). The second measurement is the same field component with the plate in place in front of the radiator, and is denoted as $E^{\mathrm{m}}_{\mathrm{covered}}$ (or $H^{\mathrm{m}}_{\mathrm{covered}}$). The shielding effectiveness for this configuration is then evaluated as

$$SE = 20\log_{10}\left(\frac{\left|E^{\mathrm{m}}_{\mathrm{removed}}\right|}{\left|E^{\mathrm{m}}_{\mathrm{covered}}\right|}\right)\ \mathrm{dB} \tag{10}$$

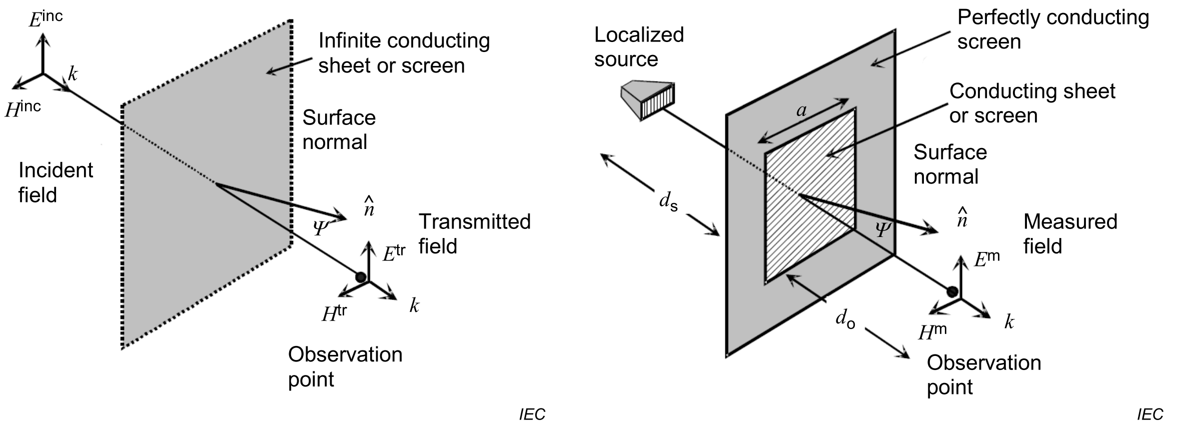

a) **Idealization** b) **Experimental realization**

Figure 16 – Concepts for shielding effectiveness measurement of conducting sheets and screens

As an example of the plane-wave shielding effectiveness of a plate of different material, Figure 17 presents calculated data for copper, aluminium and iron sheets, each having a thickness of 0,01 mm. Similar results are expected for materials having other conductivities.

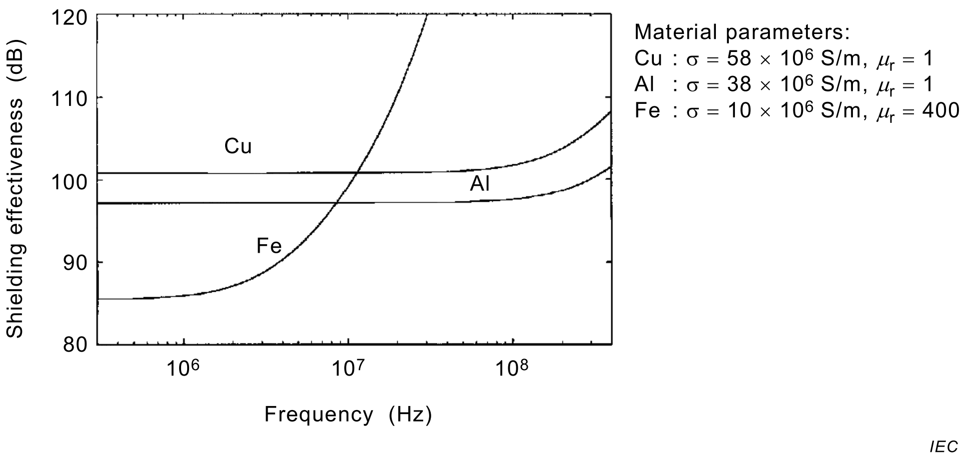

Figure 17 – Example of the calculated plane-wave shielding effectiveness of a 0,01 mm thick plate of different material as a function of frequency

4.4.4 Cut-off waveguides and honeycombs

Another type of HEMP protection measure is to use one or more cut-off waveguides or honeycomb structures in a conducting wall, as illustrated in Figure 18. This permits the easy flow of air or other non-conducting material in and out of an enclosure, while at the same time providing large attenuation to the EM field environment. The test concept for this penetration protection method is identical to that for the conducting mesh or screen shown in Figure 15.

As before, the waveguides or honeycomb protection shall be located in a highly conducting wall, and shielding effectiveness measurements shall be made with and without the wall present, as described in 4.4.3.

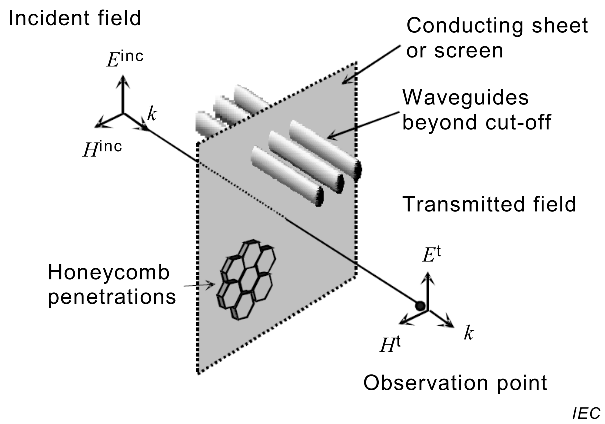

Figure 18 – Cut-off waveguides and honeycomb used as protective elements

4.5 Summary of test concepts

A number of different test concepts have been presented in Clause 4 for different aspects of shielded systems. Table 1 summarizes the recommended test concepts for the different system components. In selecting the various tests, it is important to realize that there is never a "best" test for a system. Each test has its strong points and its flaws. Each test has uncertainties and errors in the result, for example test object and measurement equipment interaction, test object variability, uniformity of fields, non-linear effects and measurement errors. In selecting a test, therefore, the user should carefully consider the following requirements for the proposed test:

– why is the test being conducted?
– is the test really necessary?
– what is the expected result from the test?
– what is the required accuracy of the test results?

Answers to these questions will serve to put the various test procedures into better perspective and will allow the user to select the proper test and minimize the cost of the testing.

Table 1 – Recommended test procedure for different test objects

Test object	Test procedure						
	Full- & reduced scale transient illumina-tion	Full-scale CW illumination	TEM cell simulation	Small simulator pulse excitation	Local excitation of PoEs	Current injection testing	Specialized test fixtures
Buildings	a	b	-	-	c	-	-
Shielded rooms	a	b	-	-	c	c	-
Equipment enclosures	-	-	a	a	b	c	-
Apertures	-	-	-	-	a	b	c
Gaskets and seams	-	-	-	-	b	a	c
Cable and conduit characterization	-	-	c	c	-	b	a

[a] Recommended test concept(s).

[b] Back-up test concept.

[c] Test of last resort.

5 Test methods for measuring the shielding effectiveness of HEMP protection facilities

5.1 General

Because of the diverse ways to simulate the effects of HEMP on a system, there is a wide variety of facilities, equipment configurations, and procedures that can be used to perform tests on protection devices. Clause 5 summarizes test procedures for each of the test concepts presented in Clause 4.

5.2 Electromagnetic field testing

5.2.1 General

As noted in the interaction sequence diagram of Figure A.1, testing can be done either by generating the excitation E- and H-fields at a testing interface within the system, or by simulating the effects of these fields interacting with the system barriers by injecting appropriate current and charge on the surfaces. Subclause 5.2 discusses simulation methods for the field excitation of the system under test.

5.2.2 Pulse field testing

5.2.2.1 Full-scale system illumination

Full-scale pulse testing is most suitable for performing a high-confidence, system-level assessment. Because it is capable of providing much more information about the system response to HEMP, it is seldom used to evaluate only the shielding behaviour of a single protective element of the system, such as the outer shielding barrier.

The incident HEMP fields are typically produced by a capacitive discharge MARX generator which stores energy in capacitor banks over a period of several minutes and then discharges the energy in a time of the order of several nanoseconds into a physically large radiating structure (typical dimensions being of the order of 50 m to 100 m). The radiating structure can behave like a waveguide to conduct the fields to the test object, or it can behave like an antenna radiating in free space. In either case, the test object is illuminated by a transient HEMP field and it responds in the appropriate manner. Typically, the test object should not be greater than one-third to half the height of the working volume of the simulator so as to minimize the plate interaction and to better approximate free-space conditions. Figure 19 illustrates several example types of full-scale simulators. Alternative types of simulators having different properties can also be considered.

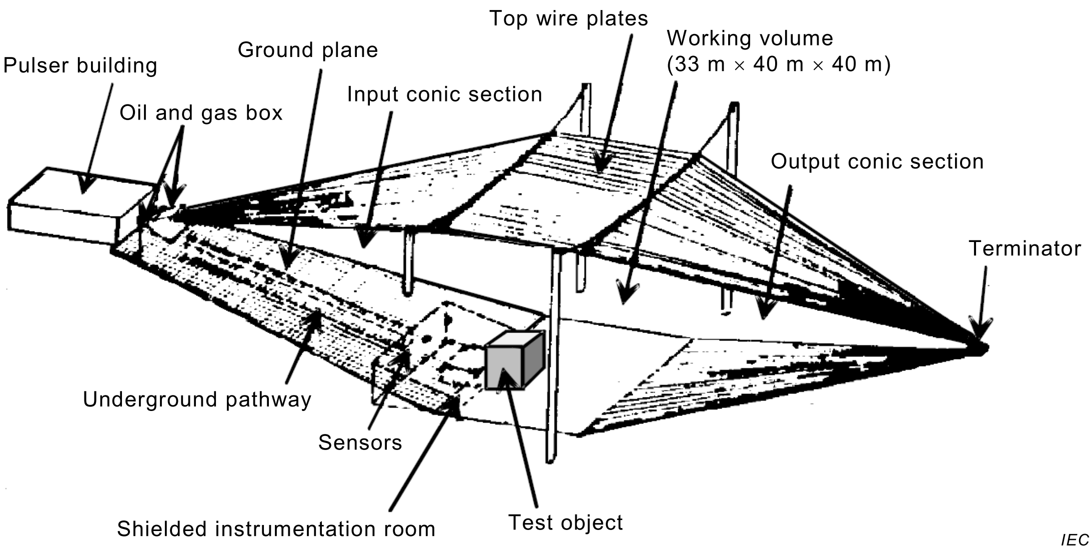

a) Vertically polarized, bounded-wave simulator

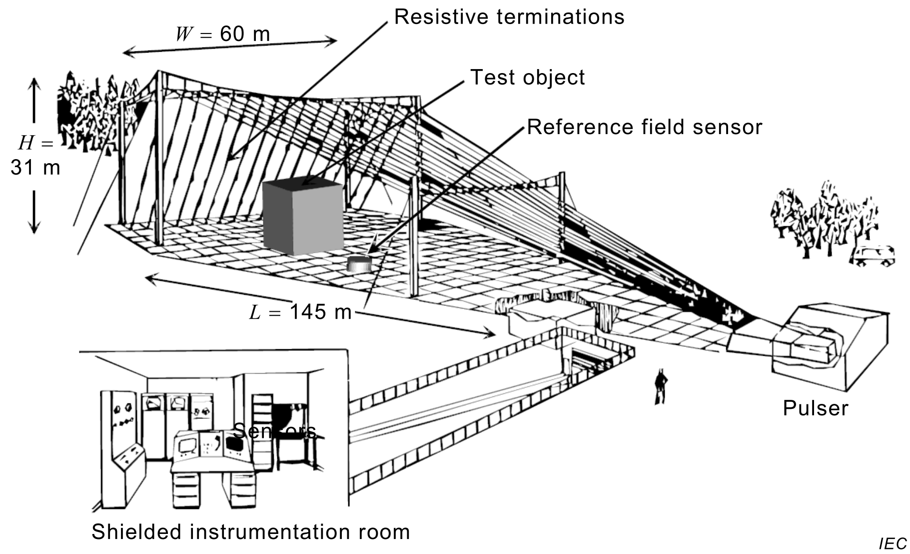

b) Alternate configuration for a vertically polarized, bounded-wave simulator

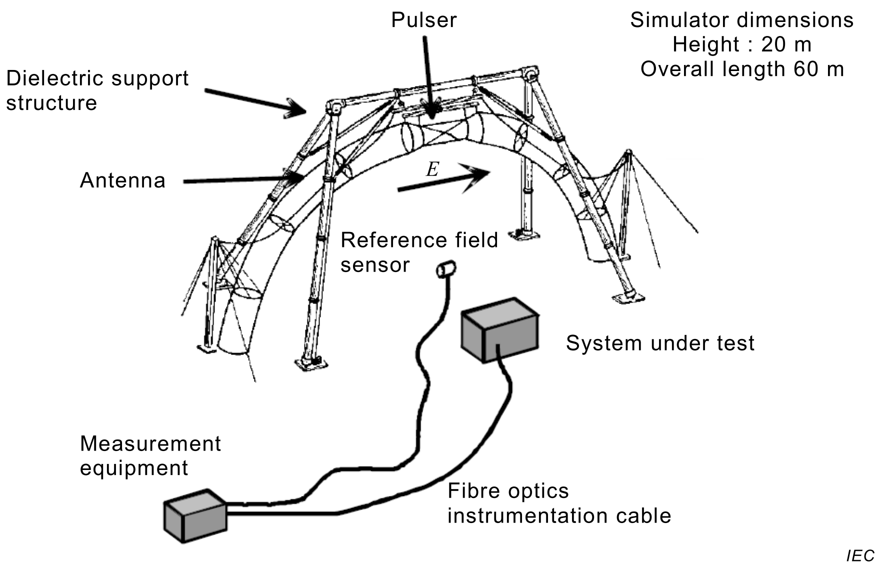

c) Horizontally polarized radiating simulator

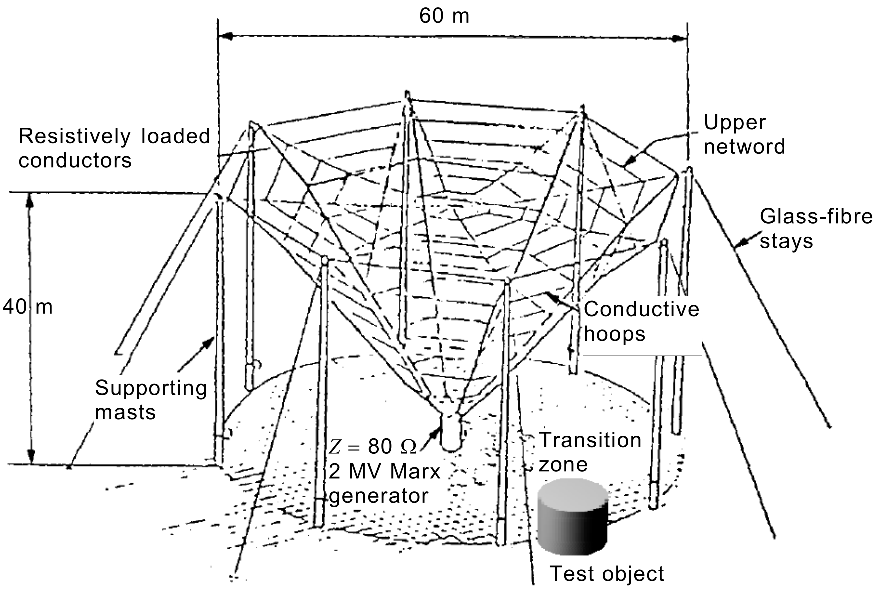

d) Vertically polarized radiating simulator

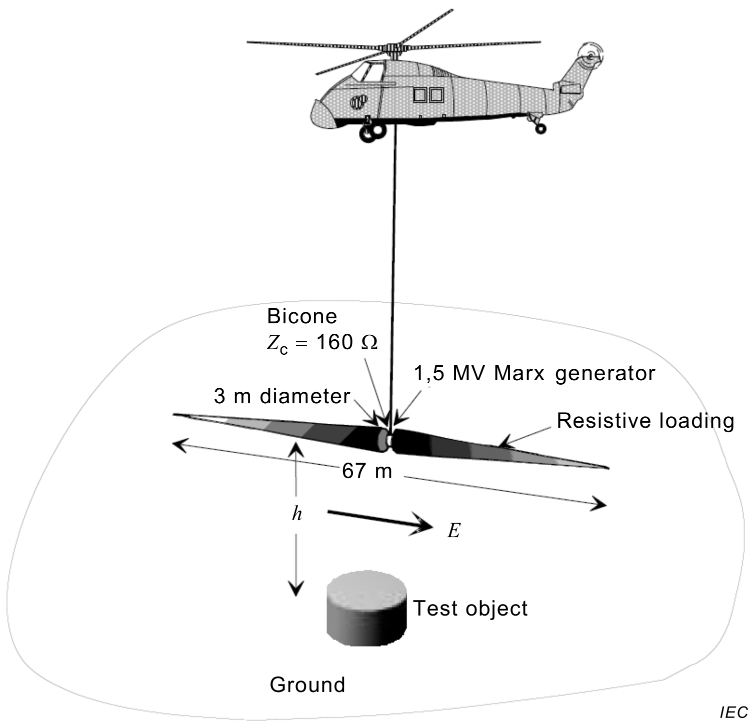

e) Airborne horizontally polarized radiating simulator

Figure 19 – Examples of full-scale, pulse-radiating HEMP simulators

Test set-up

Figure 19b) illustrates the typical test set-up for this type of HEMP testing. The test object is located in the "working volume" of the simulator. A reference field sensor is located in the working volume at a location where it will not be severely affected by the scattered fields from the test object. (The manufacturer of the facility will usually provide information as to the optimum locations of the working volume and reference sensor.)

The test object is instrumented according to the goals of the particular test. This involves placing E- or H-field probes, current probes or voltage probes at pre-selected points within the system, and connecting these to the data acquisition computer by means of the non-conducting fibre optic cables. Depending on the test objective, the test object configuration may involve connections to the power mains and to other connected equipment, which can affect the test results.

Control of the pulser and the data acquisition system is carried out in an equipment room which is located under or near the simulator structure. It should be designed so that it does not interfere with the simulator fields, and it is usually shielded so that the simulation fields do not adversely affect the data recording and processing equipment.

Test equipment

Aside from the basic simulator facility needed to simulate the HEMP environment, the following types of equipment are needed for this type of testing:

– E- and H-field reference sensors for measuring the transient excitation simulator fields;
– E- and H-field sensors for measuring fields within the system under test;
– current and voltage sensors for measuring internal wire responses;
– calibration equipment for all sensors;
– fiber optic transmitters, receivers and cable for data extraction;
– transient digitizers for each data channel (rise time of 1 ns);
– data acquisition computer and mass storage medium;
– data processing computer and plot capability.

Details of these equipment items are provided in Annex C.

Test procedure

This is a transient test: the pulser is fired and the transient response of the system is measured with the waveform digitizing equipment. If this test is used to characterize the first layer of shielding of the system, as defined in Annex A and in Clause 4, it is necessary to convert the measured transient responses into the frequency domain to evaluate the system transfer function $T(\omega)$ or the shielding effectiveness, SE. Figure 20 summarizes the steps in this test procedure. It should be noted that after the response ratio $R(\omega)/F(\omega)$ has been computed, corrections to the transfer function may be needed. This situation arises when the design of the simulator is such that the spectrum $F(\omega)$ has a very small value at certain frequencies. At these frequencies, the response $R(\omega)$ is dominated by noise and the ratio can have a large pseudo-resonance.

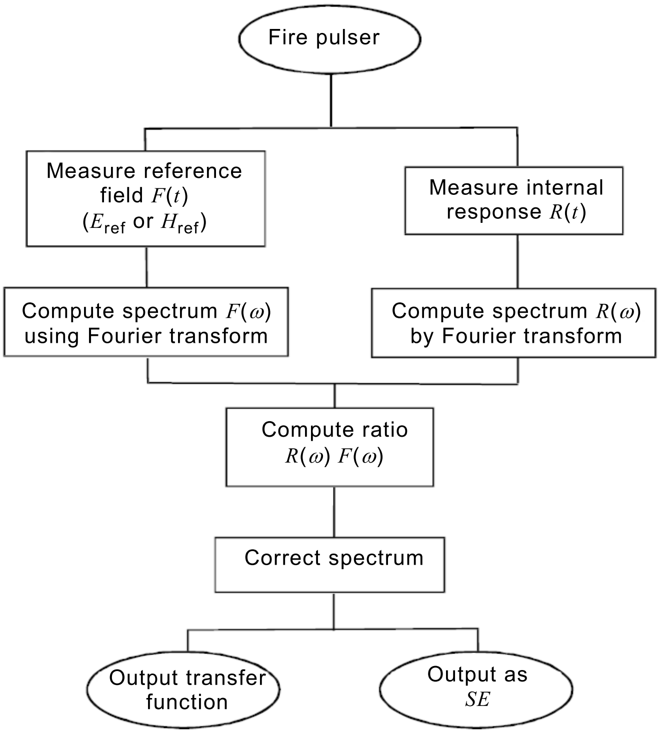

Figure 20 – Test procedure for the pulse test

It is important to realize that HEMP can arrive with different angles of incidence relative to the test object. Therefore, the test procedure in Figure 20 should be carried out for different polarizations of the excitation field (if permitted by the simulator) and with different orientations of the test object.

5.2.2.2 Small HEMP simulators

Smaller versions of the full-scale transient HEMP field simulators discussed in 5.2.2.1 are often found in university laboratories, research organizations and manufacturing companies. These simulators are similar to their larger counterparts, with the exception that entire systems cannot be tested, due to the small working volume. Usually, these simulators are used to test individual boxes, small cabinets or cables.

The small size of these simulators provides a benefit in that the rise times of the fields are usually faster than in the larger, full-scale simulators. However, the peak voltages of the pulser, and consequently the peak E- and H-field strengths, are limited by the dielectric breakdown characteristics of the air near the feeding section.

The test equipment, test set-up and procedures for these small-scale simulators are the same as indicated in 5.2.2.1.

5.2.2.3 Reduced-scale system illumination

A solid state hyperband generator connected to a full IRA, adapted half IRA or another 50 Ω directed antenna represents a reduced-scale system illumination method with characteristics according to 5.2.2.2. Such a medium power pulse source is easily transportable to a test site and has a field strength which is detectable within the shielding enclosure with a high probability.

With the exception of the signal source the test equipment, test set-up and procedures for these reduced-scale simulators are the same as indicated in 5.2.2.1.

5.2.3 CW field testing

5.2.3.1 General

An alternative to pulse testing is to make the measurements in the frequency domain. Such tests are significantly less expensive than the transient tests, due to the relatively inexpensive equipment involved. Moreover, because it is possible to dwell on each frequency for a long time, this test method can be used for highly shielded systems in which pulse testing is inefficient due to the low signal strength.

5.2.3.2 Global illumination with active radiators

A typical test configuration for a CW test is shown in Figure 21. This figure shows the facility being tested, the CW antenna, the measurement equipment enclosure and associated cable connections. The measuring equipment is located on the ground near the facility. Because this is a field illumination test, it is important to have the CW radiating antenna located at least several wavelengths from the facility so that the illuminating field appears as a plane wave.

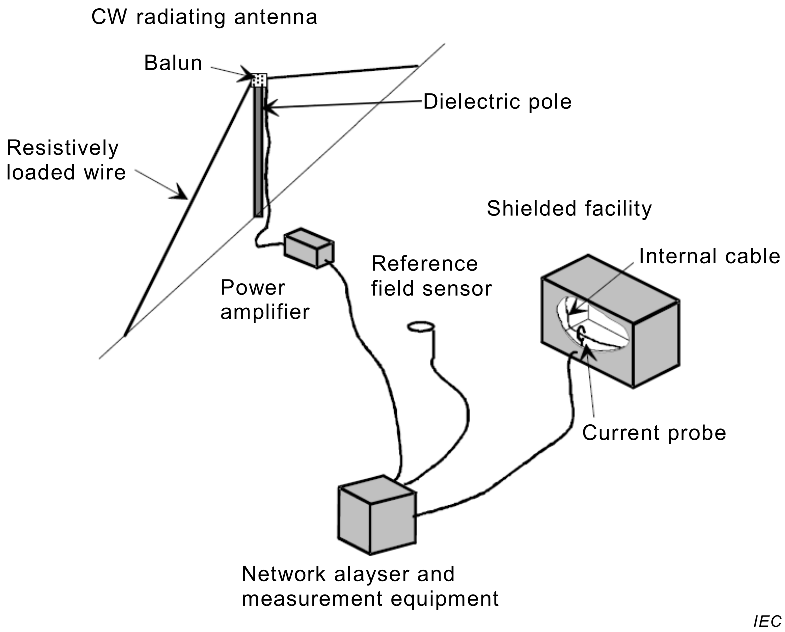

Figure 21 – Typical configuration of a CW test facility

Test set-up

Figure 22 illustrates the details of the CW measurement set-up. The heart of the system is a network analyser, which has the capability of measuring two responses simultaneously: a reference channel and channel A, which is the desired system response. The network analyser is controlled by a personal computer (PC). Both pieces of equipment should be located in a shielded region, well away from the radiated field produced by the incident field of the CW antenna.

Associated with the measurement computer is a data analysis computer. This analysis function can be contained within the measurement computer itself, or it can be performed by a separate computer, linked directly to the measurement computer.

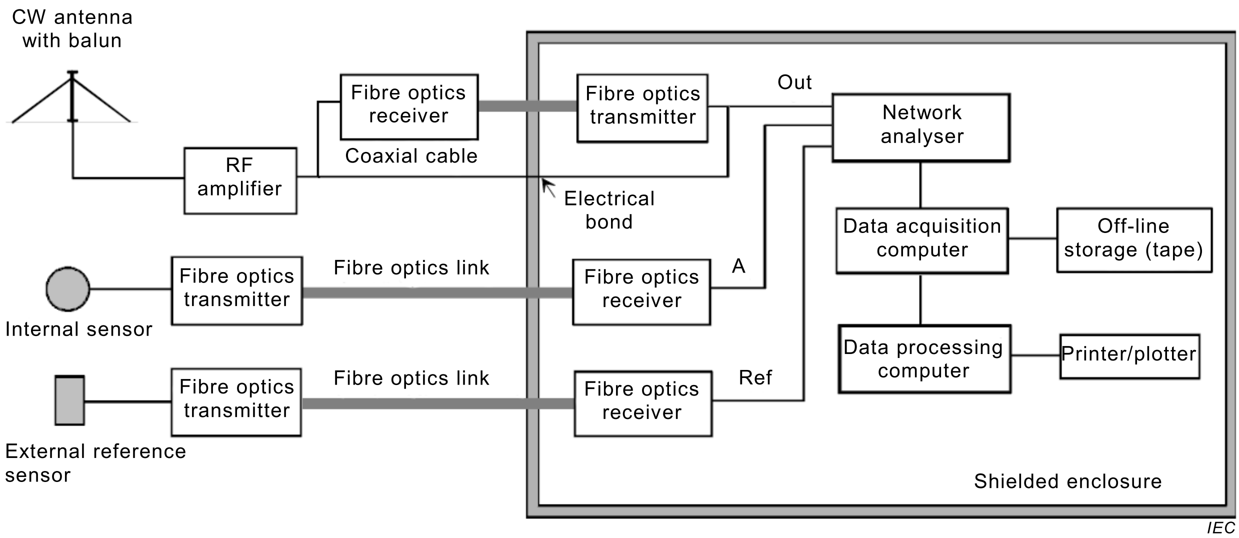

Figure 22 – Example CW measurement set-up

The external field/current sensors for the reference and the measurement channels should not violate the shield topology surrounding the measurement equipment. A common way of ensuring that the shielding is maintained is to use fibre optic links for both of these channels. This requires a conversion of the electrical signals at the sensors to optical signals by means of a fibre optics transmitter, the transmission of the optical signals via an optical cable, and the reconstitution of the electrical signal within the equipment enclosure by a fibre optics receiver.

The network analyser provides an output RF signal which is swept over the frequency range of interest. This signal is transmitted via a 50 Ω coaxial cable to an RF power amplifier, which boosts the signal level and then feeds it to a specially designed antenna to radiate the signal.

The coaxial cable shield should be electrically bonded to the shielded equipment enclosure at the penetration point to isolate the external and internal regions, as indicated in Figure 22. In addition, ferrite bead attenuators can be located at about 30 cm intervals along the cable to help minimize the unwanted external field coupling and propagation along the cable. An alternative to the use of a hard-wired connection between the network analyser and the amplifier is to use a fibre optics link, as illustrated in Figure 22.

Test equipment

For this test, the following types of equipment are needed:

– CW radiating antenna;
– power amplifier;
– network analyser;
– reference and response sensors;
– fiber optics transmission system;
– data acquisition computer and mass storage medium;
– data processing computer and plot capability.

Pertinent details of this equipment are discussed in Annex D.

Test procedure

To ensure that the CW test is conducted properly, a series of steps should be performed in setting up the measurement equipment and conducting the measurements. As shown in Figure 23, these procedures consist of activities that pertain directly to the conduct of the test (labelled as "CW test activity"). The other analysis support tasks (denoted as "CW data processing activity") serve to ensure that the test configuration is correct and that the test data are of sufficient quality for the data analysis, and finally to perform the desired analysis on the measured CW data.

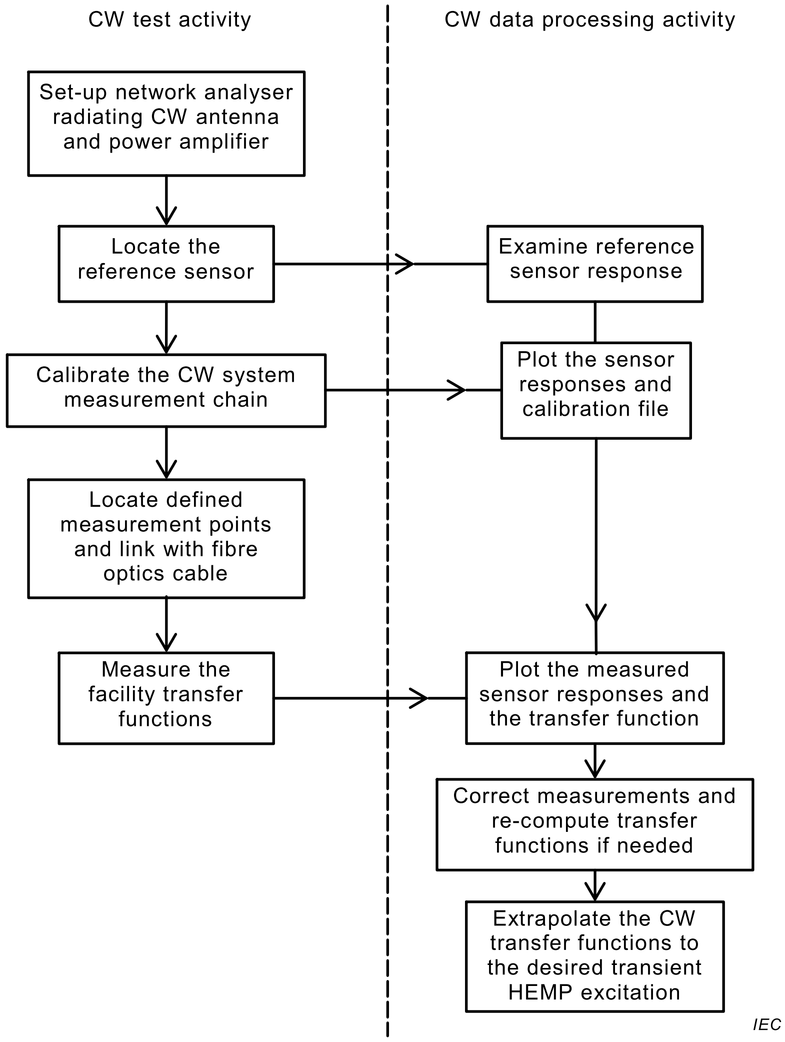

Figure 23 – Test and analysis procedures for conducting a CW test

The first step in conducting the CW test is to decide upon the location of the CW test antenna. In the direction broadside to the antenna, the radiated EM field is primarily horizontally polarized. Thus, this CW antenna is suitable for simulating the effect of an incident horizontally polarized HEMP field. Details of antenna placement are provided in Annex D.

Once the antenna location is fixed, the reference sensor is selected and the calibrations of the response and reference sensors are performed. The next step in the CW test procedure is to locate the desired measurement points (presumably within the facility or test object), connect the previously calibrated sensors, and run the fibre optic cables from the transducer near the network analyser to the measurement location. In doing this, care should be taken to ensure that the shielding topology of the test object is not violated. For example, even though the fibre optic cables do not conduct electrical signals, if they pass through a door into a shielded enclosure, the door shall remain open to let the cable pass. Such an open door constitutes a shielding violation and should be avoided.

With the appropriate equipment connected at the internal measurement points, the measurement process can proceed, with the simultaneous measurement of the reference and the response sensors. Generally, the calibration transfer function $T_o(\omega)$ is applied to these responses during the measurement process and, as a result, there are three data files provided for each measurement:

– the reference sensor spectrum;

– the response sensor spectrum;

– the corrected transfer function.

As noted in Figure 23, concurrent with the measurements, data analysis should be performed, with plotting of these data files, and a preliminary examination of the reasonableness of the results should be made. If there are any bad data points in either of the sensor responses, they should be checked and a new transfer function calculated.

After the measurements of the transfer functions are completed, Figure 23 indicates that the remaining task is the processing of the measured data. Usually, for a CW test, this will involve taking the measured (and corrected) transfer function spectrum and converting it to a transient, HEMP response of the system. To describe this extrapolation process, the signal flow diagram shown in Figure 24 can be used. In addition, if only the shielding effectiveness of the enclosure is desired, this quantity can be determined from the transfer function, as discussed previously in Clause 4.

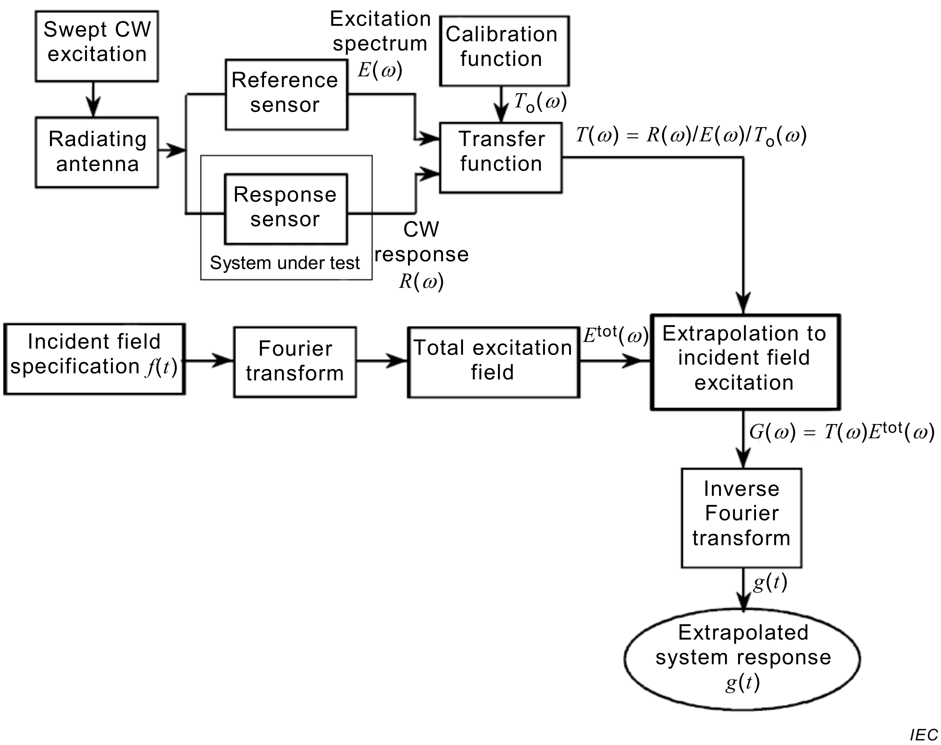

Figure 24 – Analysis flow diagram for extrapolating a measured CW spectrum to the HEMP response

5.2.3.3 Global illumination with existing CW sources

An alternative to the CW or pulse testing of a system, using an active transmitter and antenna, is to consider a passive approach in which ambient EM signals around the system provide the excitation. These signals arise from stationary transmitters and, consequently, there can be a large variability in the results. Consideration should be given to the illumination direction of the stationary transmitter.

Figure 25 illustrates an example scan of the EM spectrum (from 9 kHz to 3 GHz) which could be used to excite a test object in this manner.

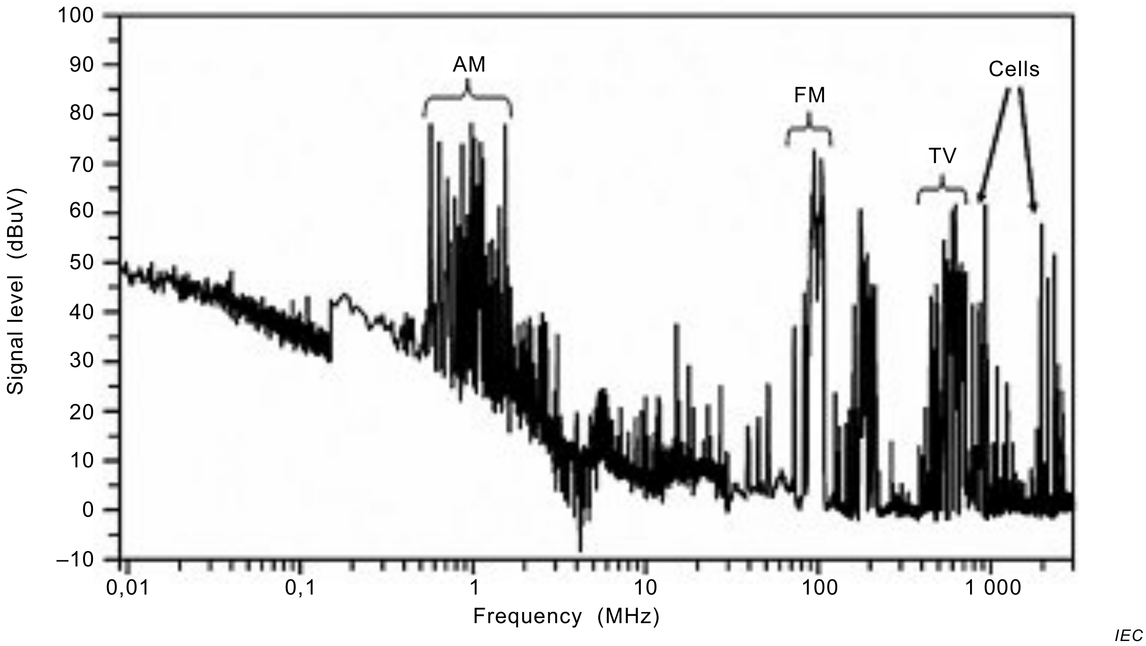

Figure 25 – Example scan from 9 kHz to 3 GHz for the ambient electromagnetic field from communication signals

There are several advantages in performing tests in this manner:

– the incident EM environment is a plane wave, exciting the entire system under test simultaneously;

– there is no interference with nearby equipment;

– no regulatory (PTT, FCC, etc.) approval is needed;

– the test is inexpensive, due to minimal equipment costs;

– there is no equipment liability issue.

However, this method presents the following disadvantages:

– there is no control over the characteristics of the excitation EM environment (amplitude, polarization, etc.);

– the signal/noise ratio is low, making it difficult to measure in highly shielded regions;

– phase information and complete spectral information are not available, making it impossible to calculate the correct transient responses;

– the internal equipment shall be turned off due to the low signal levels provided by the external sources.

Test set-up

The test set-up in this case is similar to that shown in Figure 21, except that the transmitting antenna and power amplifier are not present. Moreover, the network analyser may be replaced by a spectrum analyser, as the phases of the external reference and internal response signals are not measured.

Test equipment

For this test concept, the following types of equipment are needed:

– spectrum analyser capable of simultaneous measurements on two channels;
– reference and response sensors;
– fiber optics transmission system;
– data acquisition computer and mass storage medium;
– data processing computer and plot capability.

Test procedure

The procedure for performing this test is illustrated in Figure 26. It is important to perform a pre-test assessment of the ambient EM field environment to determine if it is suitable for performing the test. If there are not enough EM field emissions over the desired bandwidth, then it will be necessary to perform a pulse or CW test.

An important aspect of this type of test is to ensure that the measurements of the internal and reference responses are performed simultaneously. Because the ambient EM environment changes as a function of time, there is no guarantee that the incident fields will be constant. If the measurements of these responses are not simultaneous, variations of the received signal strengths will mask the shielding of the system.

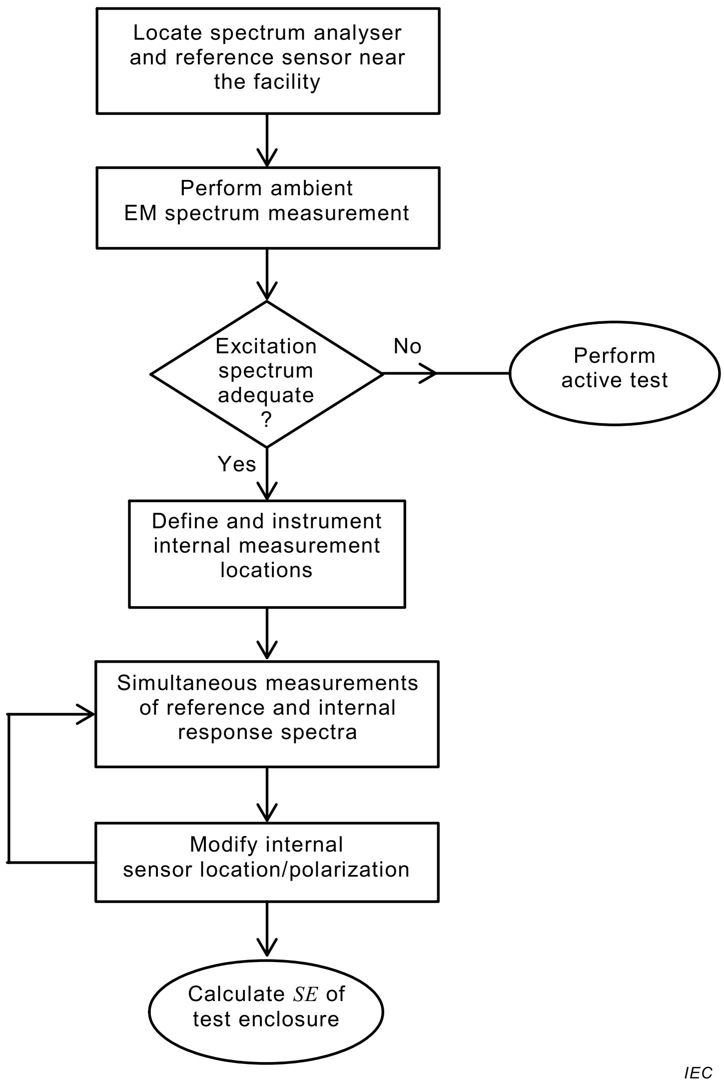

Figure 26 – Test procedure for the ambient EM excitation test

5.2.3.4 Double-ended TEM cell

The double-ended TEM cell is another way of producing a uniform and controlled EM field environment to globally excite a shielded enclosure. This device is like a coaxial transmission line, with a source at one end and a matched load at another. The source produces a transverse EM (TEM) field within the coaxial line which interacts with the test object located inside the coaxial region, and is ultimately absorbed by the termination impedance.

Figure 27 illustrates a typical double-ended TEM cell, with a cut-away view showing the centre conductor of the coaxial system and the object under test. As long as the test object is not too large compared with the cross-section of the cell, the excitation field can be taken to be approximately uniform. Because the TEM mode in this waveguide has no low-frequency cut-off, the testing may be conducted at very low frequencies – well below the frequencies permitted by a radiating antenna structure. As the frequency of operation increases, however, other modes and cavity type resonances can occur; these effectively limit the high-frequency utility of the device. Suppliers of individual TEM cells provide information as to the usable bandwidths of their equipment, which typically range from several tens of kilohertz to 100 MHz for cells having a working volume in the order of a metre in height.

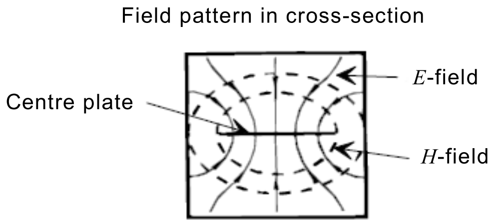

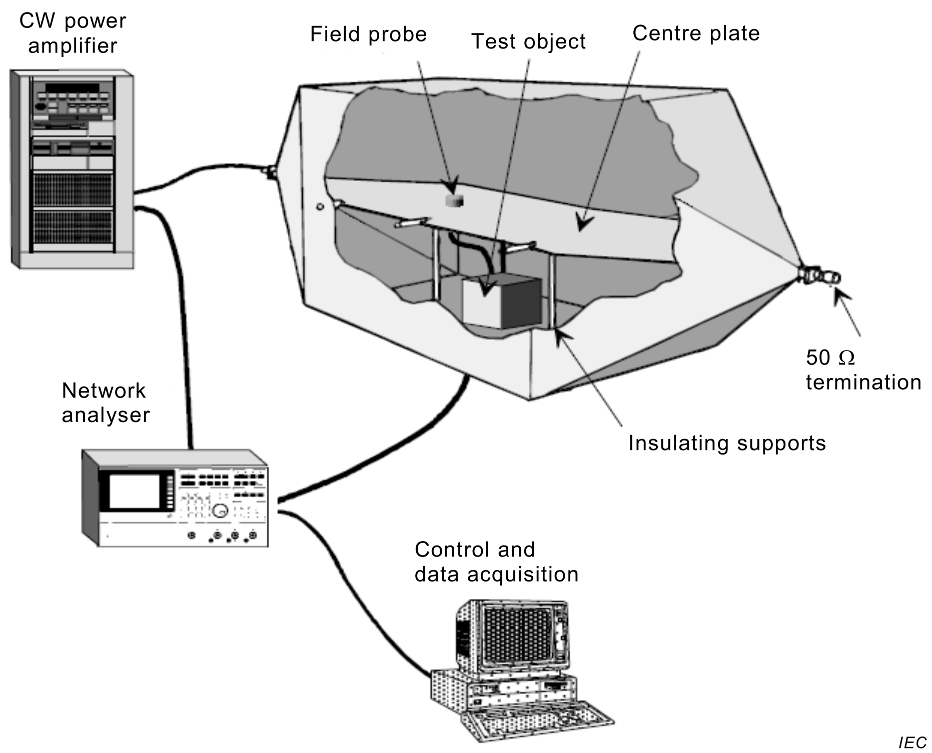

Figure 27 – Double-ended TEM cell for field illumination testing of small enclosures

Test set-up

The equipment set-up for testing in the TEM cell is similar to that used for the CW field illumination testing discussed in 5.2.3.2, with the exception that the shielded enclosure surrounding the equipment in the CW case is not needed, because of the shield surrounding the TEM cell. Figure 28 illustrates the equipment connections for this test.

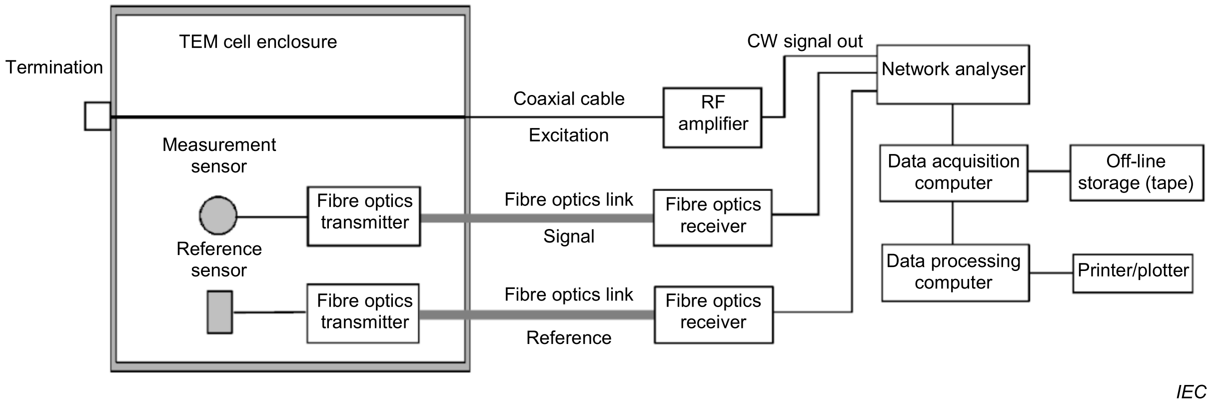

Figure 28 – Example test set-up for field illumination in the TEM cell

Test equipment

For this test concept, the following types of equipment are needed:

– TEM cell with matched termination resistance;
– CW power amplifier, network analyser or spectrum analyser capable of simultaneous measurements on two channels:
– reference and measurement sensors;
– fiber optics transmission system;
– data acquisition computer and mass storage medium;
– data processing computer and plot capability.

Test procedure

Testing in the TEM cell proceeds in a manner similar to the other tests described previously: the network analyser drives the power amplifier and sweeps from a low frequency to a high frequency which is determined by the upper limits of operation of the TEM cell. Measurements of the reference field sensors and the internal system response are made simultaneously by the network analyser and the transfer function between these two quantities is developed directly in the spectrum analyser. If an extrapolated transient response is desired from these measurements, then the analysis procedure illustrated in Figure 24 is used. However, if the shielding effectiveness of the enclosure is desired, such a detailed analysis is not performed: only the SE response is formed from the transfer function, as described by Equation (2).

5.2.3.5 Single-ended TEM cell

An alternative to the double-ended TEM cell described above is the tapered TEM cell as shown in Figure 29. In this test chamber, the inner conductor is offset vertically so as to create a larger test volume, and it has a gradually flared rectangular coaxial cross-section, terminating in a matched load.

The end termination consists of a combination low-frequency circuit element of 50 Ω load and a high-frequency absorber wall for absorbing the incident propagating wave as in anechoic chambers. The crossover between these two regimes depends on the cell size and the absorber length. The broadband impedance match provided by the termination acts to suppress higher modes. The absorbing material significantly reduces the Q of the chamber cavity, thereby reducing the resonance effects of the cavity modes. Field variability inside the empty chamber should be less than ± 4 dB for frequencies from d.c. to 1 GHz.

The cells have been given the name "GTEM" cells to emphasize their gigahertz capability. Cells have been constructed with test chamber heights from 0,5 m to over 3 m for use in testing printed circuit boards up to box-size equipment. Larger cells, capable of complete rack or vehicle testing, are under study.

Testing in these modified TEM cells is identical to that discussed in 5.2.3.4, with the exception that the upper frequency range is higher. Consequently, similar equipment is used (but perhaps with a larger bandwidth), and the same test procedure as that discussed in 5.2.3.4 is used. See also IEC 61000-4-20 for information on testing with the use of TEM cells.

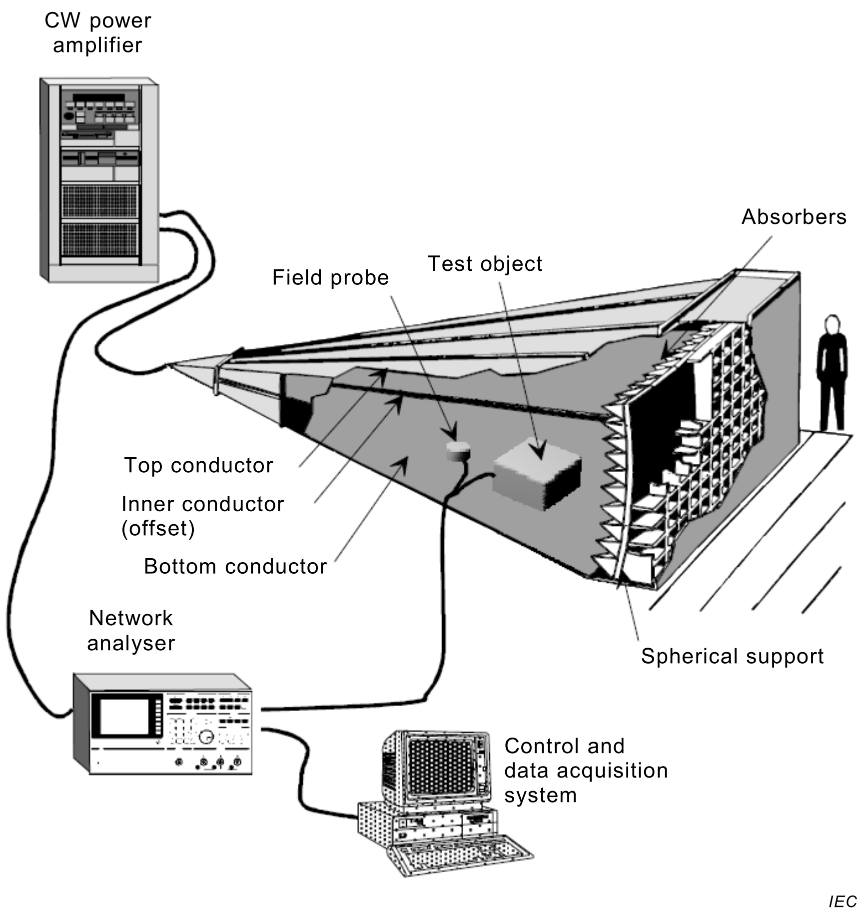

Figure 29 – Illustration of the single-ended TEM cell and associated equipment

5.2.3.6 Localized barrier shielding effectiveness test method

In some instances, a shielded enclosure cannot be viewed as being a “good” shield. Such is the case if there are many openings in the shield or if the shield material is not highly conducting. In these instances, the testing of the shielding can be accomplished by performing a local barrier illumination using a small antenna that provides EM field illumination in the vicinity of the barrier penetration. Such tests are less reliable than are the full system illumination tests, because the shielding effectiveness values depend on the location of the internal measurement sensor, as well as the location of the external antenna. Thus, a range of SE values can be obtained for any particular system. For example, as illustrated in Clause 4, local illumination tests can be applied to the measurement of the overall shielding of the enclosure (as in Figure 5), to the localized measurement of the shielding provided by wire mesh or conducting panel protection over apertures (as in Figure 15), or to the localized testing of other PoE protection methods (as suggested in Figure 18).

Due to the localized nature of the excitation source, this measurement provides information only about the shielding in the region where the excitation EM field is strongest. For localized PoE measurements the testing is performed in the vicinity of the penetration point.

As noted in Clause 4, the shielding behaviour of an enclosure at low frequencies is different for the E- and H-fields. Because the E-fields are relatively easy to shield for these frequencies, only tests of the magnetic field shielding effectiveness are required. As the frequency increases, the E- and H-shielding effectiveness becomes identical, and it is equivalent to the plane-wave shielding effectiveness. This quantity is also measured by the test method.

Since the electromagnetic barrier has to remain intact during the conduct of the shielding effectiveness measurements, and since the use of electrically noisy equipment has to be restricted, construction activity or unusual operations (facility modification, maintenance) may be affected. Radiated signal levels are low and present no hazard to equipment, but frequency adjustments may be required to avoid self-interference or interference with nearby facilities. Normal electrical safety precautions apply during this test.

Test set-up

In conducting these low-frequency magnetic field or plane-wave shielding effectiveness tests of the enclosure, the basic test set-ups illustrated in Figure 29 and Figure 31 shall be used. Measurements of the receiving antenna responses, with and without the shield present, are made, and the ratio of these responses provides an indication of the shielding effectiveness of the local barrier as

$$SE = 20\log_{10}\left|\frac{V_{\mathrm{c}}}{V_{\mathrm{m}}}\right| \mathrm{dB} \tag{11}$$

where

V_{c} is the measured receiver response under calibration conditions (without the barrier);

V_{m} is the measured response with the barrier in place.

This procedure should be applied to shielded enclosures large enough to accommodate the test equipment inside the enclosure.

Test set-up for plane-wave measurements

The set-up for calibration and measurement of plane-wave shall be placed in accordance with Figure 30a) and Figure 30b).

If it is not possible to place the transmitting antenna outside due to physical constraints, the set-up for the measurement follows Figure 30c). The oscillator and power amplifier may be placed inside the shielded enclosure with an additional shielded rack. When using a vector network analyser, the oscillator is part of the network analyser and therefore in its location.

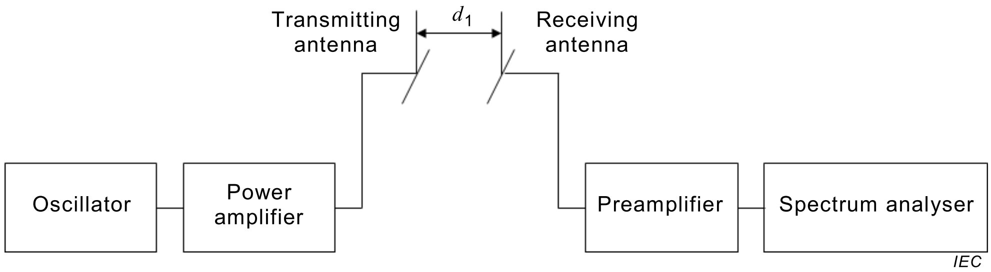

a) Calibration

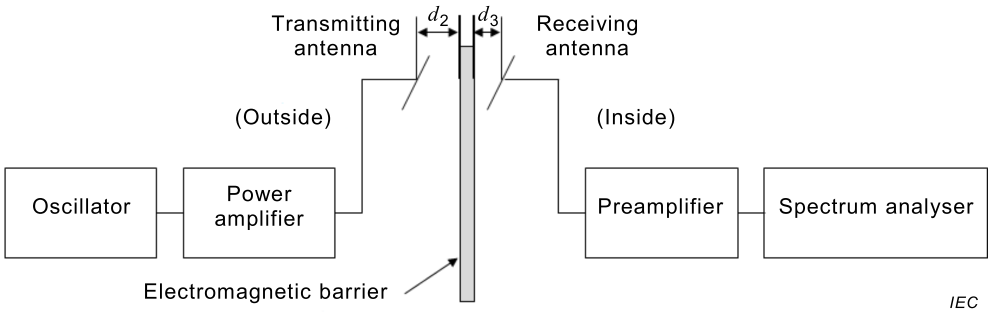

b) Measurement

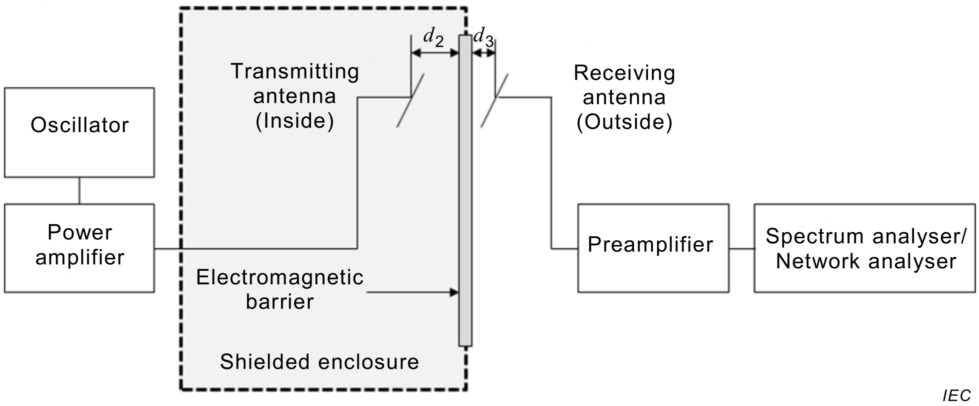

c) Measurement (inside-to-out)

Figure 30 – Test set-up for the plane-wave shielding effectiveness measurements

The dimensions and composition of the various distances d_1 to d_3 are given in Table 2.

Table 2 – Dimensions and composition of distances d_1 to d_3, with reference to Figure 30

Term	Minimum dimension	Composition
d_1	2 m	$d_2 + d_3$ + barrier thickness
d_2	30 cm	$d_1 - d_3$ – barrier thickness (within dynamic range and physical constraints)
d_3	30 cm	$d_1 - d_2$ – barrier thickness (within dynamic range and physical constraints)

Test set-up for magnetic field measurements

The set-up for magnetic field calibration and measurement shall be used in accordance with Figure 31a) and Figure 31b).

If it is not possible to place the transmitting antenna outside for a separation distance of twice the loop antenna diameter and the thickness of the electromagnetic barrier due to physical constraints, the transmitting loop antenna shall be placed at a distance of 30 cm from the test area surface. In this case, the distance of the receiving antenna from the test surface shall also be 30 cm, and the distance between two loop antennas for the calibration shall be twice the loop antenna diameter and the thickness of the electromagnetic barrier.

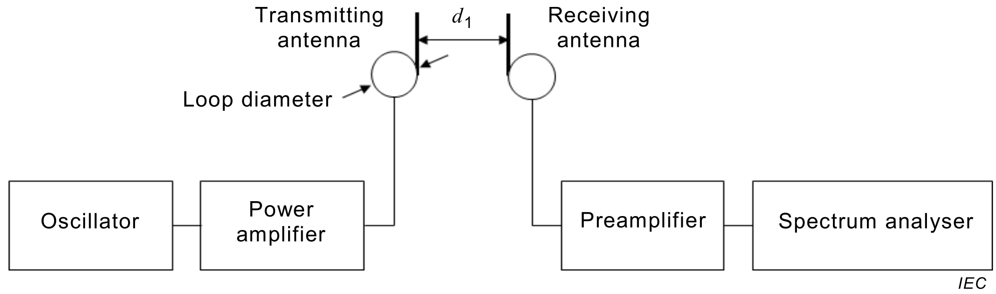

a) Calibration

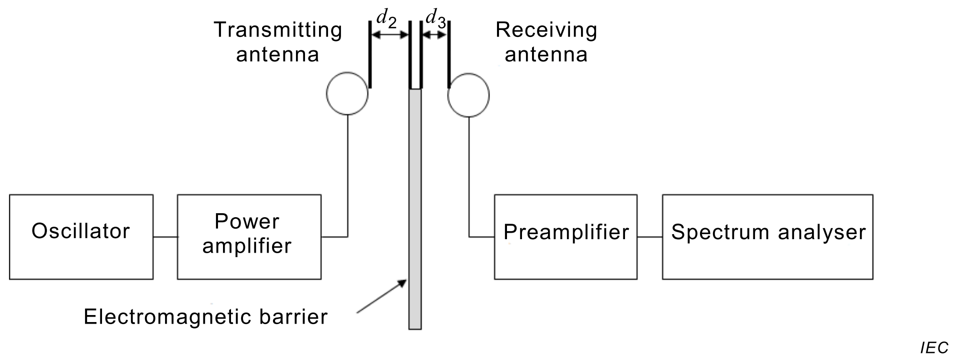

b) Measurement

Figure 31 – Test set-up for the *H*-field shielding effectiveness measurements

The dimensions and composition of the various distances d_1 to d_3 are given in Table 3.

Table 3 – Dimensions and composition of distances d_1 to d_3, with reference to Figure 31

Term	Minimum dimension	Composition
Loop diameter	-	Usually 30 cm
d_1	60 cm + barrier thickness	$d_2 + d_3$ + barrier thickness
d_2	30 cm	$d_1 - d_3$ – barrier thickness (within dynamic range and physical constraints)
d_3	30 cm	$d_1 - d_2$ – barrier thickness (within dynamic range and physical constraints)

The localized antennas are used to illuminate various portions of the shielded enclosure. For the plane-wave shielding measurements, the entire surface (including the floor when both sides of the shield are accessible) of the electromagnetic barrier shall be divided into numbered plane areas not greater than 2,5 m × 2,5 m, as illustrated by the example in Figure 32. The circles in this figure in the centre of each area indicate the various transmitting antenna locations for these measurements. The magnetic field shielding effectiveness measurements shall be performed at seams and PoEs, such as air vent, access panel, filter and so on.

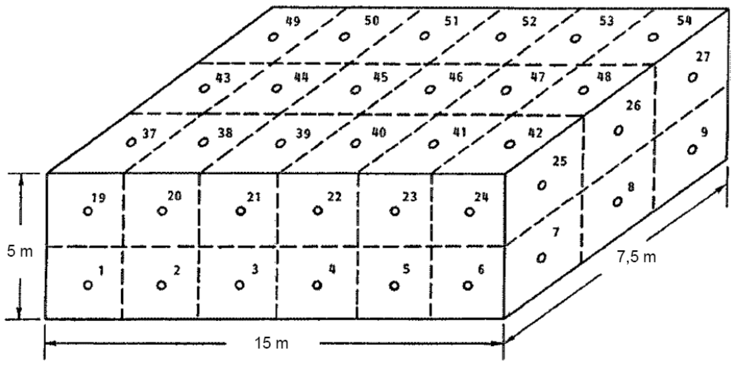

Figure 32 – Example of antenna locations for the localized antenna tests for a hypothetical shielded enclosure or facility

Test equipment

The test equipment required for shielding effectiveness measurements includes the following:

– RF signal oscillators;
– RF power amplifier(s) with a power output as required for dynamic range;
– preamplifier(s);
– receivers/spectrum analyser(s);
– antenna(s);
– miscellaneous cables and attenuators – as required.

NOTE 1 Alternatively a vector network analyser can be used in place of RF signal oscillators and receivers/spectrum analysers.

Test procedures

Plane-wave shielding effectiveness measurements

For each plane-wave test area defined in Figure 32, eight shielding effectiveness measurements shall be made by sweeping the receiver antenna position. These measurements shall be made at four distinct frequencies in the HEMP band, for each of two transmitting antenna polarizations, as follows.

a) Frequencies

One test frequency in each frequency range of Table 4 shall be chosen according to the approved test plan by the owner.

Table 4 – Measurement frequencies and antennas in plane-wave

Frequency range	Antenna type
20 MHz to 100 MHz	Biconical
100 MHz to 300 MHz	Biconical
300 MHz to 600 MHz	Dipole or log periodic
600 MHz to 1 GHz	Dipole or log periodic

NOTE 2 Instead of measuring only four single test frequencies, a vector network analyser can be used to measure a sweep over the frequency range listed in Table 4. If available, transmitting antennas with a broad frequency range (usually log periodic) can be used and the frequency ranges of the sweeps according to Table 4 can be adjusted to the frequency range of the chosen transmitting antennas. Receiving antennas with fibre optic systems with corresponding sensors of a broad frequency range can be used as well.

b) Transmitting antenna polarizations

Dipole (or antenna aperture) parallel to the test area surface in two orientations, at 90° to each other and parallel to the principal weld seams in the shield.

The plane-wave calibration for each frequency and transmitting antenna polarization shall be performed in accordance with Figure 29a). The transmitting and receiving antennas such as biconical, dipole, log periodic, or other linear antennas shall be oriented parallel to each other (or aperture antenna planes parallel to each other). The distance between antennas shall be as large as possible, within dynamic range constraints, but shall be at least 2 m. The receiving antenna position shall be varied by ± 30 cm from its nominal location to ensure that it is not located at a minimum of the radiation pattern. Test equipment shall be chosen to provide a dynamic range at least 20 dB in excess of the shielding effectiveness requirement at the test frequency. During calibration, no equipment or other electromagnetic reflector (except ground) shall be closer than three times the antenna separation. The antennas shall be at least 0 m above ground. The received signal strength for each frequency and transmitting antenna polarization shall be recorded as the calibration signal (V_c) for that configuration.

NOTE 3 To get an idea of the limits of the measuring system and the truth of the test results a noise measurement can be performed over all frequency ranges of interest. Therefore the receiving antenna can be replaced by a 50 Ω terminator (or packed into an aluminium foil in case of a small fibre optic field sensor).

After the calibration is completed, the plane-wave shielding effectiveness measurements for each test area, and at each required frequency and transmitting antenna polarization, shall be performed as shown in Figure 29b). Identical equipment, antennas, cable and equipment settings (except attenuator settings) shall be used in the calibration and measurement sequences.

The transmitting antenna shall normally be placed outside the electromagnetic barrier and centered on the test area. The transmitting antenna's axis (or plane in the case of an aperture antenna) shall be parallel to the test area surface and parallel to one of the two principal weld seam directions. The distance from the closest points of the transmitting antenna to the test area surface shall be 30 cm less than the separation at which calibration was performed.

To perform the swept measurements, the receiving antenna shall be swept over the entire test area at distances of approximately 5 cm to 60 cm from the test area surface and shall be rotated in orientation until a maximum received signal is obtained. The maximum received signal strength shall be recorded as the swept measure signal V_m for that test area, frequency, and transmitting antenna polarization. Shielding effectiveness values are calculated using Equation (11).

If it is not possible to place the transmitting antenna outside due to physical constraints, the transmitting antenna can be placed in the shielded enclosure. The plane-wave calibration is the same as in Figure 29a) and the shielding effectiveness measurements shall be performed as shown in Figure 29c). For measurements, all equipment except for the transmitting antenna shall be placed outside or shielded inside the enclosure to avoid interference with the transmitting EM wave. It is recognized that testing of the shielded enclosure shall be avoided at, or very near, the shielded enclosure resonant frequency. The test procedure for shielding effectiveness measurements is the same as that of placing the transmitting antenna outside.

Magnetic field shielding effectiveness measurements

For each 2,5 m × 2,5 m magnetic field test area shown in Figure 32, six shielding effectiveness measurements shall be made at three frequencies for each of two transmitting antenna polarizations, as follows:

1) Frequencies

One test frequency in each frequency range of Table 5 shall be chosen according to the approved test plan by the owner.

Table 5 – Measurement frequencies and antennas in magnetic field

Frequency range	Antenna type
10 kHz to 16 kHz	Loop
140 kHz to 160 kHz	Loop
14 MHz to 16 MHz	Loop

NOTE 4 Instead of measuring only three single test frequencies, a vector network analyser can be used to measure a sweep over the frequency range listed in Table 5. As receiving antennas, fibre optic systems with corresponding sensors of a broad frequency range can be used as well.

2) Antenna polarizations

Plane of the loop antenna normal to the test area surface in two orientations, at 90° to each other and parallel to the principal weld seams in the shield.

For these measurements, magnetic field calibration at each frequency and transmitting antenna polarization shall be performed in accordance with Figure 31a). The loops of the transmitting and receiving antennas shall be in the same plane.

The receiving antenna position shall be varied by ± 30 cm from its nominal location to ensure that it is not located at a minimum of the radiation pattern. Test equipment shall be chosen to provide a dynamic range at least 20 dB in excess of the shielding effectiveness requirement at the test frequency. During calibration, no equipment or other electromagnetic reflectors (except ground) shall be closer than three times the antenna separation. The antennas shall be at least 2 m above ground. The received signal strength for each frequency and transmitting antenna polarization shall be recorded as the calibration signal V_c for that configuration.

NOTE 5 To get an idea of the limits of the measuring system and the truth of the test results a noise measurement can be performed over all frequency ranges of interest. Therefore the receiving antenna can be replaced by a 50 Ω terminator (or packed into an aluminium foil in case of a small fibre optic field sensor).

After the calibration is completed, magnetic field shielding effectiveness measurements for each test area, and at each required frequency and transmitting antenna polarization, shall be performed as shown in Figure 31b). Identical equipment, antennas, cable and equipment settings (except attenuator settings) shall be used in the calibration and measurement sequences.

The transmitting antenna shall normally be placed outside the electromagnetic barrier and centered on the test area. The plane of the transmitting loop antenna shall be normal to the test area surface and parallel to one of the two principal weld seam directions. The distance from the closest points of the transmitting antenna to the test area surface shall be 30 cm less than the separation at which calibration was performed.

The receiving antenna shall normally be inside the barrier. To perform the swept measurement, the receiving antenna shall be swept over the entire test area at distances from approximately 5 cm to 60 cm from the test area surface and shall be rotated from vertical to horizontal polarization until a maximum received signal is obtained. The maximum received signal strength shall be recorded as the swept measure signal V_m for that test area, frequency, and transmitting antenna polarization.

Test frequencies and pass/fail criteria

The owner shall define test frequencies and all pass/fail requirements. However, as a guide for owners, this standard recommends frequencies like Table 4 and Table 5 that can be selected for testing their shielded enclosures. Successful tests at these frequencies should provide very high confidence that a shielded enclosure provides a “good” shield at all the frequencies from 10 kHz to 1 GHz.

5.3 Current injection test procedures

5.3.1 General

Tests in 5.3 deal with those that involve the excitation of a HEMP protection device or material by a direct injection of current (and charge), as opposed to the excitation by an electromagnetic field. This corresponds to the excitation of the system shielding topology at observation points inside the principal shielding surface, as discussed in Annex A.

5.3.2 Injection testing of enclosures

The low-frequency testing of the shielding provided by an enclosure or box by current injection is discussed in 4.2.4 and is illustrated conceptually in Figure 7. This diagram is repeated in Figure 32a) which shows current being injected at one location on the external shield and extracted at another location. The internal open-circuit voltage is measured across two sense wires connected to the inside of the enclosure.

This test is not designed to simulate the effects of an incident HEMP field acting on the enclosure; rather, it simulates the effects of an HEMP-induced current on long cables being conducted onto the shielding enclosure. Thus, the locations of current injection shall correspond to points at which there would be current flowing onto the enclosure when it is in its normal operating configuration. In some cases, there may be multiple cable attachment points, requiring several different current injection simulations to account for the different possible excitations of the shield.

Test set-up

Figure 32b) illustrates the set-up for this test. A network analyser, controlled by a data acquisition computer, feeds a low-level excitation signal to a power amplifier. This amplifier, typically with a coaxial cable output, feeds a balun-like splitter which injects current onto one connection on the enclosure exterior and removes the current from another point. These injection points shall correspond to locations having electrical connections in the normal operating configuration of the system.

A suitable voltage is measured across an internal sense wire and is conducted back to the network analyser by a fibre optic link, so as not to interrupt the current path on the system exterior. With a measurement of this internal voltage, a measure of the shield transfer impedance Z_t is obtained from Equation (3).

In performing this test, it is important to ensure that the frequency of operation is sufficiently low, so that $\lambda = c / 2\pi f > L$, where L is the longest dimension of the enclosure.

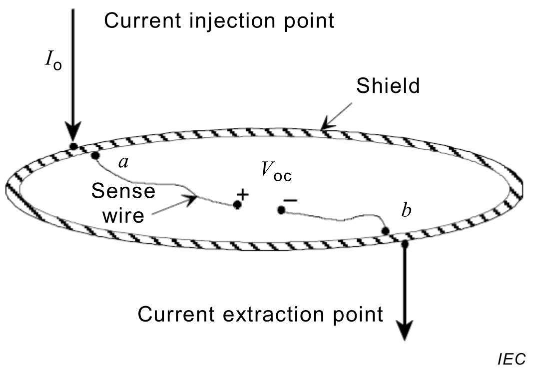

a) **Test concept**

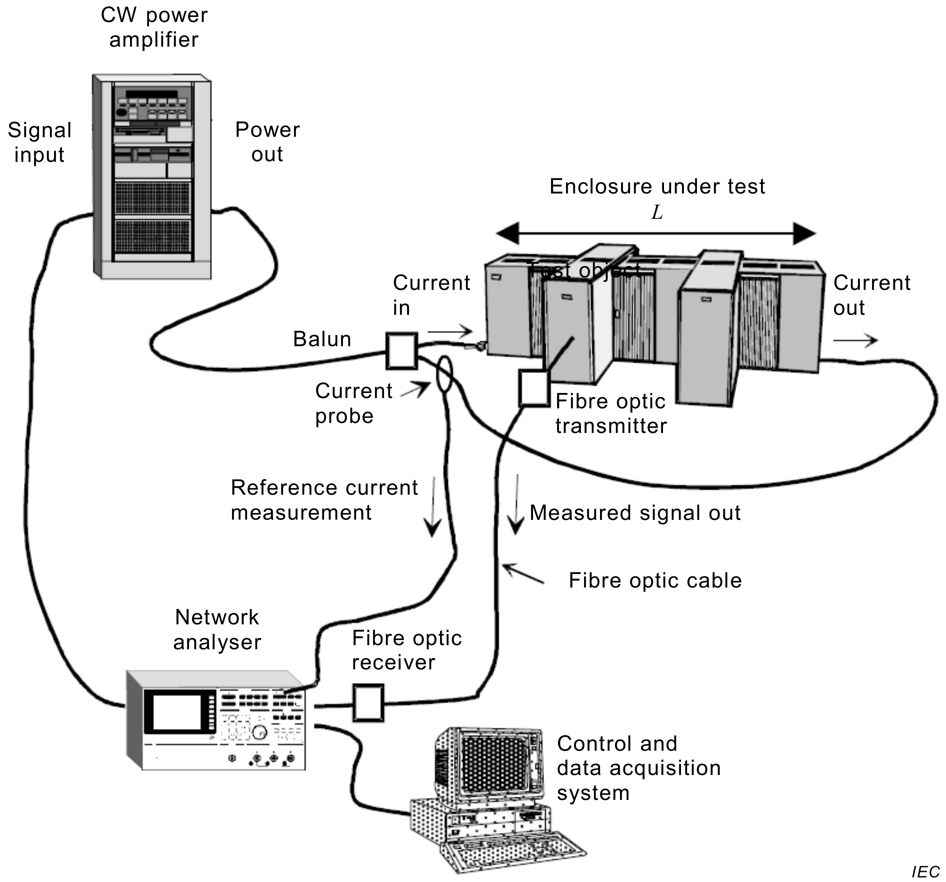

b) **Equipment configuration**

Figure 33 – Test concept and equipment configuration for current injection testing of a shielded enclosure or box

Test equipment

For this test, the following types of equipment are needed:

– network analyser or other suitable detector capable of measuring the injected current on the enclosure exterior and the internal voltage;

– low-frequency amplifier suitable for injecting the amplified current onto the enclosure;

– balun or other coaxial balanced line transition device for injecting current onto the system;

– voltage and current probes;

- fiber optic transmission unit or other data transmission medium suitable for passing the internal measured voltage back to the network analyser without causing perturbations in the external current path;
- controlling computer and data analysis station;
- assorted cables and connectors.

Test procedure

This test is conducted by first examining the system to determine the various current injection points that would normally be excited by an HEMP event. The size of the enclosure (L) is measured, and the highest frequency of operation (f_{max}) is then determined, so that the minimum wavelength (λ_{min}) is $\lambda_{\text{min}} = c/2\pi f_{\text{max}} > L$. Then, the network analyser is swept from the lowest possible frequency to the computed maximum frequency, and the complex valued transfer impedance ratio of V_{oc}/I is evaluated.

This measurement is repeated for different internal voltage collection points, so as to obtain a representative sampling of the variations of the internal responses. In addition, if there are other external current injection points possible, these measurements shall be repeated with the injection of the CW current being made at these points.

The total set of measured responses should be presented in the form of summary curves showing the response distributions as a function of frequency. Furthermore, the shielding effectiveness of the enclosure can be computed using Equation (4).

5.3.3 Transfer impedance and admittance of cable shields and connectors

Test procedures for determining the transfer impedance and admittance of cable shields are defined for example within the IEC 62153-4-x series. Annex A provides information on these measurement techniques.

5.3.4 Testing of gasket material

5.3.4.1 Resistivity measurement

The testing of the resistivity of a gasket material has been described in 4.4.2. Such measurements may not be indicative of how it might actually perform as a hardening element when installed in a facility or enclosure, but, nevertheless, such tests of the d.c. resistivity are useful in characterizing the gasket material.

Test set-up

The test set-up for this measurement is illustrated in Figure 14. In this figure, the material under test is located between two electrodes; a current is caused to flow by the excitation voltage source, and the resulting voltage is measured across the sample. In the actual test set-up, the excitation source and the voltmeter are all contained in one unit – the four-probe voltmeter, as specified below.

Test equipment

For this test, the following types of equipment are needed:

- a four-probe ohmmeter having a measurement range of 10^4 Ω to 10^{-5} Ω;
- silver- or gold-plated electrodes having a contacting area A = 1,6 cm^2 (corresponding to a circular diameter of 1,43 cm) for holding the sample. These electrodes should have suitable provisions for attaching the ohmmeter electrodes;
- a thickness gauge for measuring in increments of 0,02 mm;

– an appropriate fixture or apparatus having capabilities of supporting the electrodes and test specimen, and suitable means of applying a pressure of $(6{,}89 \times 10^6)$ Pa on the sample.

Test procedure

Gasket specimens with thicknesses ranging from 0,1 cm to 0,3 cm and a cross-sectional area at least the same as the electrodes shall be obtained for testing. Prior to testing, the surfaces of the material should be cleaned and any dirt or foreign matter removed. The electrodes should also be cleaned. Prior to testing, the test specimen and test fixture and electrodes should be conditioned for at least 3 h at a standard temperature of 23 °C and at a relative humidity of 45 % to 75 %.

Measure the area A of the silver- or gold-plated electrodes. Using the thickness gauge measure and record the thickness L of the material at the contact location with the electrodes. The material being tested shall have sufficient area to contact the entire electrode area. Then, position the material between the electrodes and apply a pressure of $(6{,}89 \times 10^6)$ Pa ± 5 % across the sample. While maintaining constant pressure, measure and record the sample resistance R.

With these measured quantities, the d.c. resistivity of the gasket material is calculated as

$$\rho_{\mathrm{DC}} = R\frac{A}{L} \tag{12}$$

where

ρ_{DC} is the d.c. resistivity (W·m);

R is the measured resistance (W);

A is the smallest cross-sectional area of part or sample between probe electrodes (m^2);

L is the distance between the two electrodes (m).

5.3.4.2 Material resistivity using the surface probe method

An alternative test method for the resistivity of a gasket may be used for cases where the gasket material cannot be cut. This involves making a surface measurement of the resistance of the sample.

Test set-up

For this test, the two-point probe shown in Figure 34 is used. This probe has an electrode separation of L = 2,54 cm, and other typical dimensions are indicated in the figure. For parts too small to be measured with this probe, a different probe with a smaller electrode separation may be used, with the electrode’s width and spacing being reduced together.

Each electrode should touch the gasket at one point. In the case of a part whose cross-section configuration makes it difficult or impossible to measure using this method, the smaller test probe described above should be used.

Dimensions in centimetres

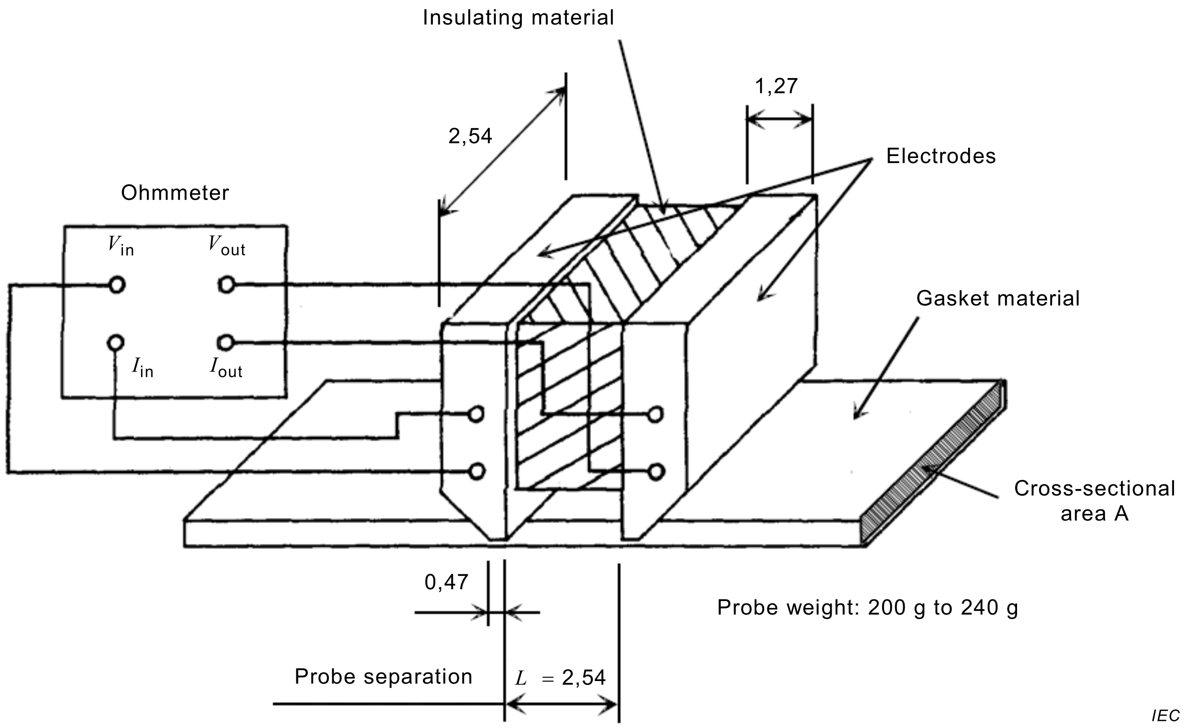

Figure 34 – Surface probe for volume resistivity measurement

Test equipment

For this test, the following types of equipment are needed:

- a four-probe ohmmeter having a minimum sensitivity of 1 mΩ;
- silver- or gold-plated electrodes having the dimensions shown in Figure 34, and suitable provisions for attaching the ohmmeter electrodes.

Test procedure

The d.c. volume resistivity of the material shall be measured using an ohmmeter capable of measuring to a minimum of 1 mΩ. The sample to be measured shall be placed on a nonconductive surface. The measurement probe shall be placed on the gasket part being tested, or alternatively, on a piece of sample material that is 1,27 cm wide by 7,62 cm long by 0,14 cm to 0,3 cm thick, in such a manner that the weight of the test probe is uniformly distributed on the part or test sample. The entire width of the part shall be in contact with each electrode. After a 30 s stabilization period, the resistance R on the ohmmeter shall be recorded. The d.c. volume resistivity shall be calculated using Equation (12).

Annex A
(informative)

HEMP test concepts for electrical systems

A.1 Overview

HEMP testing of an electrical system is necessary because mathematical and numerical models do not provide sufficiently accurate results to give a high confidence level in the assessment of a system's survivability in an HEMP environment. Many different factors enter into the decision to perform an HEMP test:

– relative importance of the system and its survivability requirements;
– type of system, its physical configuration and location;
– available funds, time and personnel for testing;
– desired accuracy of the results.

Before determining the test requirements for a system, the above factors should be carefully weighed to see if a test is actually needed.

A.2 Types of HEMP tests

A.2.1 General

There are several different types of tests that can be performed on systems to determine the response to an HEMP excitation. Some tests are rather simple and straightforward, while others require large facilities and significant data processing capabilities. The following subclauses A.2.2 to A.2.6 briefly describe the major types of HEMP tests.

A.2.2 System-level transient tests

Perhaps the most thorough test of a system (aside from using an actual nuclear environment) is to perform a threat-level test on the entire system. This type of test involves locating a threat-level, pulsed EMP simulator near the facility being investigated, and conducting a series of measurements by changing parameters such as the angles of incidence or the system's electrical configuration (i.e. doors open or shut, etc.).

Typically, in this type of test, a large amount of transient data is measured and saved for analysis after the test is completed. The results of the post-test analysis are usually expressed as a probability of survival of the system in the event of an HEMP event, and involve the concept of waveform norms.

The principal advantage of this type of test is that the entire system is subjected to the desired threat-level environment. As a result, any non-linear protection devices will be stressed and the resulting system response will include the effects of these elements. Furthermore, the effects of other unintended non-linearities such as flashovers in cables, which are very difficult to predict analytically, will be included.

On the other hand, the equipment involved in such tests is bulky, expensive and not easily transportable. Consequently, a fixed site simulator is usually used for this type of testing. If the system to be tested cannot be easily moved, this test is difficult to conduct. Furthermore, there is usually a large amount of data generated by this type of test, and the post-test analysis effort can be considerable.

A.2.3 CW field illumination tests

An alternative to the full-scale, threat-level pulse testing is to use the CW field illumination test concept. This test concept is similar to that of the system-level pulse-testing concept in that a radiating structure (i.e. an antenna) is located near the system under test. Unlike the pulse test, however, the excitation of the antenna is time harmonic (e.g. CW) and is swept or stepped through a range of frequencies, starting at a low frequency of 10 kHz to 100 kHz and stopping at a high frequency of 100 MHz to 200 MHz. Some newer CW testing systems operate up to the gigahertz (GHz) frequency range.

The basic goal of the CW test is to measure a transfer function from a suitable reference electromagnetic EM field quantity outside the facility to a response inside the facility. As this measurement is conducted in the frequency domain, the transfer function is a complex valued function, characterized by its magnitude and phase or conversely by its real and imaginary parts.

Suitable external reference quantities include a component of the incident or total E- or H-fields, a current induced on a long external cable, or perhaps the input current in the CW antenna itself. In cases when the measured response has to be extrapolated from an HEMP response, the choice of the external reference should be made so that it can be related to an incident HEMP field. Internal response quantities can include E- and H-fields inside the facility, currents on internal cables and voltages at equipment terminals.

This form of testing has several advantages over the full-scale pulse testing described earlier. The equipment used is readily available and is significantly less costly than that required for pulse testing. Furthermore, the entire system can be easily transported to remote sites and quickly erected. Because of the narrowband characteristics of the excitation and measurement process, the effects of noise can be reduced. Typically, it is easier to get a "clean" CW spectrum than to get a clean transient waveform.

The major disadvantage of CW testing is that, because of the low power level and non-transient mode of operation, non-linear protective devices within the system are not triggered. In addition, other unpredictable non-linearities, such as cable insulation flashover, are not noted. Consequently, this test method only provides the linear (or low-level) response and systems tested in this manner may appear to be more vulnerable than they really are, since the non-linear effects can add extra protection – if they operate.

This deficiency may not be serious in some circumstances, as many systems use both nonlinear devices together with electrical filters. CW testing on these systems provides a reasonable worst-case estimation of the response – namely, the response that would be obtained if the non-linear device were not to function properly. Moreover, there exist methods to combine analytically the low-level CW measurements of a system with the non-linear device characteristics to permit a calculation of the pulsed, non-linear behaviour of the system.

A second disadvantage of this test approach is that the final measured result is usually not the final desired result. To obtain the extrapolated transient HEMP response, some additional data processing should be undertaken, and this can give rise to errors in the resulting transient response.

A.2.4 Current injection testing

The two previous tests are applied to the entire system. An alternate test concept is to excite only parts of the system. One way of doing this is to identify important electrical conductors entering a facility and inject pulse or CW currents onto the cables. The injected currents will then re-distribute themselves within the facility and provide an indication of the system response under external field excitation conditions.

Typically for this type of test, a pre-test analysis should be performed in order to identify the important conductive current paths into the facility or system being considered. These might include power lines, communication cables or mechanical conductors. For each of these conductors, an analysis of the external EM-field coupling should be performed to estimate the amplitude and waveshape of the HEMP response. A current injection source having the proper transient (or spectral) characteristics is then applied to each of the selected conductors and the internal responses are measured.

The advantage of this type of test is that pulse injection equipment is typically smaller and less expensive than the full-scale simulator and associated equipment. Furthermore, threat-level currents are easier to induce by pulse injection methods than by an EM-field illumination. When operated in a pulsed mode, this type of testing also provides the possibility of exciting nonlinear devices located along the conducting paths being excited. Thus, a pulsed current injection test and a CW field illumination test can complement each other.

This type of test is fundamentally incomplete, as the possible synergistic effects of simultaneous excitation of the whole system are not taken into account. Thus, there is always some unknown error in this simulation technique. Furthermore, a key feature of this type of test is that the linking of the injected current levels on the external conductors to the incident HEMP field is often done by analysis. This step can introduce uncertainties in the results.

A.2.5 Partial illumination testing

Partial illumination testing is the counterpart to pulse injection testing, except that the system excitation is viewed as arising from a partial EM-field excitation of the system instead of a current injection on one of the system's conductors. This testing approach is sometimes denoted as the piece-wise application of radiation through an EMP simulator (PARTES) concept.

This test is accomplished by using small electric or magnetic dipole antennas referred to as "drivers" at various locations on the exterior surface of the system being tested. Locally, these drivers produce an EM field excitation of the system and a suitable internal response can be measured. Either CW or pulse testing is possible using this concept. By considering a suitably large number of driver locations and by analytically combining the measured responses for each, the response of a plane-wave excitation of the system can be inferred.

The main advantage of this approach is that electrically large systems can be tested. Although such systems might require many measurements as the driver location is changed, the method can allow for such testing.

The principal disadvantage of this testing is that considerable analytical work should be done to correctly combine the measured data files to obtain the final desired result. In addition, there is always the open question of deciding upon the best locations of the driver sources. Finally, the question of non-linear device operation is not addressed completely in this type of test.

A.2.6 Subsystem and component testing

Besides full-scale system testing, testing also exists at the subsystem (i.e. "black-box") level and at the component level. In this test, a piece of electronic equipment or perhaps even a discrete component within the equipment is tested for its response. In doing this the HEMP stress at the component should be determined, either from a test or by analysis.

This type of test is advantageous because component testing is relatively inexpensive and is rapidly conducted. Furthermore, if the component or equipment fails, hardening procedures can be determined by analysing the mode of failure of the device.

However, the major disadvantage of this type of testing is that it is difficult to ensure that the component is tested with the same electrical stress that would be found under HEMP excitation conditions. The HEMP stress inside a complex system is difficult to know exactly without performing a system level test. (If such a test were to be performed, then there would be no need to perform a component test.) Typically, the HEMP stress at a component is usually determined by analysis, and this is then used to design the proper pulse or CW excitation of the component.

A.3 Definition of the testing interface

A key aspect of testing is the definition of the testing interface within the system. This can be thought of as the location at which the simulated HEMP stress shall be applied to the system. It is generally recognized that an electrically complex system can be represented by a series of shielding surfaces, or "EM barriers," which are penetrated at selected points by one of several "EM penetration mechanisms," such as diffusion, aperture penetration or conducting penetration. Figure A.1 illustrates such a diagram for a generic electrical system, showing regions of different HEMP-induced electrical stresses (within the horizontal lines), together with the various coupling paths and penetration mechanisms.

It should be noted in Figure A.1 that the HEMP interaction with the system has been divided into two parts: one which deals with penetrations through the shielding barrier by diffusion and apertures, and another part dealing with penetrations along deliberately made conducting paths, such as signal lines, control lines, power lines, etc. This standard deals with testing concepts for the first type of penetration, namely test methods for shielding enclosures. IEC 61000-4-24 discusses the test methods for protective devices for HEMP-conducted disturbances, which concentrate on test methods for appropriate signal injection onto the signal and/or power leads of equipment, as indicated in Figure A.1.

Testing of the shielding of the system can be conducted at any one of the interface locations denoted by the letters A through H, which move progressively into the system. These interface locations are not actual "test points", as they do not refer to specific locations on cables or components in the system. Rather, they denote generic locations of possible test points within the system. The most straightforward testing is at interface point A at the exterior of the system, where the excitation is due to the external E- and H-fields produced by the HEMP. At this location, it is necessary to simulate the behaviour of the incident HEMP fields over the entire system (plus any reflected fields from nearby objects, such as a ground plane). If this simulation is carried out properly, the response of the system will be comparable to that of the system under HEMP illumination.

Interface point B is still located on the exterior of the system, but it occurs after the incident field has coupled to the system exterior and induced currents and charges on the exterior shield. Thus, the system excitation at this point is one step removed from the incident field. As noted in Figure A.1, HEMP stress at this level of the interaction diagram can penetrate into the system through apertures, diffusion, or by conductive penetrations, often referred to as points of entry (PoEs). In the field-illuminated case, all of these penetration mechanisms are excited simultaneously by the incident field. In the testing at interface level B, however, each penetration is usually tested separately, due to the size of the system. Consequently, testing at this level gives rise to potential errors, not only because of a more complicated requirement on the temporal behaviour of the excitation sources, but because PoEs are usually not all tested at the same time.

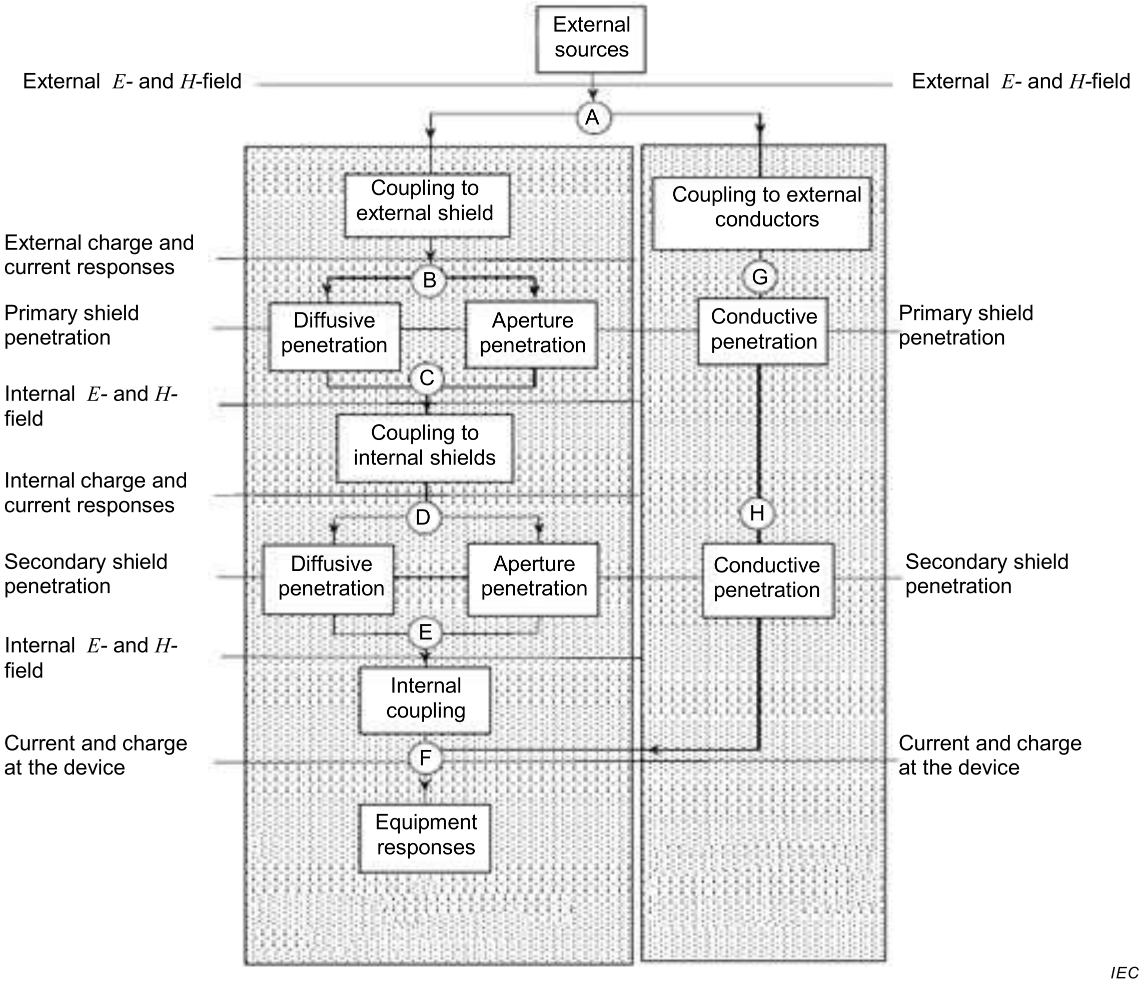

Figure A.1 – Sample HEMP interaction diagram illustrating penetration mechanisms, system responses and generic test interface locations

The necessary test excitations at this location can be described in terms of an injected current density and a corresponding charge density on the surface of the shield, or, if long conductors are considered, the sources are external currents and voltages relative to a suitable reference conductor (ground plane). Because the behaviour of these electrical responses depends on the nature of the HEMP excitation and on the electrical nature of the exterior of the system, these responses are more complicated than are the required simulation sources at location A.

Moving further into the system, interface point C is a field point at a location just inside the penetration points of the primary EM barrier. At this location, the HEMP responses consist of the local E- and H-fields within the shield. These fields propagate into the interior of the system, and couple to the surfaces of secondary shields in the system. These shields usually consist of the enclosures of individual boxes or equipment racks and the shields of cables. This gives rise to local current and charge on the inner shielding surfaces, denoted by interface D. The responses at D contain all of the effects of internal cavity resonances, internal cable resonances, local field perturbations due to internal loading and a myriad of other complications arising from a realistic system.

Finally, the currents and charges at D penetrate through the secondary shielding layer, again by diffusive or aperture type penetrations, to create internal excitation E- and H-fields at location E. These fields couple to internal cables or wires and eventually lead to test interface F at the component or "black-box" level.

HEMP testing can be performed at any one of the aforementioned interface locations. However, the deeper the test interface is located within the system, the more difficult it is to accurately describe the HEMP stress needed to apply to the test. Thus, there will be considerable uncertainty in the test results for internal test interfaces. However, the closer the test location is to the components, the more accurate is the knowledge as to the behaviour of the components or black boxes due to the stress. Consequently, one trade-off that occurs in HEMP testing is choosing between the ease of describing and simulating the desired stress on the system, and the accuracy of knowing the response of the system to this stress.

As mentioned earlier, there is an additional coupling path arising from the conducting penetrations through the shields, and these give rise to testing interface points G and H. Although these are not discussed further in this standard, they are shown in Figure A.1 for completeness.

A.4 Use of test data

A.4.1 General

Data acquired under test programs can have several different uses, depending on the nature of the test and on the functional requirements of the system. Different uses of test data are summarized below.

A.4.2 Acceptance of new systems

A new system which is designed to be hardened against the effects of HEMP will have one or more hardness specifications for the design. At the end of the construction of the system and just before formal delivery by the manufacturer, it is common to require an acceptance test to demonstrate that the system meets the required HEMP specifications.

The data acquired in test programs can be used for acceptance purposes. Such tests can be simple "proof" tests where the survivability of the system is validated, or they can amount to detailed measurements of stress levels at the defined interfaces and a verification of safety margins by determining the strength of critical components or critical inputs to subsystems.

A.4.3 System assessments

For a system that is not subject to HEMP survivability requirements, or which has not been previously tested, a test program can provide data useful for assessing the current state of HEMP hardness. This amounts to making detailed measurements of HEMP-induced stress at the defined interface points and then comparing these stresses with the known (or estimated) susceptibility of the components. This comparison of the stress/response characteristics permits an estimation of the system behaviour.

A.4.4 Hardness surveillance monitoring

Once a system is determined as hardened against HEMP, periodic measurements of the system can be made to ensure that the state of hardness remains intact. Frequently, such measurements consist of CW transfer functions from an observation point outside the system to one inside. Changes in this transfer function over a period of time indicate a degradation in the hardness of the system or a reduction of the safety margin.

A.4.5 System design

Another use of test data is in the area of new system design. Experience in system testing can lead to an understanding of how better to harden equipment and how to design, from the ground up, a HEMP hardened system. In addition, component testing (or laboratory "bench" testing) can provide information about component and subsystem responses to HEMP transients that can ultimately be useful for system-level testing and assessments.

A.5 Testing uncertainties

In each of the testing concepts described above, there are uncertainties which add errors to the final test results. Generally, these errors are difficult to know quantitatively, but a list of the uncertainties will at least help the test personnel to be aware of potential difficulties with the testing. Significant uncertainties can result from the following:

a) A lack of knowledge of the incident HEMP environment, as described by its angle of incidence and polarization relative to the earth.

b) The variability of the HEMP waveform as a function of the system location on the earth, and the inability to simulate this waveform precisely because of

   1) non-ideal spatial variations of the simulated HEMP field;

   2) an imprecise knowledge of the electrical properties of the ground;

   3) errors in the calculations for extrapolating a low-level response to HEMP levels;

   4) measurement errors;

   5) lack of precise information of the failure levels of components;

   6) unknown degradation of the system hardness over time.

c) A final source of uncertainty in the test process is often introduced by the desire to know too much from a single limited test. Only a finite number of excitations can be considered in a test, and consequently, any statistical inference about the probability of system survival against HEMP will be incomplete. Furthermore, even if one system is thoroughly tested and characterized, it is difficult to extrapolate the results to an ensemble of similar systems. Each system can be (and usually is) electrically distinct from the others, and consequently, the details of the HEMP responses can vary considerably from system to system. This is why the use of a safety margin in hardening is useful.

Annex B
(informative)

Characterization of shielded cables

B.1 Fundamentals of cable shielding

In its simplest configuration, a shielded transmission line system consists of a cable with the shield connected to each of the enclosures. The enclosures and the cable are usually located over a conducting ground plane with the cable at a height h. As shown in Figure B.1, the two enclosures are connected to the ground plane by external impedances $Z^{(e)}$ so that either a grounded or open-circuit configuration can be considered.

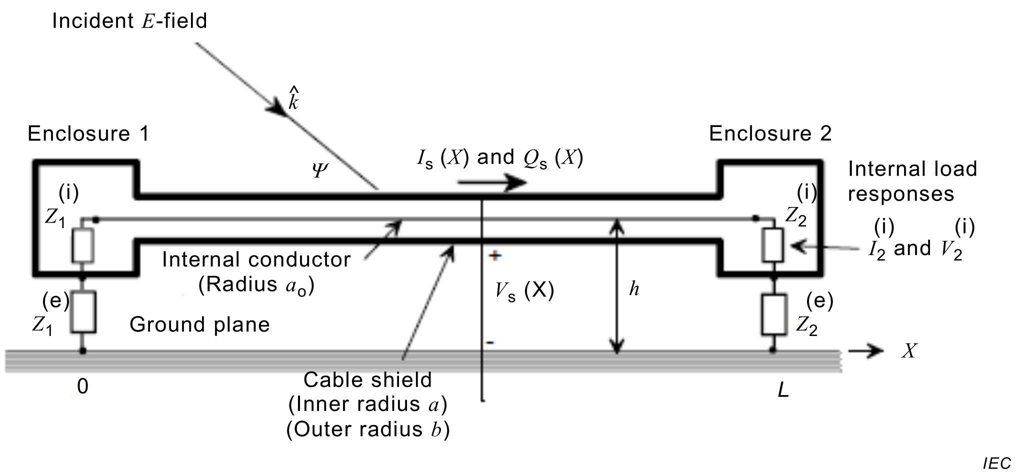

Figure B.1 – Geometry of a shielded coaxial line with an internal circuit

For a shielded cable illuminated by an electromagnetic field, the external electric and magnetic fields can penetrate through imperfections in the cable sheath and give rise to disturbing currents and voltages on the internal conductors. Annex B does not cover additional field penetration that may occur through the enclosures at either end of the line.

The coupling through the cable shield between the external electromagnetic field and the inner conductors occurs through three basic phenomena:

– diffusion of the E- and H-fields through the sheath material;

– penetration of the fields through the small apertures of the braided shields;

– a more complicated induction phenomenon due to the overlapping of the individual strands (or carriers) of the shield.

The last two phenomena occur only for braided shields.

The behaviour of the induced response on the inner conductors of a shielded cable can be described in terms of a transfer impedance Z_t and a transfer admittance Y_t of the shield. To understand the transfer impedance and admittance concepts, a time-varying external EM field which induces both a cable sheath current I_s and a sheath-to-ground voltage V_s (or equivalently, a sheath charge density) is considered. Portions of the external electric and magnetic fields are able to penetrate through the shield, and these induce internal voltage and current responses, V_i and I_i, respectively. These quantities and their assumed polarities are shown in Figure B.1. For this conductor system, a return current I_g flows in the ground; this current is the sum of I_s and I_i.

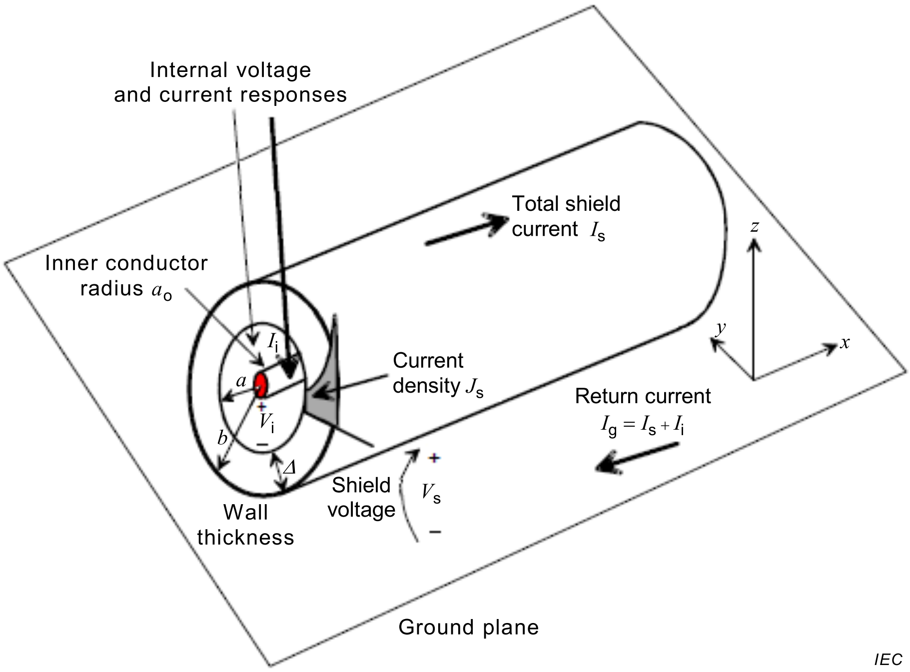

Figure B.2 – Coaxial cable located over a conducting ground plane

The current flow in the cable sheath creates an axial electric field inside the sheath. Due to the skin effect, the current distribution and the associated electric field distribution in the sheath cross-section are not uniform. If I_s is the total current flowing in the sheath, the electric field E_i on the inner surface of the shield is produced by an attenuated current density, with the reduction being determined approximately by δ, the skin depth in the shield material, given by

$$\delta = \sqrt{1/(\pi f \sigma \mu)}\ \text{m} \tag{B.1}$$

where

σ is the conductivity of the sheath material;

f is the frequency of the induced current;

μ is the permeability of the sheath material.

This axial electric field component on the inner surface of the sheath creates a voltage between the internal conductors and the sheath, and, depending on the termination impedances of the inner signal conductor, a current may flow. The protection capability of the cable shield is determined by the amount of reduction of the electric field component due to the skin depth attenuation. This reduction capability is determined more precisely in Clause B.2 through the concept of a transfer impedance, which is defined as the ratio between the inner electric field E_i and the total shield current I_s in the frequency domain.

The electrical dual of the transfer impedance is the transfer admittance, which describes the process by which a portion of the induced charge on the cable sheath finds its way onto the internal wire inside the shield. This induction of charge on the inner conductor amounts to an injected current on the internal cable. This effect can be related to the external shield-to-ground voltage V_s by a transfer admittance.

B.2 Definitions of transfer impedance and transfer admittance

The cable sheath with its external return (generally a ground plane) and the internal conductor form two coupled circuits, as shown in Figure B.2. Figure B.3 shows two per-unit-length circuits formed by the sheath and its ground return, and the sheath and the internal conductor. In this development it is assumed that the external circuit is independent of the behaviour of the internal circuit, and that the internal circuit has both a voltage- and current-controlled source providing the excitation from the external circuit. This circuit configuration results from the assumption that the cable performs as a good shield.

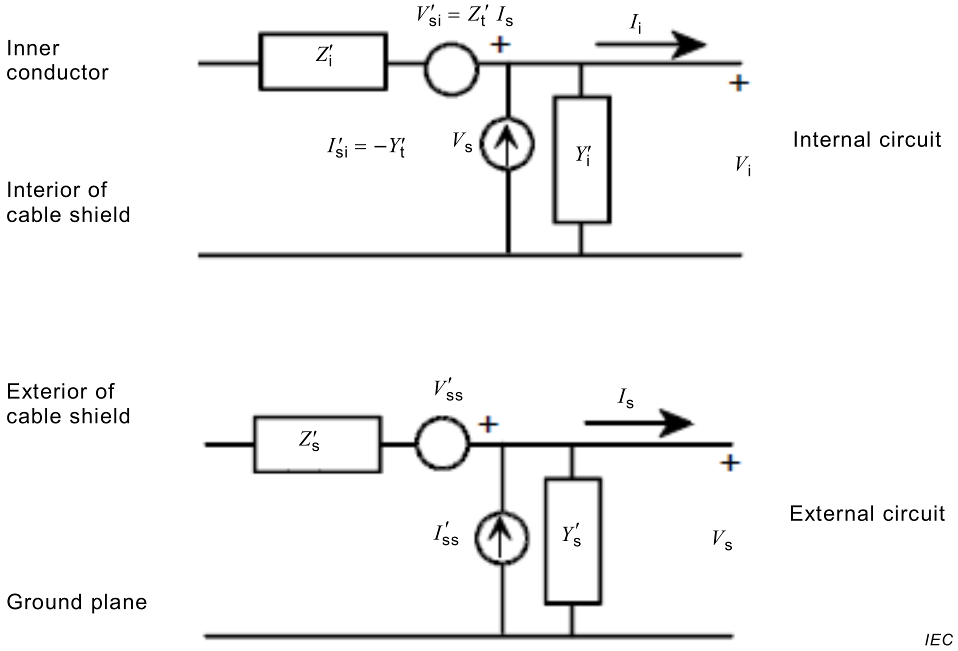

Figure B.3 – Two per-unit-length circuits formed by the sheath and its ground return, and the sheath and the internal conductor

For these two coupled lines, the current and voltage I_s and V_{ss} of the outer shield and the current and voltage I_i and V_i of the inner conductor are described by the following set of differential equations:

External circuit $$\frac{dV_s}{dx} + Z'_s I_s = V'_{ss} \text{ V/m} \quad (B.2)$$

$$\frac{dI_s}{dx} + Y'_s V_s = I'_{ss} \text{ A/m} \quad (B.3)$$

Internal circuit $$\frac{dV_i}{dx} + Z'_i I_i = V'_{si} \text{ V/m} \quad (B.4)$$

$$\frac{dI_i}{dx} + Y'_i V_i = I'_{si} \text{ A/m} \quad (B.5)$$

In these expressions, the external transmission line is described by the per-unit-length impedance and admittance parameters Z'_s and Y'_s, which for a lossless line are related to the external per unit length line inductance and capacitance quantities by $Z'_s = j\omega L'_s$ and $Y'_s = j\omega C'_s$. Similarly, for a lossless cable the internal line parameters Z'_i and Y'_i are related to the internal per unit length line inductance and capacitance by $Z'_i = j\omega L'_i$ and $Y'_i = j\omega C'_i$.

The primary excitation sources in this problem are the distributed voltage and current sources V'_{ss} and I'_{ss} on the external circuit. The excitation sources for the internal circuit are the voltage and current sources shown in Figure B.1 and are denoted by V'_{si} and I'_{si} respectively. These internal sources are related to the external line responses by

$$V'_{\mathrm{si}} = Z'_{\mathrm{t}} I_{\mathrm{s}} \text{ V/m} \tag{B.6}$$

$$I'_{\mathrm{si}} = Y'_{\mathrm{t}} V_{\mathrm{s}} \text{ A/m} \tag{B.7}$$

where

Z'_{t} *and* Y'_{t} are the transfer impedance per unit length and transfer admittance per unit length of the shield.

These quantities may be formally defined from Equations (B.4) and (B.5) by setting I_{i} and V_{i} to zero, as

$$Z'_{\mathrm{t}} = \frac{1}{I_{\mathrm{s}}} \frac{dV_{\mathrm{i}}}{dx}\bigg|_{I_{\mathrm{i}}=0} \ \Omega/\text{m} \tag{B.8}$$

$$Y'_{\mathrm{t}} = \frac{1}{V_{\mathrm{s}}} \frac{dI_{\mathrm{i}}}{dx}\bigg|_{V_{\mathrm{i}}=0} \ \text{S/m} \tag{B.9}$$

In the definition of the transfer impedance in Equation (B.8), the resulting parameter Z'_{t} depends only on the electrical and physical composition of the shielded cable. This is not true for the transfer admittance in Equation (B.9), however, because the external shield voltage, V_{s}, depends on the geometry of the external conductor. More specifically, the transfer impedance depends on the external capacitance of the cable shield to the reference ground plane.

An alternative to evaluating the internal current excitation source as in Equation (B.7) is to consider the pertinent external response to be the external charge density on the cable shield, q'_{e}, instead of the external shield-to-ground voltage. In this manner, the internal current source can be written as

$$I'_{\mathrm{si}} = -j\omega C'_{\mathrm{i}} S_{\mathrm{s}} q'_{\mathrm{e}} \tag{B.10}$$

where

C'_{i} is the per-unit-length capacitance of the internal line;

S_{s} is a shield leakage factor (measured in m/F) which depends only on the shield characteristics.

Typically, the shield leakage factor S_{s} is the more desirable indicator of cable shield behaviour, as it is independent of the external line geometry. However, measurement techniques frequently provide a direct knowledge of Y'_{t} instead of S_{s}. Once Y'_{t} is known for a particular test set-up, the actual cable shield parameter can be determined by the expression

$$S_s = \frac{1}{j\omega C_i'} \frac{Y_t'}{C_e'} \tag{B.11}$$

B.3 Relative significance of Z'_t and Y'_t

The definitions of the transfer impedance and admittance of the cable shield in Equations (B.8) and (B.9) as described above are valid for both solid tubular and braided cables. For a solid tubular shield, the electrostatic shielding is much greater than the magnetostatic shielding, and, as a result, the transfer impedance term dominates at low frequencies. This fact has led some investigators to neglect the transfer admittance term in EMC coupling problems.

For braided cables, the coupling mechanisms giving rise to the transfer impedance and admittance are enhanced, due to the E- and H-field penetration through the shield apertures. Again, at low frequencies, the electrostatic shielding of the braid is much better than the magnetic field shielding, and Y_t' is usually small compared with Z_t'. However, as the frequency increases, both the E- and H-fields are able to penetrate through the braid apertures. In this case, the induced effects on the inner conductor from both field components can be of the same order of magnitude. For shields that are not well designed to exclude the E-field, neglecting the transfer admittance may lead to roughly factors of 2 error in the estimated internal responses.

Annex C
(informative)

Equipment for HEMP pulse measurements

C.1 General

Over the years, specialized equipment has evolved for performing fast transient measurements on systems. This equipment falls into three broad categories:

1) sensors designed to measure a transient response;
2) data links to transmit the measured information from the test point to an analysis station;
3) transient recording device capable of storing the measured data.

For each of these components, considerable effort has gone into their design and performance optimization. Considerations have included the following:

– sufficient bandwidth to accurately measure the fast HEMP-induced transients;
– minimal phase distortion to maintain the integrity of measured pulse shapes;
– minimal end-to-end loss in the measurement chain to provide a high signal-to-noise ratio;
– standard calibration of the measurement probes and sensors.

Annex C provides basic information on the key elements of a HEMP pulse measurement system.

C.2 Sensors for HEMP measurements

C.2.1 *B*- and *H*-field sensors

Sensors for measuring the transient magnetic field are essentially small loops which may be configured in such a way as to minimize any additional response that the *E*-field may induce on the sensor. All of these sensors create a voltage across the loops that is proportional to the time rate of change of the magnetic flux passing through the loops. Thus, they are often referred to as *B*-dot sensors, as they actually respond to the derivative of the *B*-field.

Figure C.1 illustrates several common configurations for such measurement loops. The first two (on the top of the figure) are configured to work in conjunction with a reference conductor as a ground plane. Hence they can provide an indication of induced surface current flowing on the conductor. The others are for operation away from a reference conductor, and thus they measure the "free-field" response of the *H*-field.

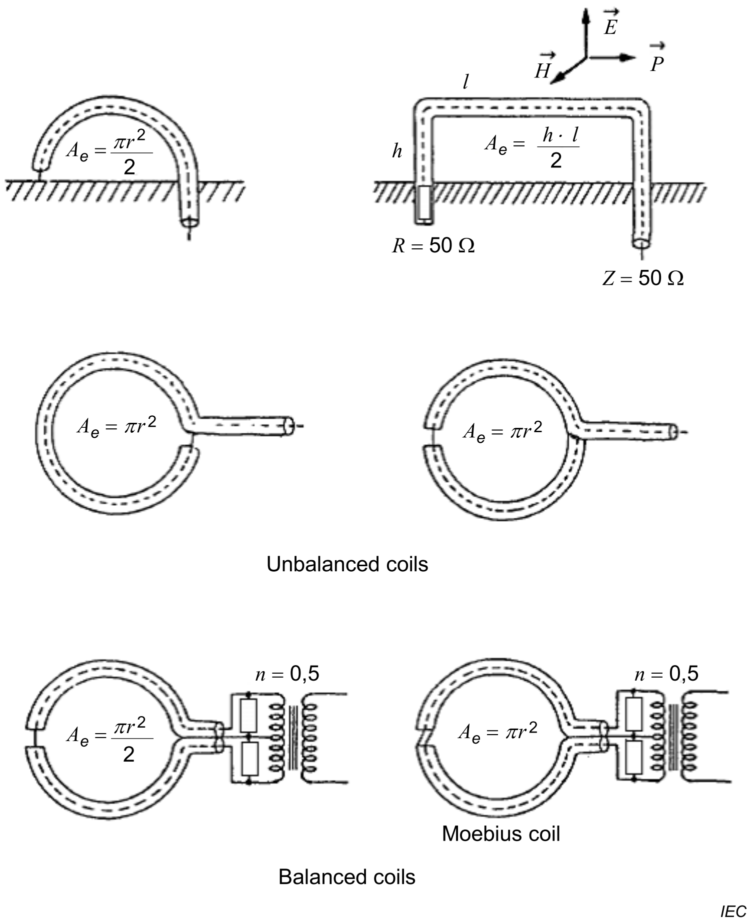

Figure C.1 – Magnetic field sensors [23]

Other types of coil configurations are also found in H-field HEMP sensors. Figure C.2 illustrates a cylindrical coil sensor having a single slot across which the induced voltage is measured with two shielded coaxial cables, providing a balanced output. Figure C.3 shows two- and four-gap configurations for the cylindrical coil.

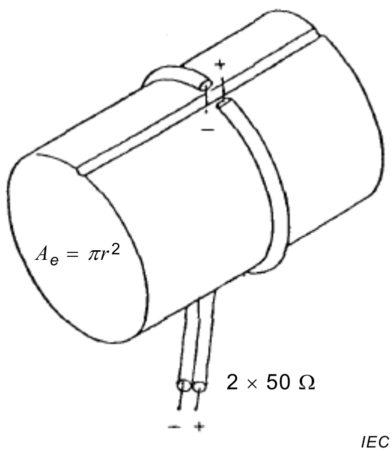

Figure C.2 – Single-slot, cylindrical coil sensor [23]

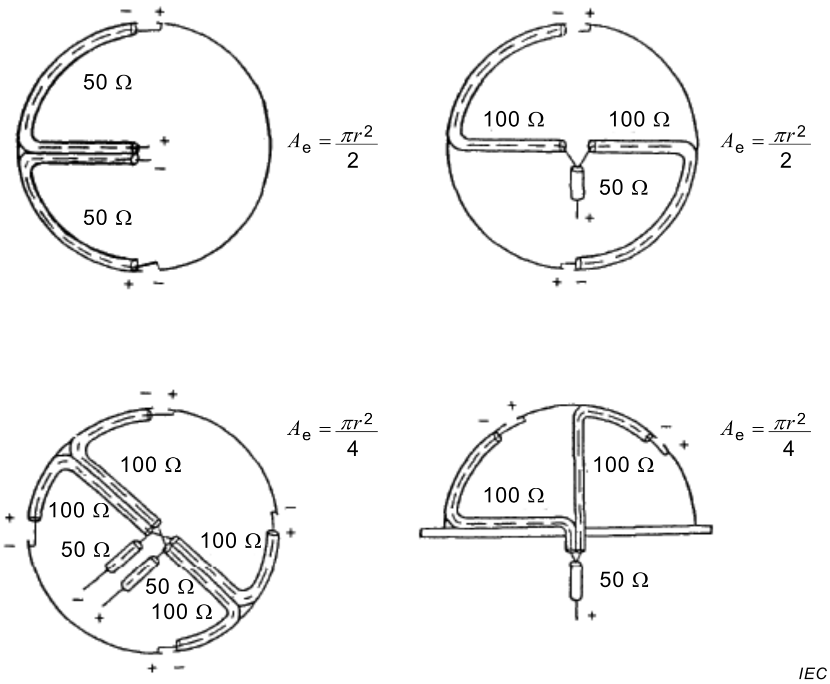

Figure C.3 – Two- and four-slot cylindrical coil sensors [23]

The basic limiting factor of these types of sensors is their size, since the sensor should be electrically small in order for it to function properly in HEMP tests. Large (~0,5 m diameter) sensors are available for measuring the B-fields in a range of 10 kHz to 30 MHz. Smaller sensors (approximately 10 cm diameter) are available for higher frequency measurements, typically with an effective bandwidth of 9 kHz to 150 MHz.

C.2.2 *D*- and *E*-field sensors

The basic configuration for an E-field sensor is shown in Figure C.4. The two plates, when immersed in a time-varying E-field, produce a short-circuit current that is proportional to the time rate of change of the field. This signal is often integrated (either passively as shown, or by an active integrator) to provide an indication of the actual E-field.

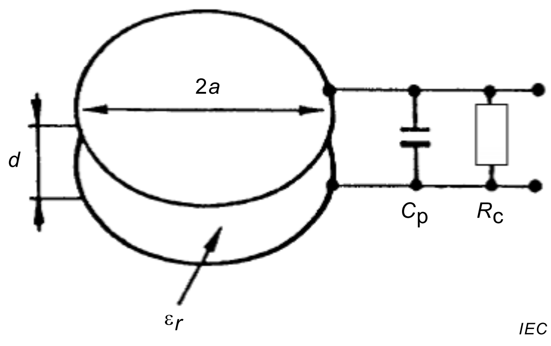

Figure C.4 – Electrical configuration of an *E*-field sensor [23]

E-field measurements made in free space usually use an antenna (or sensor) similar to that illustrated in Figure C.5. This sensor responds to the E-field component that is parallel to the long dimension of the antenna. This antenna can be relatively large (about 1,4 m in overall length) and this size limits the practical upper frequency response of the antenna to about 30 MHz, if frequency dependent calibration curves are not provided. However, in the event that the antenna manufacturer provides such a calibration factor relating the measured voltage at its terminals to the incident E-field at a specified frequency, this type of antenna can be used at frequencies up to about 200 MHz.

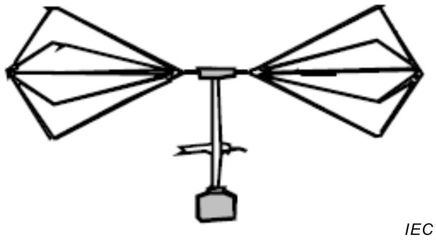

Figure C.5 – Biconical E-field sensor

Other types of smaller E-field sensors are possible. Figure C.6 illustrates a spherical dipole sensor which is used to measure the E-field on a conducting surface. Larger sensors of this type have a maximum frequency of about 45 MHz with a rise-time measurement capability of about 7,4 ns. Smaller units of this type have a maximum frequency of 150 MHz and a rise time of 2,3 ns.

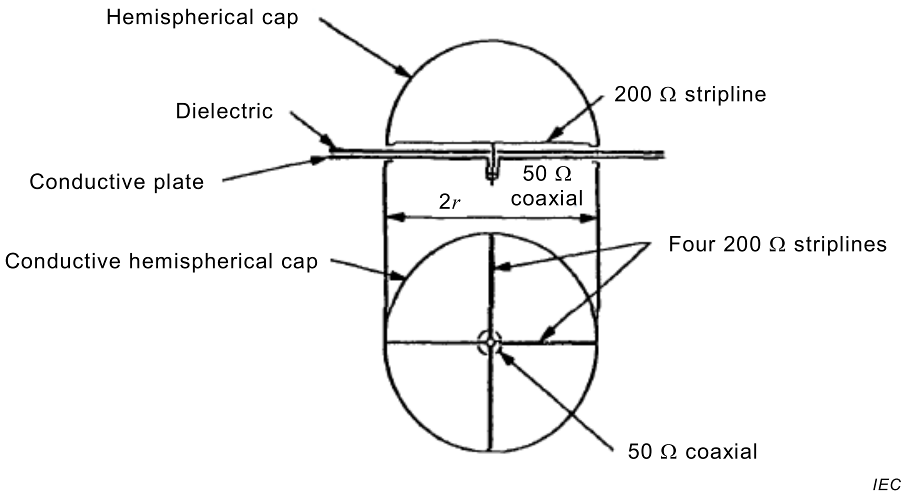

Figure C.6 – E-field sensor mounted on a conducting ground plane [23]

Other types of E-field sensors have rather odd cross-sectional shapes, as shown in Figure C.7. This is the asymptotic conical dipole (ACD) sensor which is designed to provide a known response by simply measuring some geometrical factor. This is known as "calibration by the ruler" and is only possible for a limited number of antenna shapes.

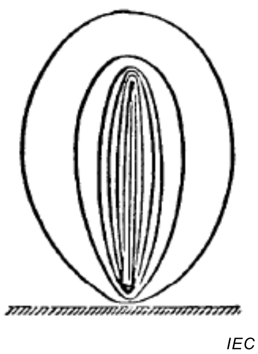

Figure C.7 – Equipotential shapes for an optimally designed E-field sensor [23]

C.2.3 Current sensors

Current sensors (or probes) are essentially small transformers which are clamped over a cable carrying a current and provide a voltage which is proportional to the current flowing through the cable. The operation of these devices is similar to that of a Rogowski coil, as pictured in Figure C.8.

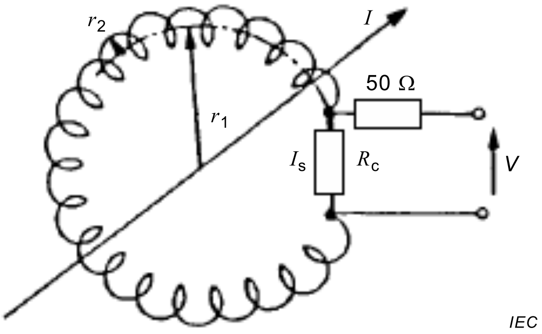

Figure C.8 – Rogowski coil used for current measurements [23]

Usually, these coils are made of a single-turn loop of high permittivity material to increase the measurement sensitivity. Figure C.9 illustrates this configuration, in which a voltage is induced across the slot in the high permeability toroid by the current in a wire passing through the hole in the sensor.

Typical realizations of these devices are the probes which use multiple voltage pick-up points as shown in Figure C.10. Large versions of these probes have a bandwidth of 100 kHz to 100 MHz. The smaller versions of these probes are of the "clip-on" type and can operate typically from 200 kHz to 300 MHz.

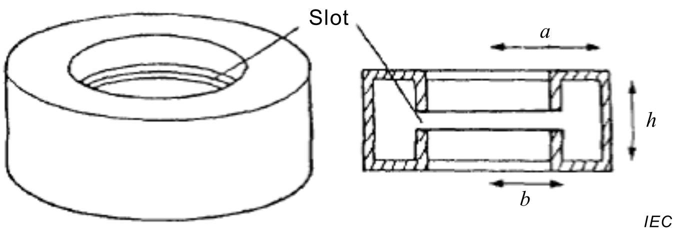

Figure C.9 – Toroidal current sensor made of magnetic material [23]

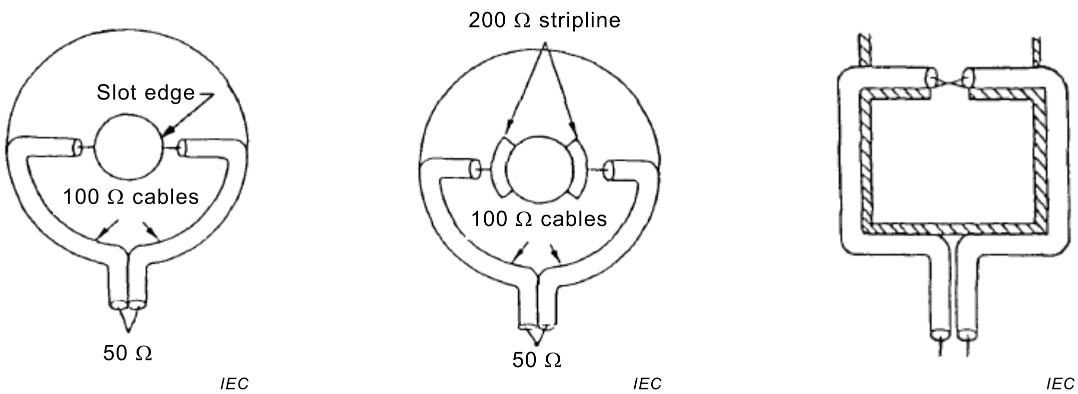

a) – Unbalanced at two points **b) – Unbalanced at four points** **c) – Balanced pick-up**

Figure C.10 – Voltage pick-up points on the edges of the toroidal sensor [23]

C.3 Signal transmission

C.3.1 General

Measured responses from the sensors should be relayed from the sensor to the measurement equipment. The preferred technique for doing this is to employ fibre optic links, because they have a minimal influence on the EM environment surrounding the test equipment.

C.3.2 Fibre optic links

Many different methods are used to transmit information in HEMP tests, for example wires, coaxial cables, waveguides and radio. For the highest quality signal transmission, hard-wired electrical connections from the sensors to the transient digitizers should be used. However, such wires can also pick up part of the HEMP signal and corrupt the responses of the sensors. Furthermore, the presence of long electrical cables inside a facility can distort the normal EM fields and may even introduce an inadvertent EM coupling path.

Weight is one of the main disadvantages of coaxial cables: the RG14 and RG19 cables weigh 350 kg/km and 1 100 kg/km respectively: a typical single-fibre cable weighs only 12 kg/km. This difference may become much more drastic in multichannel cables. Noise immunity is also a problem in coaxial cables. They are sensitive to the electric and magnetic fields generated by machinery, lightning or EMP. Ground loops and oscillations are also severe potential problems in coaxial cable systems.

As a result of these difficulties, the use of fibre optic links is often recommended for HEMP testing. The use of such links eliminates filtering and grounding problems, and minimizes to a few millimetres the aperture sizes for pass-through connectors in the shielding structure. An additional benefit is that the fibres are practically free from crosstalk: even if light is radiated by one fibre, it cannot be recaptured by other fibres.

Figure C.11 illustrates a single-channel fibre optic transmission system. Typically, there are actually two fibre channels: one for transmitting the signal, and another for controlling the settings of a signal attenuator located in the transmitter unit near the sensors.

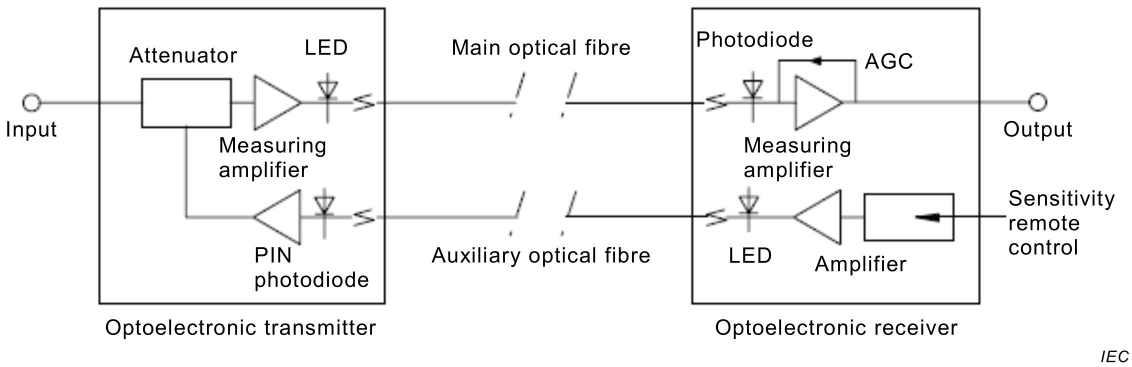

Figure C.11 – Example of a single-channel fibre optic transmission system [23]

Figure C.12 compares the attenuation and bandwidth characteristics of two RG type cables with those of typical fibres. The skin effect in a coaxial cable causes the attenuation to rise with the square root of the frequency, typically starting below 1 MHz. As a result, for very long coaxial lines, serious dispersion effects arise which should be corrected with filters.

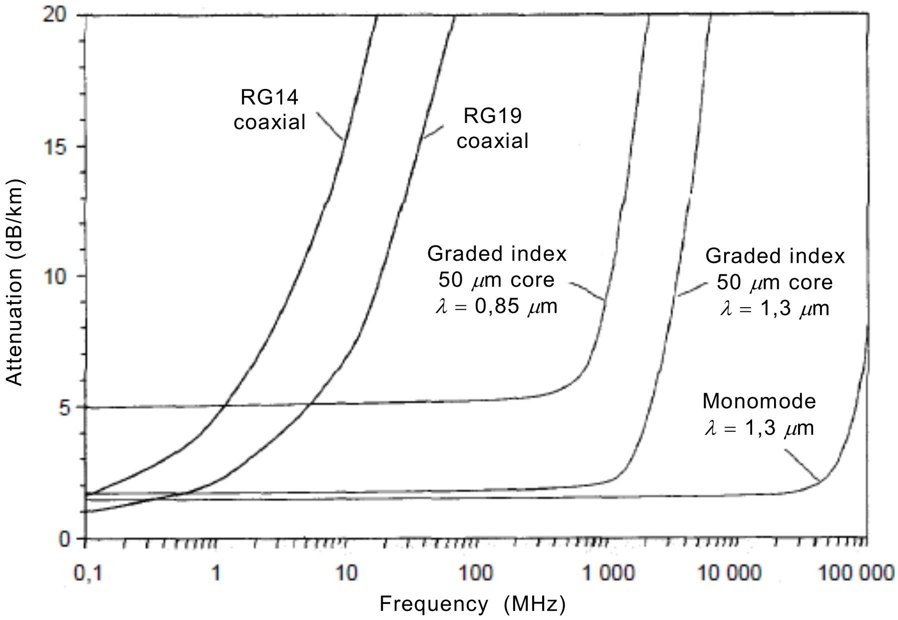

IEC

Figure C.12 – Attenuation of coaxial lines and fibre optic cables as a function of frequency

C.3.3 Fibre optic transducers

Transducers should be located at each end of the fibre optic cable to convert the electrical signals to modulated light beams, and to then convert the light back to electrical signals. Such units can take many forms, but the more modern units consist of a microprocessor controller and internal bus system which can house, power and control different modules. This permits the system to be tailored for specific applications.

A typical plug-in system consists of a base module fitting into the main unit, a fibre optic cable for signals, a fibre optic cable for control if necessary, one or two battery-powered, small-sized, shielded (more than 200 V/m CW and 100 kV/m pulsed electromagnetic fields) modules and one or two battery chargers. Each plug-in can be individually managed by the microprocessor control system inside the mainframe. Most modules are remotely controllable via a dedicated control optic link. These modules are powered by batteries which provide more than 8 h continuous operation. The maximum optic link length for standard models is 1 km.

A wide range of fibre optic plug-ins is available, providing a large selection of working modes (acquisition, telemetry, stimulation, EM field monitoring, audio and video transmissions), frequency ranges (from d.c. up to 1 GHz) and variable gain attenuation.

C.4 Signal detection and processing

The detected signal from the fibre optic transducer is digitized, processed and then archived. A number of different transient digitizers are currently available on the market. The one selected should be capable of measuring the leading edge of the fastest HEMP waveform that is to be measured. Typical rise-time requirements will be of the order of 1 ns. Furthermore, the digitizer should have an adequate dynamic range (number of bits in the representation of the digitized data) so as to avoid the digitization errors in the responses. Finally, the digitizer should have sufficient memory to be capable of measuring the complete transient response, from start to finish, without the requirement of having multiple digitizers sampling different portions of the same waveform.

The present-day capabilities of personal computers make it unnecessary to use the older, larger and slower computers that have traditionally been used for data acquisition and analysis purposes, both for pulse and CW testing. Similarly, the initial data processing (plotting and correcting) of the raw data and the subsequent extrapolation analysis can be performed on a PC using standard signal processing programs.

Annex D
(informative)

Equipment for CW testing

D.1 General

Annex D discusses the equipment and calibration techniques needed for conducting a CW test. Some of the equipment, such as the field sensors and the fibre optic links, is the same as that used for transient tests. However, other items such as the CW network analyser and the radiating antennas are different.

D.2 Antenna system

Several different types of radiating antennas are possible, depending on the desired polarizations and the frequency range of operation. For frequencies between about 1 MHz to 100 MHz, the antenna shown in Figure D.1a) radiates an E-field in the direction broadside to the antenna that is mainly horizontally polarized. At lower frequencies, the radiation efficiency drops and at the high-frequency end, the radiation field contains side lobes due to the large electrical size of the antenna.

The antenna is connected to the earth at both ends, through a resistance of the order of 400 Ω to 500 Ω. This electrical connection serves to enhance the low-frequency radiation characteristics of the antenna. The antenna is fed at its apex by a power amplifier which is connected via a coaxial cable. This unbalanced line should be matched to the balanced antenna input at the top of the dielectric support tower by a balancing transformer, referred to as a balun. Care should be exercised to ensure that during the testing the power level of the amplifier does not exceed the rated operational power level of the balun.

If a vertical incident E-field is desired, a vertical antenna can be employed. This is illustrated in Figure D.1b). A vertical conductor is fed by a voltage source between the antenna base and the ground, producing a vertically polarized E-field. At low frequencies (i.e. frequencies such that $\lambda >$ antenna length), the radiation from this type of antenna is very poor.

Figure D.1c) illustrates another type of radiating antenna, known as the P × M antenna. It appears as a simple end-fed transmission line, having a load at the end equal to the characteristic impedance of the line. This line has the beneficial property of radiating an EM field having a characteristic impedance of exactly 377 Ω – even at very low frequencies. This radiation occurs in the "backward" direction, that is to say, to the right of the source in Figure D.1c). This antenna is effective in this manner only for low frequencies, however. As the frequency begins to increase so that $\lambda >$ the line length, the beam of the radiation begins to move to the forward direction and the antenna becomes the well-known Beverage antenna.

For both horizontal and vertical antennas, it is important to add resistive loading along the wires. This resistance serves to damp out the natural antenna resonances, thereby creating a smoother radiated field spectrum. In addition, by properly choosing the level of impedance loading on the antenna, the E/H ratio of the fields near the antenna can be made more like that of a plane wave in free space, namely 377 Ω.

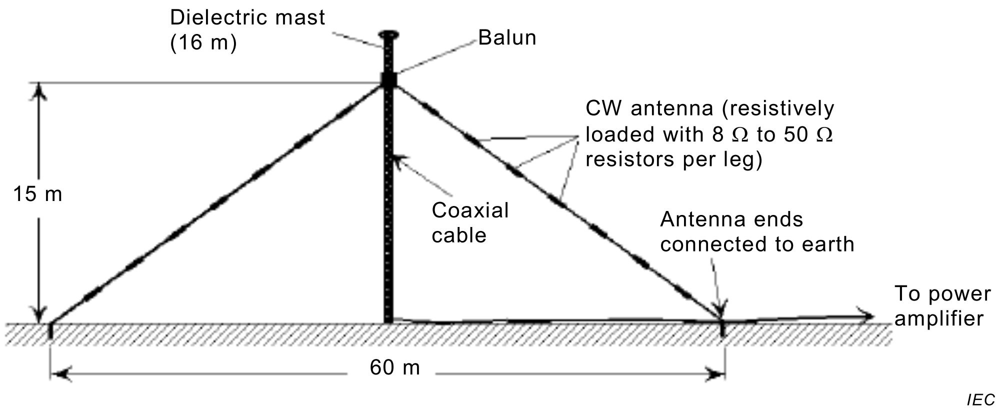

a) Horizontally polarized antenna

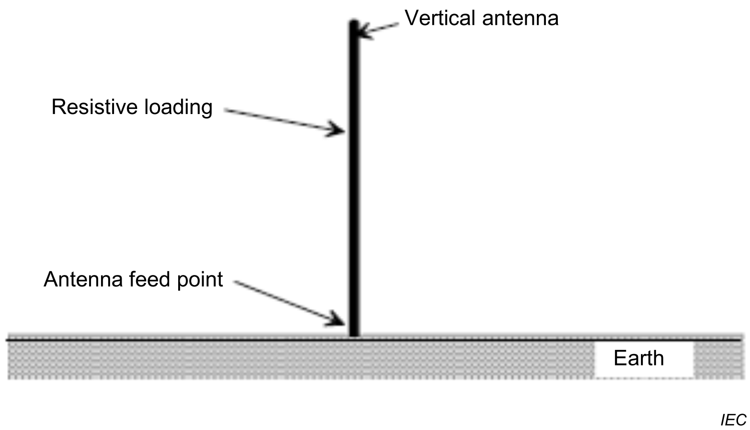

b) Vertically polarized antenna

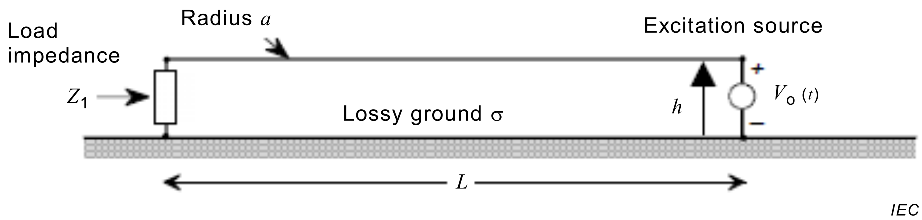

c) P × M antenna

Figure D.1 – Various antennas for CW testing

As the presence of the antenna feed cable can perturb the radiated fields, care should be used in locating the cable near the antenna. For optimal performance, the cable should run directly down the support mast and then out from the antenna in a perpendicular direction to the antenna broadside. Periodically placed ferrite beads on the exterior of the coaxial cable can help to eliminate unwanted coupling effects to this cable.

CW antennas are used to provide an incident CW field on the system under test that approximates a plane wave. As shown in Figure D.2, the angle of incidence of the simulated HEMP field, denoted by the angle ψ, is defined by the angle from the top (apex) of the antenna down to the facility under test. Thus, the location of the antenna relates to the angle of incidence of the HEMP being simulated.

For the simulated EM field to appear as a plane wave, the antenna should be located as far from the facility as possible. Specifically, the distance d in Figure D.2 should be larger than the typical dimensions of the facility under test. In addition, the distance d should be larger than the dimensions of the antenna. Often these requirements cannot be met, due to the large size of the facility. It should be noted that this difficulty concerning antenna placement also occurs in pulse testing.

If the facility being tested is very large and the antenna cannot be located so that d is larger than the facility dimension, the CW test can be conducted using the PARTES concept discussed in annex A. This involves determining the principal points of entry (PoEs) of the facility and locating the antenna so that this part of the facility is suitably illuminated by the simulated plane-wave excitation from the antenna.

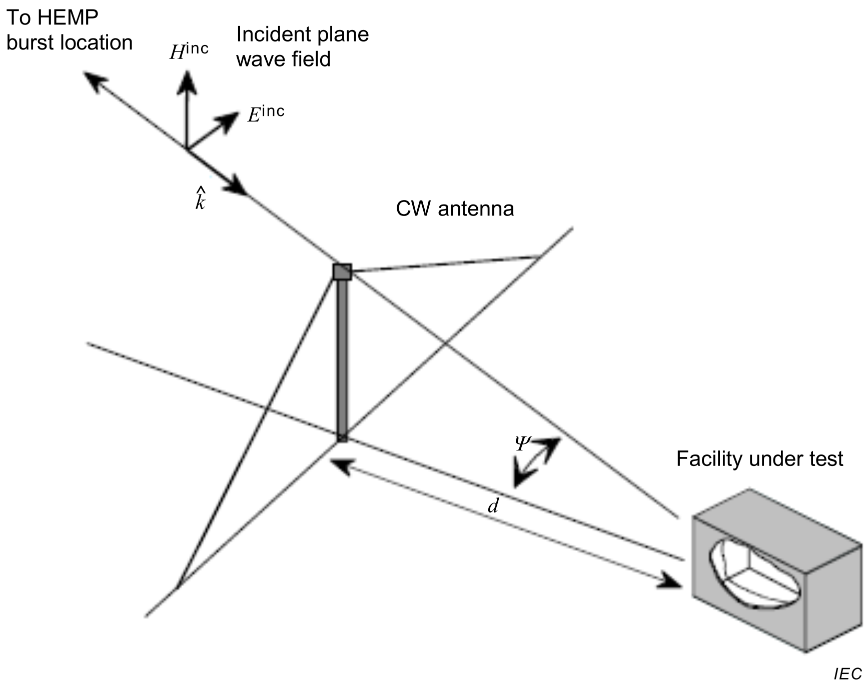

Figure D.2 – Relationship between the CW antenna and the incident HEMP field

In addition to the proper placement of the antenna, there is a need to locate the antenna power amplifier, the motor-generator unit and the measurement equipment (network analyser). As discussed earlier, the location of this equipment should be chosen in such a way that the EM fields produced by the antenna do not severely interact with the equipment and cause perturbations in the measured results. This implies that all conducting cables should be run closely to the ground and in such a direction that they are orthogonal to the E-fields produced by the antenna. If possible, the measurement equipment should be located away from the facility or in a separate shielded enclosure to minimize the effects of direct EM interaction with the antenna fields.

D.3 Power amplifier

The power amplifier takes a low-level CW signal from the network analyser as an input, amplifies it to a power level of the order of 50 W to 100 W, and then feeds the signal to the CW antenna through a 50 Ω coaxial cable. A typical amplifier operates from a low frequency of 10 kHz to a high frequency of 250 MHz. The frequency of the signal provided to the amplifier is swept over a range of frequencies by the network analyser. The amplifier should not be overdriven at its input by the analyser, and the output power should not overdrive the antenna balun, which would result in possible damage to the balun coils.

The power amplifier is located near the base of the antenna so that the feed cable from the amplifier to the antenna balun is as short as possible.

D.4 Receiver (network analyser)

The receiver for this system is typically a network analyser. For this application, the network analyser is swept from approximately 10 kHz to 200 MHz in a mode that is controlled by the computer connected to the analyser through the IEEE bus. The network analyser provides a low-level, 50 Ω sinusoidal output as it sweeps through the designated frequencies, which serves to control the aforementioned power amplifier.

Two input channels to the network analyser are used: one is the reference channel from the reference sensor located on the exterior of the facility and the other is the measurement channel which is connected to a suitable measurement sensor or probe, normally located inside the facility. As noted in Figure 22 in 5.2.3.2, these sensor connections should be made with fibre optic transducers, so as to eliminate electrical coupling with the measurement equipment.

The network analyser provides a transfer function for the measurement $T(\omega)$, which is a complex valued quantity defined at each angular frequency ω by a magnitude and a phase. The phase quantity provides information of the relative times of arrival of the responses at the sensors and shall be retained for high-quality CW measurements. Frequently, when CW test results are presented, only the magnitude of the response is plotted and discussed. The phase is equally important, but it is often omitted in discussion.

D.5 Reference and response sensors

Many of the same sensors used for transient HEMP testing can be used for CW testing. Annex C provides information about these sensors. An important aspect of the CW test configuration is the proper location of the reference sensor. The purpose of having a reference sensor measurement is to provide a way of relating the measured results in the facility using the CW antenna to the response that would be obtained if the excitation were an incident plane wave. Thus, it is necessary to understand how the reference sensor is excited.

As shown in Figure D.3, the response measured by the reference sensor consists of an incident wave contribution plus a contribution reflected from the ground. This resulting field is the total excitation field at the sensor. If the reference sensor is located far from the CW antenna, it can be seen that the direct and ground-reflected rays from the antenna apex (i.e. from the driving source on the antenna) will have about the same path length as will the contributions for the equivalent incident HEMP plane wave. In this case, the response of the sensor will be easily related to the response of a plane-wave excitation. However, if the sensor is too close to the antenna, the sensor response for the CW case will be different from that of the plane-wave excitation. A general rule of thumb is that the reference sensor should be located at a distance equal to several antenna lengths away from the antenna.

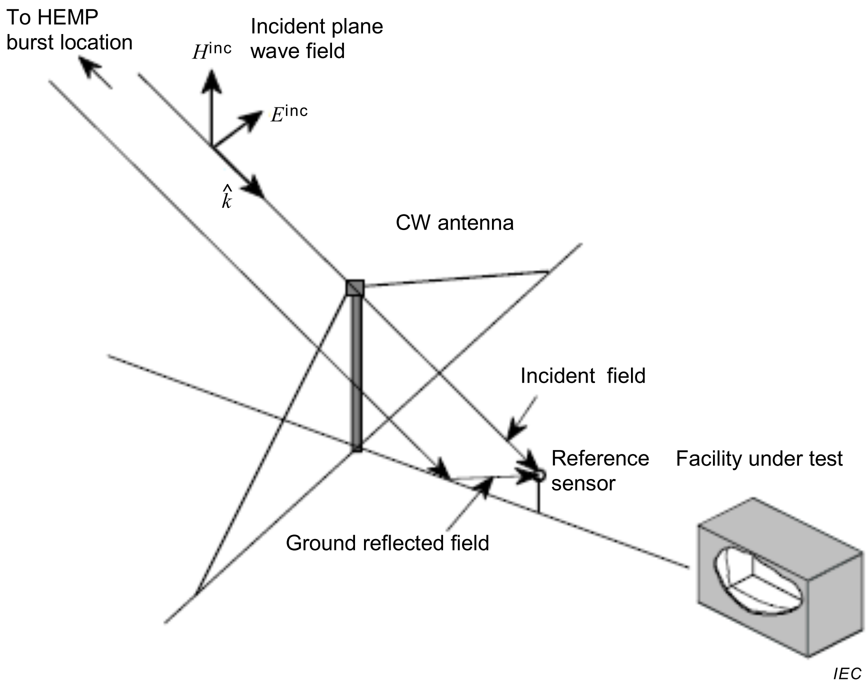

Figure D.3 – Incident and ground-reflected field contributions to the reference sensor excitations

There is another important rule in locating the reference sensor: it should not be located close to other conducting structures which can contaminate the local EM fields. This implies that the reference sensor should not be located too close to the facility under test.

Figure D.4a) serves as an example of this, by illustrating the measured H-field reference sensor spectrum taken in an actual CW test. This response was taken using equally spaced sample points and exhibits a very rapid fall-off of the response at high frequencies due to the sensor limitations. The resonances in the response are due to antenna resonances and reflections from nearby objects. The first null in this total field response due to the reflection in the groundplane occurs at about 200 MHz, and this also accounts for the high-frequency fall-off of the spectrum.

Figure D.4b) illustrates the delta-function response of this spectrum, obtained by taking the inverse Fourier transform of the spectrum. This transient response clearly illustrates the initial response of the sensor, arriving with a time delay determined by the antenna and reference sensor geometry and the details of the fibre optic cables. Later in time, smaller impulses arrive at the sensor. These have been reflected from a nearby building and should be eliminated if possible by moving the sensor further away from the building.

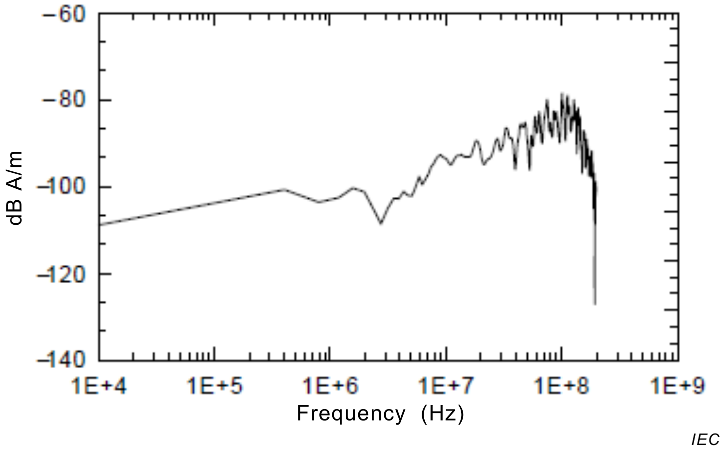

a) Measured *H*-field spectrum

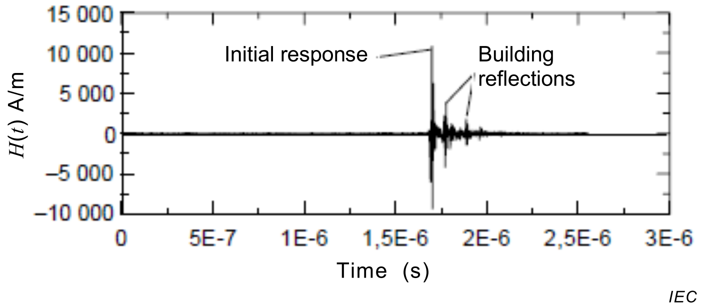

b) Computed delta-function response from spectrum

Figure D.4 – Measured reference *H*-field spectrum and its inverse Fourier transform

D.6 Fibre optic system

As in the transient test case, a fibre optic system for extracting the reference and response signals from the system and carrying them to the network analyser is needed. Characteristics of this transmission system are provided in Annex C.

After the location of the reference sensor has been determined, it is necessary to calibrate the measurement chain. This is important, as it corrects any differences in the sensor magnitude responses, but it also removes any unwanted phase shifts in the responses. These phase shifts amount to time shifts in the transient response and can cause errors in data interpolation if they are present in the measured data.

The calibration is accomplished by locating the measurement sensor next to the reference sensor and making a sweep of the spectrum. Figure D.5a) illustrates the results of such a measurement. Denoting the reference spectrum for the calibration process as $R_o(\omega)$ and the calibration response spectrum as $S_o(\omega)$, a transfer function between the two is defined as

$$T_o(\omega) = \frac{S_o(\omega)}{R_o(\omega)} \tag{D.1}$$

This derived transfer function is illustrated in Figure D.5b). Because the two sensors are not identical and because they are in slightly different locations, the transfer function $T_o(\omega)$ is not equal to unity. In addition, differences in the lengths and optical characteristics of fibre optic cables can contribute to variations in $T_o(\omega)$. If both sensors are of the same type, such variations should be small, and large variations indicate the possible presence of standing waves in the vicinity of the reference sensor, which is something to avoid.

Once the calibration transfer function $T_o(\omega)$ has been determined, a check of the calibration process should be performed. This involves making a new measurement of the reference sensor response, denoted by $R_1(\omega)$, and a new response sensor measurement, $S_1(\omega)$. With these measurements, a new, and corrected, transfer function is defined as

$$T(\omega) = \frac{S_1(\omega)1}{R_1(\omega)T_o(\omega)} \tag{D.2}$$

Ideally, this new transfer function should be unity. However, slight variations in the measurements will cause it to be different. Figure D.6 illustrates this second transfer function and shows that it is indeed close to unity. This calibration procedure and check of the calibration should be used for each test and recalibrations should be performed routinely. The calibration transfer function $T_o(\omega)$ should be applied to all transfer function measurements made using the calibrated sensors and the fixed system configuration.

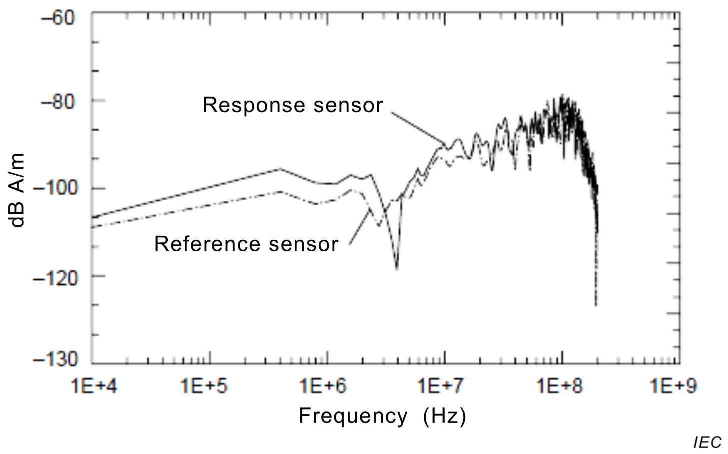

a) Reference and response sensor spectra

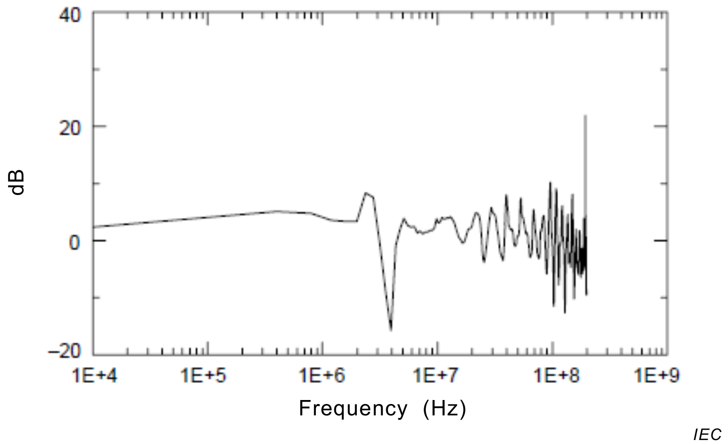

b) Derived calibration function

Figure D.5 – Measured sensor responses and calibration function

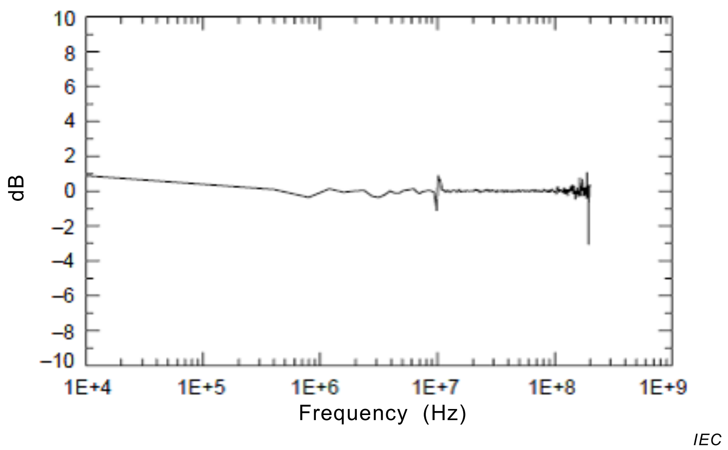

Figure D.6 – Measured transfer function, corrected by calibration file

D.7 Limitations of measurements

In developing a calibration procedure for the measurement chain, there are several limiting factors that should be remembered and taken into account. The dynamic range of the measurements can be limited by the following:

– noise in the fibre optic transmission system;

– insufficient bandwidth of the network analyser;

– amplifier gain setting.

These limitations can be understood and partially alleviated by making noise floor measurements with the amplifier turned off, changing the emission levels of the antenna by changing the amplifier gain and by changing the network analyser bandwidth.

Annex E
(informative)

Characterization of a planar shield for HEMP protection

E.1 General

The protection of equipment against the effects of HEMP is often accomplished by using the principles of electromagnetic shielding. As denoted in Figure E.1, localized electric or magnetic sources of EM energy create external E- and H-fields in the vicinity of a shielded enclosure. Due to the reflection and attenuation of these fields at the enclosure boundary, the internal E- and H-fields are reduced inside the shield.

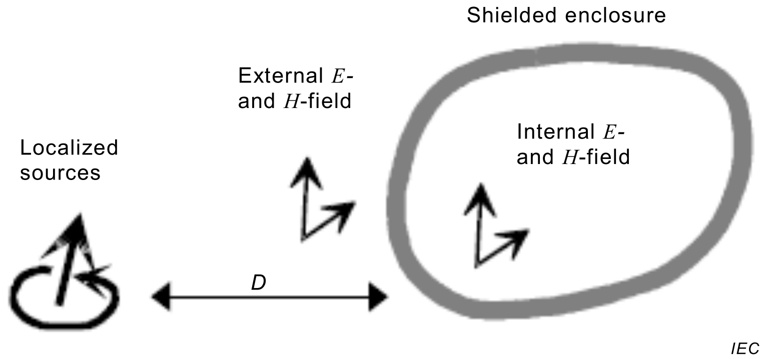

Figure E.1 – Example of a general shielding problem

The characterization of this problem is difficult in the most general case, because the shielding depends not only on the electrical characteristics of the shield, but also on the nature and location of the excitation sources. For example, if the external source is magnetic in nature (caused by circulating electric currents in a loop), the fields near the source are predominately magnetic. Similarly, if the source appears as a linear current flowing on a thin wire, the fields are predominately electric in their composition. Of course, Maxwell's equations dictate that both E- and H-fields exist together (except at d.c.). This implies that there is a different impedance level for the two sources – with the magnetic source producing EM fields with a low E/H ratio, and the electric sources producing fields with a high E/H ratio.

Strictly speaking, the concept of the field impedance is valid only in the radiation zone (or "far" field) where the E- and H-fields are mutually orthogonal and located in the plane transverse to the direction of propagation. In this region, the wave impedance is defined as $Z_c = |E|/|H|$. In the near field, at distances closer than several wavelengths, the fields have complicated spatial dependencies and such a transverse definition of impedance is not valid. However, it is possible to consider the magnitudes of the E- and H-fields in the near field in order to arrive at an "impedance level" for the fields, and this quantity will be different, depending on whether the source is primarily electric or magnetic.

At large distances from the source ($D >> \lambda$), the distinction between the electric and magnetic sources fades and the fields become radiating transverse electromagnetic (TEM) waves with a characteristic impedance of E/H = 377 Ω. Locally, these fields appear like a plane wave. Figure E.2 summarizes the behaviour of the fields from both magnetic and electric sources, and illustrates that at far distances, they both produce the same type of field, namely the plane wave.

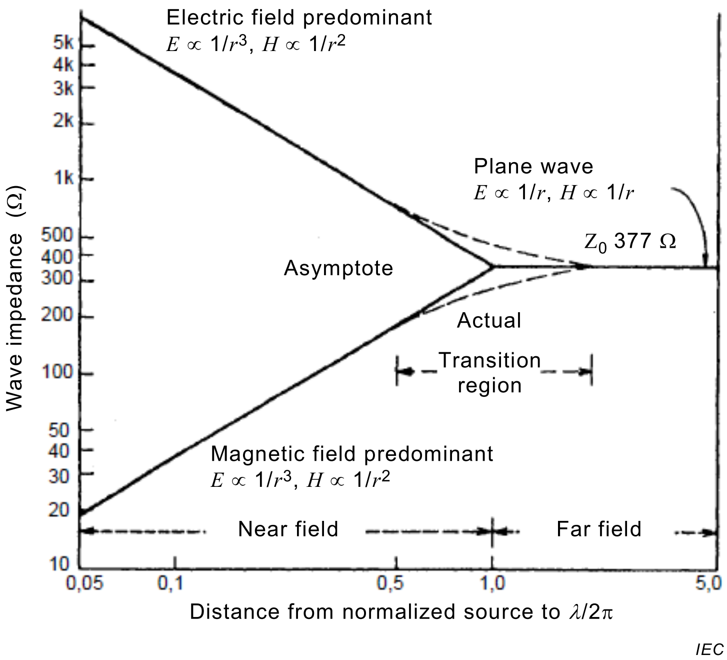

Figure E.2 – Behaviour of the impedance ratio $|E|/|H|$ as a function of distance from a source [29]

The penetration of EM fields into the enclosure also depends on the nature of the excitation fields. Generally, for sources that are close to the shield (i.e. for $D < \lambda$, or conversely, at low frequencies) the E-field is very strongly attenuated by the enclosure, but the H-field is able to diffuse through the shield. Thus, the actual internal fields depend on the shield characteristics and on the type of external source.

Frequently, this shielding problem is simplified by making the following assumptions:

– the source is very far from the shield ($D >> \lambda$), so that the external field is a plane wave;

– the shielding enclosure is an infinite planar slab.

Such infinite plane shields are often used in modelling and in trying to interpret measured data from HEMP tests, primarily due to the simplicity of the resulting expressions for the shielding effectiveness. It should be recognized that any values of shielding effectiveness for such structures can, at times, vastly overstate the shielding actually obtained in a realistic shield. This is because real structures are not infinite in two directions (as is the case of an infinite slab) and because many interference sources are not really plane waves.

Nevertheless, an examination of the shielding of a flat plate is instructional, because it clearly illustrates the connection between the resistivity of the shield material, the surface impedance presented to the incident field and the transfer impedance on the shielded side. Annex E provides a discussion of this background material for the purpose of better understanding these shielding concepts.

E.2 Problem geometry

Figure E.3 illustrates the problem under discussion in Annex E. An infinitely large, finitely conducting slab of thickness, d, is illuminated by an incident electromagnetic plane wave. This field induces a volume current density, J, to flow in the material and this current re-radiates, producing a reflected field propagating back towards the original source of the fields, plus a transmitted field which enters into the "protected" region on the opposite side of the slab. If the slab were to be perfectly conducting, the entire incident field would be reflected, with no penetrating field. In reality, however, as a slab of finite conductivity is involved, some penetrating field will occur, and it is desired to develop expressions for calculating this penetrated field in terms of shield thickness, electrical conductivity and other pertinent parameters.

In this problem, the amount of field that penetrates into the protected region depends on the polarization and the angle of incidence, ψ, of the incident field. To simplify the discussion, it is assumed that the incident field is normally incident on the slab (i.e. ψ = 0), so that the shielding factors become independent of the incidence angles.

The goal of the analysis presented here, therefore, is to summarize the analytical expressions that may be used to predict the EM fields that penetrate into the shielded region.

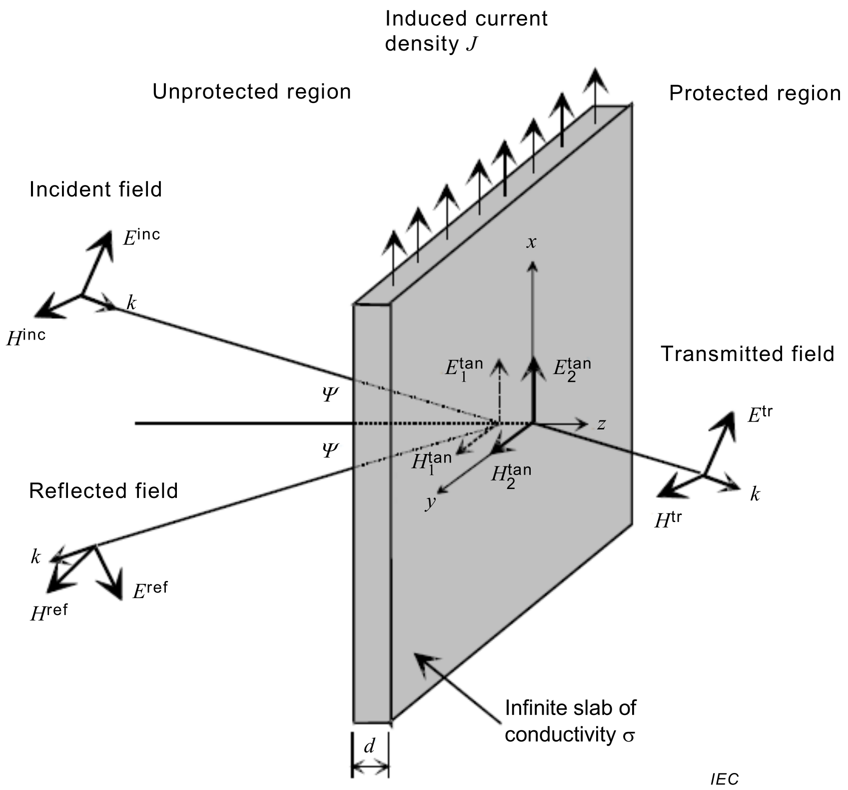

Figure E.3 – Conducting slab of thickness, *d*, and infinite extent serving as an electromagnetic barrier

E.3 Equivalent circuit representation

E.3.1 General

The behaviour of the EM fields illustrated in Figure E.4 can be described using an equivalent two-port circuit (see Figure E.4). The conducting slab in the problem is represented by a linear two-port circuit, in which the tangential E- and H-fields on the unshielded side are linearly related to the corresponding field quantities on the shielded side through a matrix equation. In Figure E.4a), the excitation is provided by a series voltage source, given by the incident E-field E_{inc}, and by a shunt current source given by the incident magnetic field, H_{inc}. The impedances of these sources (i.e. the relationship between E and H) is the characteristic impedance of free space, Z_c, and this is represented by the impedance element in the source circuit.

Figure E.4b) illustrates an equivalent representation for the excitation of this circuit. The shunt current source can be transformed into a voltage source using a Norton-to-Thevenin transformation, and the relationship E_{inc} = $Z_c \cdot H_{inc}$ can be used to arrive at the equivalent source voltage of 2 E_{inc}. A similar transformation can be used to obtain the electrically dual source: a current source of 2 H_{inc} in shunt with the impedance Z_{c}.

On the shielded side of the slab, the model contains a load impedance Z_{c}, which is equal to the characteristic impedance of free space. With either of the equivalent sources shown in exciting the slab, suitable expressions for determining the tangential E_2^{tan} and H_2^{tan} fields on the shielded side can be developed.

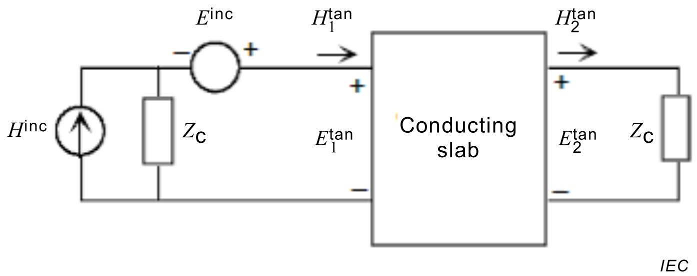

a) Circuit representation of the conducting slab

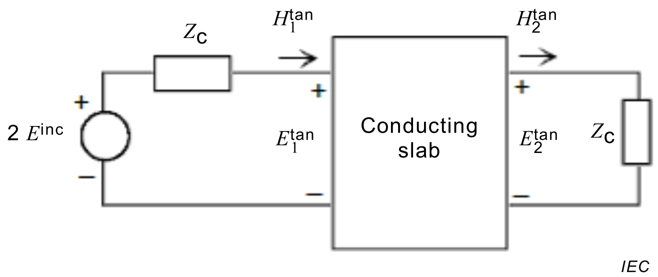

b) Alternate circuit representation of the conducting slab

Figure E.4 – Equivalent circuit representation of the shielding problem

E.3.2 Chain parameter representation of the shield

A general two-port circuit as shown in Figure E.5 can be represented by a number of different matrix relationships:

– open-circuit impedance parameters (Z);
– short-circuit admittance parameters (Y);
– chain (or $ABCD$) parameters;
– scattering parameters (S);
– hybrid parameters (h).

In the present case, the chain parameters are the most useful as they provide a relationship between the voltage and current quantities on one port of the circuit and those at the other port. With reference to Figure E.5, the chain parameter relationship can be expressed as (see [35])

$$\begin{bmatrix} V_1 \\ I_1 \end{bmatrix} = \begin{bmatrix} A & B \\ C & D \end{bmatrix} \begin{bmatrix} V_2 \\ I_2 \end{bmatrix} \tag{E.1}$$

or, by its inverse

$$\begin{bmatrix} V_2 \\ I_2 \end{bmatrix} = \begin{bmatrix} D & -B \\ -C & A \end{bmatrix} \begin{bmatrix} V_1 \\ I_1 \end{bmatrix} \tag{E.2}$$

It should be noted that in these expressions, there is a requirement that the $ABCD$ parameters shall satisfy the relationship $AD\text{-}BC$ = 1 for a linear, bilateral system.

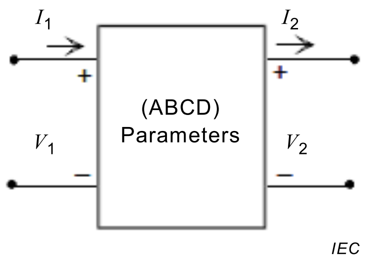

Figure E.5 – Two-port representation of a circuit

Letting the variables V_1 and I_1 represent the tangential E- and H-fields on the illuminated side of the slab ($E_1^{\tan}$ and $H_1^{\tan}$) and V_2 and I_2denote the fields $E_2^{\tan}$and $H_2^{\tan}$ on the shielded side, reference [8] has developed the following chain parameter representation for the slab:

$$\begin{aligned} \begin{bmatrix} E_1^{\tan} \\ H_1^{\tan} \end{bmatrix} &= \begin{bmatrix} A & B \\ C & D \end{bmatrix} \begin{bmatrix} E_2^{\tan} \\ H_2^{\tan} \end{bmatrix} \\ &= \begin{bmatrix} \cosh\left(\sqrt{j\omega\tau_d}\right) & R\sqrt{j\omega\tau_d}\,\sinh\left(\sqrt{j\omega\tau_d}\right) \\ \left(R\sqrt{j\omega\tau_d}\right)^{-1}\sinh\left(\sqrt{j\omega\tau_d}\right) & \cosh\left(\sqrt{j\omega\tau_d}\right) \end{bmatrix} \begin{bmatrix} E_2^{\tan} \\ H_2^{\tan} \end{bmatrix} \end{aligned} \tag{E.3}$$

where τ_d is a diffusion time and R is the d.c. slab surface resistance (in Ω), given by

$$\tau_d = \mu\sigma d^2 \quad \text{and} \quad R = \frac{1}{\sigma d} \tag{E.4}$$

In these expressions, d is the slab thickness, σ = 1/ρ is the electrical conductivity of the material and μ is the permeability of the sample.

E.3.3 Circuit responses

E.3.3.1 Expression for the surface fields

Using standard circuit analysis techniques, the responses for E and H anywhere in the problem can be determined. Specifically, the surface fields on the illuminated side of the slab can be evaluated as

$$E_1^{\tan} = \frac{\left(AZ_c + B\right)}{Z_c\left(A + Z_c C\right) + \left(B + Z_c D\right)} 2E^{\text{inc}} \tag{E.5}$$

and

$$H_1^{\tan} = \frac{\left(CZ_c + D\right)}{Z_c\left(A + Z_c C\right) + \left(B + Z_c D\right)} 2E^{\text{inc}} \tag{E.6}$$

where A, B, C and D are the slab chain parameters defined in equation (E.3).

The limiting cases of Equations (E.5) and (E.6) are instructive. When the conductivity of the slab vanishes, or equivalently, when d = 0, the chain parameters become A = 1, B = 0, C = 0, D = 1, and these equations are reduced to the free-space case where

$$E_1^{\text{tan}} = E^{\text{inc}} \quad \text{and} \quad H_1^{\text{tan}} = \frac{1}{Z_{\text{c}}} E^{\text{inc}} \tag{E.7}$$

Another case of interest is when the slab becomes perfectly conducting (i.e. $\sigma \to \infty$). For this case, the chain parameters are A = 1, B = 0, C = ∞, D = 1, and the fields in Equations (E.5) and (E.6) take on the required values

$$E_1^{\text{tan}} = 0 \quad \text{and} \quad H_1^{\text{tan}} = \frac{2}{Z_{\text{c}}} E^{\text{inc}} = 2H^{\text{inc}} \tag{E.8}$$

on the surface of the conductor.

E.3.3.2 Expression for the penetrating fields

In a similar manner, the fields penetrating into the shield region, E_2^{tan} and H_2^{tan}, can be determined by circuit analysis. These fields have the form

$$E_2^{\text{tan}} = \frac{Z_{\text{c}}}{Z_{\text{c}}\left(A + Z_{\text{c}}C\right) + \left(B + Z_{\text{c}}D\right)} 2E^{\text{inc}} \tag{E.9}$$

and

$$H_2^{\text{tan}} = \frac{1}{Z_{\text{c}}\left(A + Z_{\text{c}}C\right) + \left(B + Z_{\text{c}}D\right)} 2E^{\text{inc}} \tag{E.10}$$

Checks of these fields for the limiting cases described in E.3.3.1 indicate that for no slab present the fields become the free-space incident fields, and for a perfectly conducting slab, the fields are zero, indicating perfect shielding.

E.3.3.3 The surface impedance

Using the general field expressions in Equations (E.5) and (E.6), it is possible to develop an expression for the surface impedance on the illuminated side of the slab. This quantity is useful, in that it permits the analysis of problems on the illuminated side of the slab without requiring a further analysis of fields inside the slab or in the shielded region beyond. This impedance is defined as the ratio of E and H on the surface as:

$$Z_{\text{s}} = \frac{E_1^{\text{tan}}}{H_1^{\text{tan}}} = \frac{\left(AZ_{\text{c}} + B\right)}{\left(Z_{\text{c}}C + D\right)} (\Omega) \tag{E.11}$$

For a thin slab of finite conductivity at low frequencies, the chain parameters become A = 1, B = 0, C = 1/R and D = 1. In this case, the surface impedance becomes:

$$Z_s = \frac{1}{\left(\frac{1}{R} + \frac{1}{Z_c}\right)} \approx R \; (\Omega) \tag{E.12}$$

for cases where the surface resistance of the material is much less than the impedance of free space (377 Ω).

At higher frequencies, the chain parameters in Equation (E.11) should be evaluated using Equation (E.3). The general expression for Z_s becomes:

$$Z_s = \frac{\left(Z_c \cosh\sqrt{j\omega\tau_d} + R\sqrt{j\omega\tau_d}\,\sinh\sqrt{j\omega\tau_d}\right)}{\left(Z_c\left(R\sqrt{j\omega\tau_d}\right)^{-1}\sinh\sqrt{j\omega\tau_d} + \cosh\sqrt{j\omega\tau_d}\right)} \; (\Omega) \tag{E.13}$$

For many types of conducting materials in the HEMP frequency range, it is possible to use a low-frequency simplification to Equation (E.13):

$$Z_s \approx R\sqrt{j\omega\tau_d} = (1 + j)\sqrt{\frac{\omega\mu}{\sigma}} \equiv R_s + j\omega L_s \tag{E.14}$$

where the surface resistance R_s and the surface inductance L_s are given in terms of the frequency $f = \omega/2\pi$ as:

$$R_s = \sqrt{\frac{2\pi f\mu}{\sigma}} \quad \text{and} \quad L_s = \frac{R_s}{2\pi f} \tag{E.15}$$

Table E.1 presents the surface resistance for several materials.

Table E.1 – Surface resistance and electrical parameters for selected materials

Material	**Conductivity σ** **S/m**	**Permeability μ** **H/m**	**Skin depth δ** **m**	**Surface resistivity R_s** **Ω**
Silver	$6{,}17 \times 10^{7}$	$4\pi \times 10^{-7}$	$0{,}0642 / \sqrt{f}$	$2{,}52 \times 10^{-7}\sqrt{f}$
Copper	$5{,}80 \times 10^{7}$	$4\pi \times 10^{-7}$	$0{,}066 / \sqrt{f}$	$2{,}61 \times 10^{-7}\sqrt{f}$
Aluminimum	$3{,}72 \times 10^{7}$	$4\pi \times 10^{-7}$	$0{,}826 / \sqrt{f}$	$3{,}26 \times 10^{-7}\sqrt{f}$
Brass	$1{,}57 \times 10^{7}$	$4\pi \times 10^{-7}$	$0{,}127 / \sqrt{f}$	$5{,}01 \times 10^{-7}\sqrt{f}$
Tin	$0{,}90 \times 10^{7}$	$4\pi \times 10^{-7}$	$0{,}168 / \sqrt{f}$	$6{,}62 \times 10^{-7}\sqrt{f}$
Solder	$0{,}71 \times 10^{7}$	$4\pi \times 10^{-7}$	$0{,}185 / \sqrt{f}$	$7{,}73 \times 10^{-7}\sqrt{f}$

Material	Conductivity σ S/m	Permeability μ H/m	Skin depth δ m	Surface resistivity R_S Ω
Graphite	$3{,}0 \times 10^{4}$	$4\pi \times 10^{-7}$	$2{,}91 / \sqrt{f}$	$1{,}15 \times 10^{-5} \sqrt{f}$
Plexiglas	$5{,}1 \times 10^{-3}$	$4\pi \times 10^{-7}$	$7{,}05 \times 10^{3} / \sqrt{f}$	$0{,}028 \sqrt{f}$

E.3.3.4 Shield transfer impedance

The transfer impedance of the plate is defined as the ratio of $E_2^{\text{tan}} / H_2^{\text{tan}}$, or equivalently, the ratio of the internal E-field to the external surface current density. This is slightly different from the transfer impedance of a cable in which the impedance is defined as the ratio of the internal E-field (a distributed voltage source) to the total shield current. In this case, the transfer impedance has the units of Ω/m. Its units are in Ω. A circuit analysis of provides the following expression for the transfer impedance of the plate:

$$Z_{\text{t}} = \frac{E_2^{\text{tan}}}{H_1^{\text{tan}}} = \frac{Z_{\text{c}}}{\left(Z_{\text{c}} C + D\right)} \; (\Omega) \qquad \text{(E.16)}$$

or, equivalently:

$$Z_{\text{t}} = \frac{Z_{\text{c}}}{\left(Z_{\text{c}}\left(R\sqrt{j\omega\tau_{\text{d}}}\right)^{-1} \sinh\sqrt{j\omega\tau_{\text{d}}} + \cosh\sqrt{j\omega\tau_{\text{d}}}\right)} \; (\Omega) \qquad \text{(E.17)}$$

and for good conductors in the HEMP frequency range, this is approximated as:

$$Z_{\text{t}} \approx \frac{R\sqrt{j\omega\tau_{\text{d}}}}{\sinh\sqrt{j\omega\tau_{\text{d}}}} \; (\Omega) \qquad \text{(E.18)}$$

It should be noted that at low frequencies, the transfer impedance is $Z_{\text{t}} \approx R$, which is the d.c. surface resistance of the slab. It is interesting to note that this is the same value as the surface impedance in Equation (E.12). Thus, a low-frequency measurement of the surface impedance on the front side of the plate can serve to characterize the transfer impedance of the plate at low frequencies.

E.3.3.5 Transfer admittance

The transfer admittance of the planar sheet is defined as

$$\begin{aligned} Y_{\text{t}} &= \frac{H_2^{\text{tan}}}{E_1^{\text{tan}}} = \frac{1}{\left(Z_{\text{c}} A + B\right)} \; (\text{S}) \\ &= \frac{1}{\left(Z_{\text{c}} \cosh\sqrt{j\omega\tau_{\text{d}}} + R\sqrt{j\omega\tau_{\text{d}}} \sinh\sqrt{j\omega\tau_{\text{d}}}\right)} \end{aligned} \qquad \text{(E.19)}$$

For a thin slab of finite conductivity at low frequencies, the chain parameters are A = 1, B = 0, C = 1/R and D = 1and in this transfer admittance impedance becomes $Y_{\text{t}} \approx 1/Z_{\text{c}}$ = 0,002 7 (S).

Annex F
(informative)

Inside-to-out measurement method

F.1 Purpose

Some HEMP protection facilities in practical use do not have enough space available outside the electromagnetic barrier (due to physical constraints such as concrete walls or soil) to allow for the correct application of the measurement method described within the main body of this document (outside-to-in); practical experience has shown that many facilities have up to 1 m of available separation space. Territorial regulatory constraints can also be a prohibiting factor for conducting outside-to-in measurements.

Therefore, in many practical cases it is not possible to measure shielding effectiveness according to the standard outside-to-in test method. The constructors for HEMP protection facilities are also unwilling to build facilities with extra space for this measurement outside of the barrier due to the great expense and inefficiency of the operational working area for the existing building.

Annex F provides some experimental data that demonstrates the feasibility of placing the transmitting antenna inside the enclosure and the receiving antenna placed a short distance outside (‘inside-to-out’ method).

It is important to note that there is a risk to equipment and other materials inside the facility using this method; therefore, removal of equipment is recommended.

With this method, it may be difficult to determine whether the transmitter is actually transmitting; therefore, it is recommended that a field measurement probe with a read-out outside the chamber is utilized to confirm a field is actually present inside.

F.2 Comparison of existing SE test methods

Table F.1 provides a comparison of existing SE test methods from a variety of standards including the previous edition (Edition 1.0) of this standard.

Table F.1 – Comparison with other standards

Standard	IEC 61000-4-23:2000 (Edition 1.0)	IEEE-STD-299	MIL-STD-188-125-1
Publication	2000	2006	2005
Test frequency	15 kHz to 30 kHz: 1 point 300 kHz to 500 kHz: 1 point 1 MHz to 20 MHz: 1 point 50 MHz to 200 MHz: 3 points	9 kHz to 16 kHz: 1 point 140 kHz to 160 kHz: 1 point 14 MHz to 16 MHz: 1 point 20 MHz to 100 MHz: 1 point 100 MHz to 300 MHz: 1 point 300 MHz to 600 MHz: 1 point 600 MHz to 1 GHz: 1 point 1 GHz to 2 GHz: 1 point 2 GHz to 4 GHz: 1 point 4 GHz to 8 GHz: 1 point 8 GHz to 18 GHz: 1 point	10 kHz to 100 kHz: 20 points 100 kHz to 1 MHz: 20 points 1 MHz to 10 MHz: 40 points 10 MHz to 100 MHz: 150 points 100 MHz to 1 GHz: 150 points
Antenna type	Loop antenna Dipole antenna	Loop antenna Biconical antenna Dipole antenna Horn antenna	Loop antenna Biconical antenna Log periodic antenna
TX/RX antenna distance/location	TX: ≥ 5 m (outside) RX: 5 cm to 60 cm	TX: ≥ 1,7 m (outside) RX: 0,3 m	TX: 2,05 m (outside) RX: 1,0 m
Unit test area	2,5 m × 2,5 m	2,6 m × 2,0 m	3,05 m × 3,05 m
Pass/fail criteria	-	By owner	10 kHz to 10 MHz : $\geq 20\log_{10} f$ -60 dB 10 MHz to 1 GHz : ≥ 80 dB

F.3 Inside-to-out SE test of shielded rooms

F.3.1 Measurements of the inside-to-out SE

The conditions of testing real examples of HEMP protected facilities are shown in Table F.2.

Table F.2 – Test shielded rooms

	Shielded room #1	**Shielded room #2**	**Shielded room #3**
	 IEC	 IEC	 IEC
Chamber size	2,9 m × 3,9 m × 2,4 m	3,6 m × 5,9 m × 3,0 m 1,1 m × 2,4 m × 2,3 m	9,0 m × 6,0 m × 3,0 m 2,0 m × 3,0 m × 3,0 m
PoE	Door, waveguide, honeycomb, filter, connector panel	Door, waveguide, honeycomb, filter	Door, waveguide, honeycomb, filter
SE	Approximately 60 dB to 70 dB	Approximately 60 dB to 70 dB	80 dB
Door type	Single	Interlocks	Interlocks
Filter type	EMI	EMI	EMP

a) Test set-up for the inside-to-out SE measurement

In the outside-to-in case, the transmitting antenna was placed outside the electromagnetic barrier and the receiving antenna was placed inside. In contrast, for the inside-to-out, the transmitting antenna was placed inside the electromagnetic barrier and the TX equipment was placed in another shielded room to protect from EM disturbances. The receiving antenna was placed outside the barrier. It was then retested under the equal separation distance placing the transmitting antenna outside. The results were then compared.

Using the basic test method of MIL-STD-188-125-1 to measure the shielding effectiveness, the nominal distance from the transmitting antenna reference point to the test area surface is 2,05 m, and the nominal distance from the receiving antenna reference point to the test area surface is 1 m.

Test points for the shielded room #1 and #2 are selected at the door, and the test point of the shielded room #3 is selected at the wall. Regarding frequencies of 200 kHz, 50 MHz, 200 MHz, 400 MHz, and 1 GHz, outside-to-in measurement results were compared with inside-to-out measurement results. The shielded RF cables of 10 m were used both for calibration and measurement.

The test set-up for outside-to-in and inside-to-out SE measurement is shown in Figure F.1.

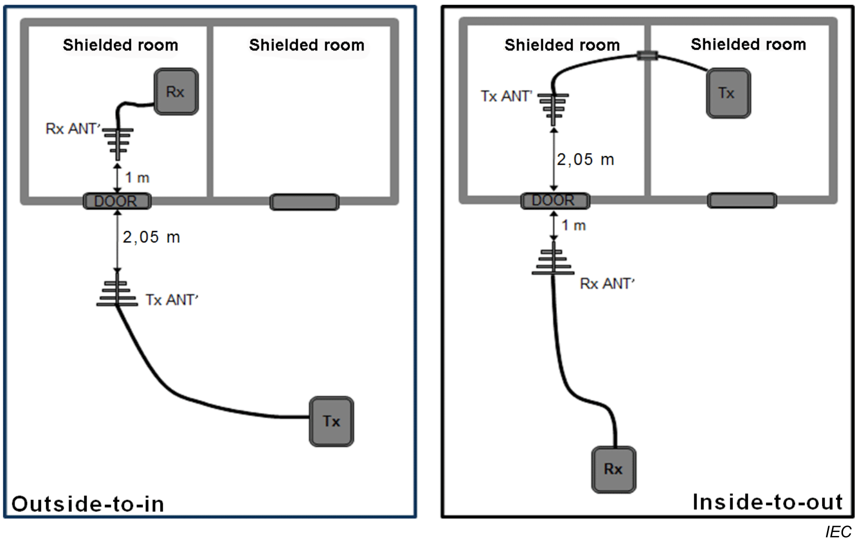

a) **Shielded room #1**

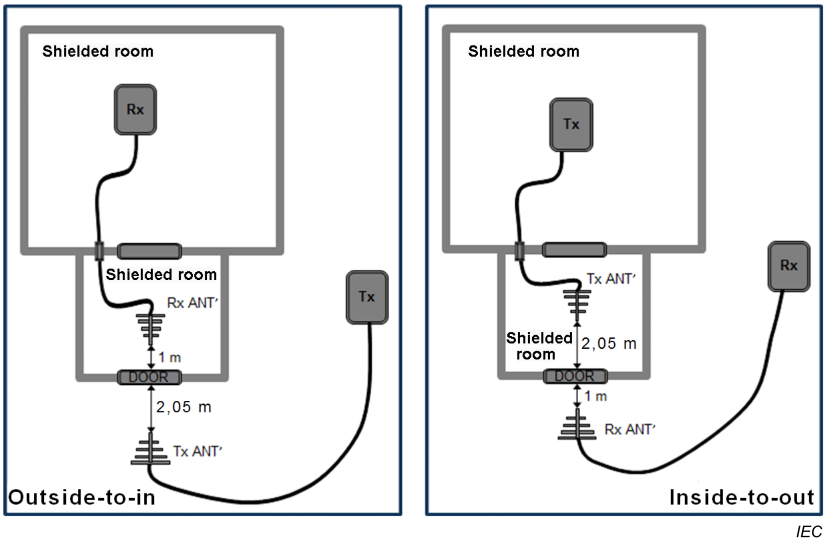

b) **Shielded room #2**

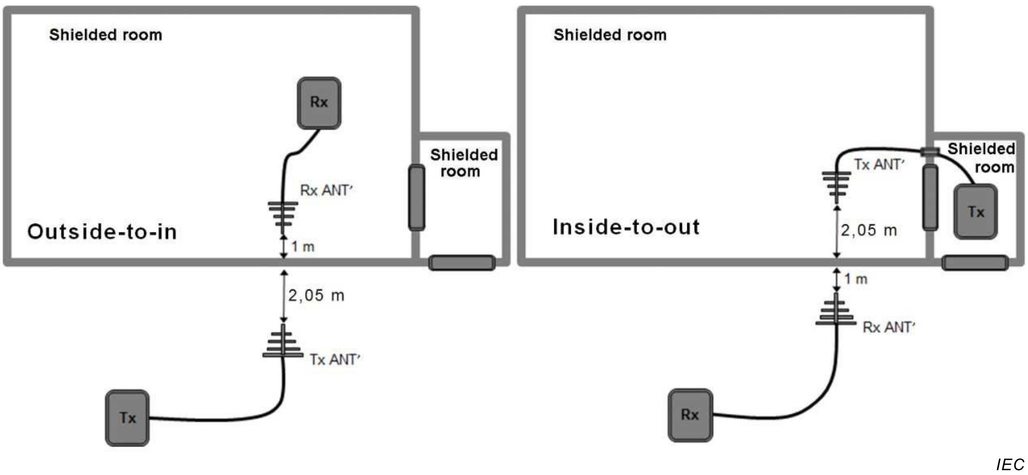

c) **Shielded room #3**

Figure F.1 – Test set-up for the outside-to-in and inside-to-out SE measurement

b) Test results for the inside-to-out SE measurement

The measurement results are shown in Table F.3.

Table F.3 – Comparison of the SE measurement results

(Unit: dB)

		Freq.	200 kHz	50 MHz	200 MHz	400 MHz	1 GHz
Shielded room #1 - Door -	Outside-to-in	SE	42	83	46	54	52
	Inside-to-out	SE	42	84	47	51	52
	Difference		0	+1	+1	-3	0
Shielded room #2 - Door -	Outside-to-in	SE	37	81	56	52	45
	Inside-to-out	SE	46	79	57	50	42
	Difference		+9	-2	+1	-2	-3
Shielded room #3 - Wall -	Outside-to-in	SE	> DR	> DR	92	82	93
	Inside-to-out	SE	> DR	> DR	95	77	89
	Difference		?	?	+3	-5	-4

NOTE "> DR" means the shielding effectiveness is superior to the DR (dynamic range) value. DR is the range in which the test system is able to measure the SE.

The actual measurement results of outside-to-in and inside-to-out shielding effectiveness for each shielded room are not identical. This is probably due to the different shielded room conditions. Care should be taken to ensure that sufficient dynamic range above the noise floor is available for the inside-to-out method or, at test frequencies where this is not possible, an alternative test frequency should be specifically selected to avoid this issue.

F.3.2 Summary

The inside-to-out method produces very comparable results to the traditional outside-to-in method, particularly where the shielding effectiveness of the installation is anticipated to be lower than a high quality shielded room (> 80 dB).

For cases where radiated HEMP protection is required to be much less than 80 dB, the inside-to-out method clearly has merit. This does not preclude the method being applied to high quality shielded rooms; however, dynamic range may be a limiting factor.

Bibliography

[1] IEC 61000-4-20, *Electromagnetic compatibility (EMC) – Part 4-20: Testing and measurement techniques – Emission and immunity testing in transverse electromagnetic (TEM) waveguides*

[2] IEC 61000-4-25, *Electromagnetic compatibility (EMC) – Part 4-25: Testing and measurement techniques – HEMP immunity test methods for equipment and systems*

[3] IEC 61000-2-10, *Electromagnetic compatibility (EMC) – Part 2-10: Environment – Description of HEMP environment – Conducted disturbance*

[4] IEC 61000-4-24, *Electromagnetic compatibility (EMC) – Part 4-24: Testing and measurement techniques –Test methods for protective devices for HEMP conducted disturbance*

[5] IEC TR 61000-2-5, *Electromagnetic compatibility (EMC) – Part 2-25: Environment – Description and classification of electromagnetic environments*

General EMP references:

[6] Baum, C.E., "EMP Simulators for Various Types of Nuclear EMP Environments: An Interim Categorization," IEEE TRANS. EMC, Vol. EMC-20, No. 1, Feb. 1978.

[7] Bell Laboratories, "EMP Engineering and Design Principles", Technical Publications Department, Bell Laboratories, Whippany, N.J., 1975.

[8] EMP Interaction: "Principles, Techniques and Reference Data", K.S.H. Lee, editor, Hemisphere Publishing Co. New York, 1989.

[9] Ghose, R., "EMP Environment and System Hardness Design", DWCI Publication, Gainesville, VA, 1984.

[10] Joehl, W., "A General and Systematic Survey of NEMP Protection Measures", Research Institute for Protective Construction (FMB), Zurich, Rep. FMB 78-1, Jan. 1978.

[11] Joint Special Issue of the Nuclear Electromagnetic Pulse, IEEE Trans EMC, Vol. EMC-20, No. 1, Feb. 1978.

[12] Vance, E.F., "Electromagnetic-Pulse Handbook for Electric Power Systems," Report DNA 3466F, Defense Nuclear Agency, Washington, D.C., Feb. 4, 1975.

Electromagnetic topology:

[13] Baum, C.E., "Electromagnetic Topology for the Analysis and Design of Complex Electromagnetic Systems," pp. 467-547 in *Fast Electrical and Optical Measurements*, Vol. I, eds. I.E. Thompson and L.H. Luessem, Martinus Nijhoff, Dordrecht, 1986.

[14] Baum, C.E., "Electromagnetic Topology: A Formal Approach to the Analysis and Design of Complex Electronic Systems", of the 4th Symposium and Technical Exhibition on EMC Zurich, pp. 209-214, March 1981.

[15] Baum, C.E., "The Role of Scattering Theory in Electromagnetic Interference Problems", in Electromagnetic Scattering, P.L.E. Uslenghi, editor, Academic Press, 1978.

[16] Karlsson, T., "The Topological Concept of a Generalized Shield," AFWL Interaction Note 461, Kirtland AFB NM, Jan. 1988.

[17] Karlsson, T., "On Grounding – Practical Procedures Based on Electromagnetic Theory", Proceedings of the 9th International Zurich Technical Exhibition on EMC, 3-5 March 1987.

[18] Tesche, F.M., "Topological Concepts for Internal EMP Interaction," IEEE Trans. EMC, 20 (1), Feb. 1978.

[19] Tesche, F.M., "Introduction to Concepts of Electromagnetic Topology as Applied to EMP Interaction With Systems", NATO/AGARD Lecture Series Publication 144, Interaction Between EMP, *Lightning and Static Electricity with Aircraft and Missile Avionics Systems*, May 1986.

[20] Vance, E.F., "EMP Hardening of Systems," Proceeding of the 4th Symposium and Technical Exhibition on Electromagnetic Compatibility, Zurich, 10-12 March 1981.

[21] Vance, E.F., and W. Graf, "The Role of Shielding in Interference Control", IEEE Trans. EMC, Vol. 30, No. 3, August 1988, pp. 294-297.

Electromagnetic compatibility references:

[22] Christopoulos, C., "Principles and Techniques of Electromagnetic Compatibility", CRC Press, Boca Raton, 1995.

[23] Degauque, P. and J. Hamelin, eds., "Electromagnetic Compatibility", Oxford University Press, Oxford, 1993 (also in French).

[24] Goedbloed, J.J., "Electromagnetic Compatibility", Prentice Hall, New York, 1992.

[25] Gravelle, L.B., and P.F. Wilson, "EMI/EMC in Printed Circuit Boards – A Literature Review", IEEE Trans. EMC, Vol. 34, No. 2, May 1992, pp. 109-116.

[26] Ianovici, (Ianoz) M. and J.J Morf, eds., "Compatibilité Électromagnétique", Presses Polytechniques Romandes, Lausanne, 1983.

[27] Keiser, B.E., "Principles of Electromagnetic Compatibility", Artech House, Inc. Dedham, Mass. 1979.

[28] Morgan, D., "A Handbook for EMC Testing and Measurement", Peter Peregrinus Ltd., IEE Electrical Measurement Series 8, London, 1994.

[29] Ott, H.W., "Noise Reduction Techniques in Electronic Systems", John Wiley & Sons, New York, 1988.

[30] Paul, C.R., "Prediction of Crosstalk in Ribbon Cables: Comparison of Model Predictions and Experimental Results", IEEE Trans. EMC, Vol. EMC-20, No. 3, Aug. 1978, pp. 394-406.

[31] Paul, C.R., "Transmission-Line Modeling of Shielded Wires for Crosstalk Prediction", IEEE Trans. EMC, Vol. EMC-23, No. 4, Nov. 1981, pp. 345-351.

[32] Paul, C.R., "Introduction to Electromagnetic Compatibility", John Wiley & Sons, New York, 1992.

[33] Perez, R., ed., "Handbook of Electromagnetic Compatibility", Academic Press, 1995.

[34] Ryser, H., "Electromagnetic Compatibility," Hasler Review, Vol. 17, No. 2, 1984, pp. 33-40.

[35] Tesche, F.M., M.V. Ianoz and T. Karlsson, "EMC Analysis Methods and Computational Models", John Wiley & Sons, New York, 1996.

Electromagnetic shielding:

[36] Casey, K.F., "Electromagnetic Shielding Behaviour of Wire-Mesh Screens", IEEE Trans. EMC, Vol. 30, No. 3, Aug. 1988, pp. 298-311.

[37] Dahlberg, E., Electromagnetic Shielding, "Some Simple Formulæ for Closed Uniform Shields", TRITA–EPP–75–27, KTH Stockholm, Dec. 1975.

[38] Kaden, H., "Wirbelstroeme und Schirmung in der Nachrichtentechnik", Springer-Verlag, Berlin, 1959.

[39] King, L.V., "Electromagnetic Shielding at Radio Frequencies", *Phil. Mag. and J. Sci*., Vol. 15, No. 97, Feb. 1933, pp. 201-223.

[40] Lee, K.S.H., "Electromagnetic Shielding", Ch. 11 in *Recent Advances in Electromagnetic Theory*, H.N. Kritikos and D.L. Jagard, eds., Springer-Verlag, New York, 1990.

[41] Schelkunoff, S.A., "Theory of Lines and Shields," *Bell System Technical Journal*, 13(1934)4, pp. 522-579.

[42] Vance, E.F., "Coupling to Shielded Cables", Krieger Publishing, 1987.

[43] Savage, E. B., J. L. Gilbert and W. A. Radasky, "Expedient Building Shielding Measurement Method for HEMP Assessments," IEEE Transactions on Electromagnetic Compatibility, Vol. 55, No. 3, June 2013, pp. 508-517.

Related specifications and standards:

[44] MIL-STD-188-125-1:2005, *High-Altitude Electromagnetic Pulse (HEMP) Protection for Ground-Based C4I Facilities Performing Critical, Time-Urgent Missions – Part 1: Fixed Facilities*

[45] IEC 62153-4-x (all parts), *Metallic communication cable test methods – Part 4-x: Electromagnetic compatibility (EMC)*

[46] IEC TR 61000-5-4, *Electromagnetic compatibility (EMC) – Part 5: Installation and mitigation guidelines – Section 4: Immunity to HEMP – Specifications for protective devices against HEMP radiated disturbance*

[47] IEEE-Std-299:2006, *IEEE Standard Method for Measuring the Effectiveness of Electromagnetic Shielding Enclosures*

[48] ANSI/IEEE Std 488.1:1987, *Standard IEEE Standard Digital Interface for Programmable Instrumentation*

____

INTERNATIONAL
ELECTROTECHNICAL
COMMISSION

3, rue de Varembé
PO Box 131
CH-1211 Geneva 20
Switzerland

Tel: + 41 22 919 02 11
Fax: + 41 22 919 03 00
info@iec.ch
www.iec.ch